



SSERD IPD BATCH 4

Team Pathfinders

'Top Level Mission Analysis and Feasibility Study of a Near-Earth Asteroid Mining Mission and Resource Return'

6 Week Research Internship in Space Mission Design

Mentors: Rashika S N, Vishnuvardhan Shaktibala

Co-Ordinators: Anisha, Prateek B

Team Members: Akanksha Maskeri, Srinithya Nerella, Lalithej Vyasam, Spandana Chilukuri, Kuljeet Kaur, Akash C, Abhijeeth Someshwar, Ria Matthews, Kallu Sudarshan, Arun Pradeep, Malavika D S, Keerthana Balakrishnan

This report is submitted in partial fulfilment of the requirements for the internship in Space Mission Design under the Internship Project Division, Batch 4 of SSERD- Society of Space Education Research and Development

©Team Pathfinders, SSERD; First Edition, November 2020



Declaration against Plagiarism

A. Authenticity of Report

We, 'Team Pathfinders' and all the members involved, hereby declare that we are the legitimate author(s) of this report and that it contains our original work. No portion of this work has been submitted in support of an application for another degree or qualification of this or any other university or institution of higher education. We hold SSERD harmless against any third party claims with regard to copyright violation, breach of confidentiality, defamation and any other third party right infringement.

B. Research Code of Practice and Ethics Review procedures

We, 'Team Pathfinders' and all the members involved declare that we have abided by the Organization's Research Ethics Review Procedures.

Title : '*Top Level Mission Analysis and Feasibility Study of a Near-Earth Asteroid Mining Mission and Resource Return'*

Candidate(s):

1. Akanksha Maskeri (Team Leader)
2. Srinithya Nerella (Assistant Team Leader)
3. V V K Lalithej
4. Someshwar Abhijeeth
5. Arun Pradeep
6. Ria Maria Matthew
7. Akash C
8. Kallu Sudarshan
9. Keerthana Balakrishnan
10. D S Malavika
11. Kuljeet Kaur
12. Spandana Chilukuri

Date : November 2020

Abstract

This report presents a feasibility study and preliminary spacecraft design for an asteroid mining mission whose objective is to return 500kg of resources and be launched between the year 2027 and 2030.

A detailed study on near-earth asteroids was conducted to select the most suitable candidates for this mission. Trade parameters included asteroid composition, size, minimum ΔV requirements and the number of possible launch opportunities within the timeframe. The asteroid selected for this mission was 1989ML due to its high metallic composition.

The mission analyses conducted to plot the optimum trajectory to the asteroid (and back), considered seven possible scenarios. The option which showed the most feasibility and fuel savings was to use a Mars fly-by to reach the asteroid. The Delta – V requirements for this option was found to be ~1.6km/s, and the mission duration is 4 years.

Preliminary spacecraft design was conducted to solve subsystem designs to meet the payload and delta-V targets. The final spacecraft mass after subsystem design is ~7 tonnes (which includes a 25% margin). Based on preliminary design results, this mission concept is considered to be feasible.

Acknowledgements

The Team Pathfinders, first and foremost would like to thank SSERD for this wonderful opportunity of working on a space mission design project through this internship. In India, where space projects are few and hard to come by, SSERD has created this wonderful platform that exposes its interns to international talent and projects through their expertise which the team is very grateful for.

This research internship is an asset to one's academic and professional career where the team not only learnt systems engineering practices but also other valuable skills such as documentation, website creation, research , presentation skills and team management.

The team would like to thank our mentors- Rashika S N and Vishnuvardhan Shaktibala for their subject matter expertise and mentoring that has changed each Individuals perspective on space mission design through which we learnt a great deal as the project progressed.

The team extends its thanks to our co-ordinators- Anisha and Prateek B whose help kept the project smooth sailing.

The team recognises each individual's contribution to their respective sub-systems despite having other academic commitments and thanks each and every fellow member of the team for their dedication, effort and time into making the 6 week internship a success.

Table of Contents

Abstract.....	i
Acknowledgements.....	ii
List of Figures	iv
List of Tables	vi
List of Equations.....	viii
1 Introduction	1
1.1 Aims and Objectives for the Asteroid Resource Return Mission.....	1
1.2 Decomposition of Report Structure.....	2
1.3 Project Management	3
1.3.1 Project Management Role	3
1.3.2 Project Timeline	4
1.3.3 Project Management Tools.....	4
1.3.4 Work Breakdown Structure	4
1.3.5 Management Challenges	6
2 Literature Review.....	7
2.1 Literature Review of previously flown Near Earth Asteroid Missions	7
2.2 Literature Review of previously flown Near Earth Asteroid Missions that have a sample return ...	8
2.3 Literature Review of Key System Architecture Elements of OSIRIS-REX	9
2.4 Literature Review of Key System Architecture Elements of Hayabusa	13
2.5 Conclusions of Literature Review and Mission Drivers for our Mission	16
3 Requirements for the Asteroid Mining Mission and Challenges	17
4 Selection of Target Asteroid.....	18
4.1 Asteroid Classification.....	18
4.2 Key Trade Elements for Selection of Asteroid	18
4.3 Trade Analysis and Conclusion.....	19
4.4 Properties of Target Asteroid and Preliminary Mission Analysis.....	26
5 Mission Analysis	33
5.1 Introduction	33
5.2 Alternative Mission Architecture Concepts	33
5.3 Selection of Mission Concept using ΔV Constraint for the Asteroid Mining Mission.....	34
5.4 ΔV Budget for Proximity Operations.....	40
5.5 Critique and Concept of Operations for Selected Mission Architecture	42
6 Propulsion Sub-System	50

6.1 Introduction	50
6.2 Trade Of Different propulsion systems for the Mission	50
6.3 Selection of Propellant and Preliminary Propellant Budget	52
6.4 Launch mass of the Spacecraft for the Mission and Selection of Launch Vehicle	54
6.5 Fuel Tank design.....	55
6.6 Pressurant Tank design	57
6.7 Conclusions	57
7 AOCS Sub-System.....	60
7.1 Introduction	60
7.2 Initial Design Options.....	60
7.3 Spacecraft Modes	62
7.4 Satellite Control Configuration and Conclusion.....	63
8 Electrical Power Sub-System.....	66
8.1 Introduction	66
8.2 Calculation of Eclipse time for the mission	68
8.3 Battery Sizing	69
8.4 Solar Array Sizing.....	71
8.5 Electrical Power System Conclusion	73
9 Communications and On-Board Data Handling Sub-System	74
9.1 Introduction	74
9.2 Link Budget.....	74
9.3 OBDH and Flight Software Architecture	76
9.4 Communications Architecture for our Mission and conclusion	76
10 Thermal Sub-System	79
10.1 Introduction	79
10.2 Selection of Multilayer Insulation.....	79
10.3 Preliminary Thermal Analysis.....	80
11 Structures Sub-System	84
11.1 Introduction	84
11.2 Orientation of Payloads within the Spacecraft	84
11.3 Material Selection	85
11.4 Critique and Final Satellite Configuration	86
12 Mining Operations Sub-System	89
12.1 Introduction to different Mining Operational techniques used in Space.....	89
12.2 Alternative Mining Architecture Concepts and Critique.....	89
12.3 Critique of the Feasibility of Selected mining Technique	90

13 Space Environmental Analysis	91
13.1 Introduction to Characteristics of Space Environment and its implications.....	91
14 Budgets	95
14.1 Mass Budget.....	95
15 Conclusion and Future Work	96
APPENDIX A.....	99
APPENDIX B.....	100
APPENDIX C.....	103
APPENDIX D.....	116
References	118

List of Figures

Figure 1. 1- The figure shows the Work Breakdown structure for the project	5
Figure 2. 1-The figure spacecraft module for OSIRIS-Rex [9] [8].....	10
Figure 2. 2- The figure shows the operational timeline of OSIRIS-Rex [9] [8].....	11
Figure 2. 3- The figure shows the mission orbits for the OSIRIS-Rex mission [8] [9]	12
Figure 2. 4 - The figure shows the operational architecture for the OSIRIS-Rex mission [8] [9]	12
Figure 2. 5- The figure shows the spacecraft module for the Hayabusa Mission [14] [15]....	13
Figure 2. 6- The figure shows the Hayabusa operational mission details [13] [12]	15
Figure 2. 7- The figure shows the Hayabusa mission orbits [13].....	15
Figure 2. 8- The figure shows the system architectural elements derived from literature	16
Figure 4. 1- The figure shows the Orbital properties of 1989ML from NASA SSD	27
Figure 4. 2- The figure shows the orbital ephemeris position of 1989ML with respect to Earth and other planets.....	27
Figure 4. 3- The figure shows the asteroid environment data.....	28
Figure 4. 4- The figure shows the pork-chop plot for the launch window 2027 to 2030.....	28
Figure 4. 5- The figure shows the different launch opportunities and preliminary ΔV calculations for 2027 to 2030	29
Figure 4. 6- The figure shows the different launch opportunities and preliminary ΔV calculations for 2027 to 2030	29
Figure 4. 7- The figure shows the different Lift-Off mass capabilities by launchers for the launch window from 2027 to 2030.....	30
Figure 4. 8- The figure shows the different Lift-Off mass capabilities by launchers for the launch window from 2027 to 2030.....	30
Figure 4. 9- The figure shows the orbital diagram for the direct transfer to Asteroid rendezvous found using the NASA SSD tool.....	31
Figure 4. 10- The figure shows the range of Lift-Off mass for Delta 4 Heavy launcher	31
Figure 4. 11- The figure shows the range of Lift-Off mass for Falcon heavy launcher	32
Figure 4. 12- The figure shows the range of Lift-Off mass for SLS Block 1 launcher	32
Figure 5. 1- The figure shows the different Mission Architectures that are considered for the Mission	33
Figure 5. 2- The figure shows the Fly-By approach angle for a planet.....	37
Figure 5. 3- The figure shows the interplanetary transfer of the Spacecraft using a hyperbolic trajectory from Earth Departure to Mars Approach.....	46
Figure 5. 4- The figure shows the Martian Fly-By of the Spacecraft which then takes a hyperbolic trajectory to the asteroid 1989ML from Mars departure to Asteroid Approach	46
Figure 5. 5- The figure shows the Inter-Asteroid phase i.e. Proximity Operations performed by spacecraft (Mapping manoeuvres).....	47
Figure 5. 6- The figure shows the interplanetary phase of the spacecraft which takes a hyperbolic trajectory from Asteroid departure to Earth Arrival	47
Figure 5. 7- The figure shows the overview of the mission timeline.....	47
Figure 5. 8- The figure shows the orbit diagram for the mission.....	48
Figure 5. 9- The figure shows the plot between ΔV and the flyby altitude to find the optimal flyby altitude	49
Figure 6. 1- The figure shows the plot for Fuel mass vs Number of Stages.....	55
Figure 6. 2- The figure shows the different stages for the mission.....	58
Figure 6. 3- The figure shows the Propulsion system and its components for the mission....	58

Figure 7. 1- The figure shows the AOCS configuration for the spacecraft.....	64
Figure 8. 1- The figure shows the architecture elements of EPS	66
Figure 8. 2- The figure shows the power distribution between different sub-systems	72
Figure 8. 3- The figure shows the power system configuration for the mission	73
Figure 9. 1- The figure shows the final Communication configuration for the mission.....	78
Figure 10. 1- The figure shows the Asteroid albedo directions on the spacecraft	82
Figure 10. 2- The figure shows the Earth albedo directions on the spacecraft	83
Figure 11. 1- The figure shows the different materials considered for the spacecraft	85
Figure 11. 2- Placement of payloads and tanks within the spacecraft configuration.....	87
Figure 11. 3- Image to compare the size of spacecraft with a reference standard Indian human of average height of 1.65m.....	87
Figure 11. 4- The figure shows the rendered spacecraft module for the mission (Nadir/Earth pointing)	88
Figure 11. 5- The figure shows the rendered spacecraft module for the mission (Sun pointing; De-orbiting operations).....	88
Figure 12. 1- The figure shows the different mining operational architectures.....	89
Figure 13. 1- The figure shows how space environment affects the spacecraft	91
Figure A. 1- The figure shows the logo created for the internship batch 4	99
Figure A. 2- The figure shows the different team members for the IPS batch 4 of the internship	99
Figure B. 1- The figure shows the orbits for our mission	102
Figure C. 1- Mission scenario 1	103
Figure C. 2- Mission Scenario 2.....	105
Figure C. 3- Mission scenario 3	106
Figure C. 4 – Mission Architecture Scenario 4	108
Figure C. 5 – Mission Architecture Scenario 5	111
Figure C. 6 - Mission Architecture Scenario 6	113
Figure D. 1- Mission lifetime	116

List of Tables

Table 1. 1- The table shows the team individual responsible the WPs for the project.....	5
Table 2. 1- The table shows the previously flown Asteroid missions and their status	7
Table 2. 2- The table shows the previously flown Asteroid sample return missions	9
Table 4. 1- The table shows rating system for Composition of Asteroid	19
Table 4. 2- The table shows rating system of the size of Asteroid	20
Table 4. 3- The table shows the rating system for the preliminary ΔV for the mission.....	20
Table 4. 4- The table shows the rating system for the inclination of the asteroid wrt Earth ecliptic plane	21
Table 4. 5- The table shows the prioritisation matrix of Trade Pass 1.....	22
Table 4. 6- The table shows the normalisation matrix for Pass 1	23
Table 4. 7- The table shows the trade table for Pass 2.....	24
Table 4. 8- The table shows the normalisation matrix for Pass 2.....	24
Table 4. 9- The table shows the trade table for Final pass.....	25
Table 4. 10- The table shows the normalisation matrix for Final pass.....	25
Table 4. 11- The table shows the Trade table with correct value of size of 1989ML	26
Table 4. 12- The table shows the normalisation matrix for the correct value of size of 1989ML	26
Table 5. 1- The table shows the ΔV calculation for the Mission using patched conics	38
Table 5. 2- The table shows the ΔV calculation for the Mission using patched conics	39
Table 5. 3- The table shows the ΔV calculation for proximity operations	41
Table 5. 4- The table shows the number of passes required for proximity operations for NAC	41
Table 5. 5- The table shows the number of passes required for proximity operations for WAC	41
Table 5. 6- The table shows the total number of passes for proximity operations for the mission.....	41
Table 5. 7- The table shows the ΔV requirements for different parking orbits.....	41
Table 5. 8- The table shows the ΔV requirements for proximity operations.....	42
Table 5. 9- The table shows the ΔV expendable in each phase.....	42
Table 5. 10- The table shows the operational elements for our mission [8] [9]	43
Table 5. 11- The table shows the operational modes of sub-systems for different phases of the mission	45
Table 5. 12- The table shows the ΔV for different fly-by altitudes	48
Table 5. 13- The table shows the optimal flyby altitude	49
Table 6. 1- The table shows preliminary fuel calculations for Asteroid rendezvous	53
Table 6. 2- The table shows preliminary fuel calculations for Earth rendezvous	54
Table 6. 3- The table shows the fuel calculations for different stage separations	54
Table 6. 4- The table shows the Total fuel required for the entire mission	55
Table 6. 5- The table shows the Calculation of Fuel and oxidiser mass for the mission	56
Table 6. 6- The table shows the mass of Helium pressurant required for the mission	57
Table 6. 7- The table shows the Effective ISP and Net Thrust required for the mission	59
Table 7. 1- The table shows the different stabilisation methods considered for the Asteroid phase of the mission.....	61
Table 7. 2- The table shows the different stabilisation methods considered for interplanetary phase of mission.....	61

Table 7. 3- The table shows the final AOCS configuration for mission for Asteroid phase of mission.....	63
Table 7. 4- The table shows the Work Breakdown structure for the project for interplanetary phase of mission.....	63
Table 7. 5- The table shows the preliminary selection of thrusters for the mission	64
Table 8. 1- The table shows the different options for power generation for spacecrafts [21]	66
Table 8. 2- The table shows the trade table for different power generation for spacecrafts ..	67
Table 8.3- The table shows the different selection of batteries considered for the mission [21]	68
Table 8. 4- The table shows the eclipse calculation for the spacecraft at 10 km parking orbit from the Asteroid	69
Table 8. 5- The table shows the eclipse calculation for the spacecraft around a 10000 km parking orbit around Earth	69
Table 8. 6- The table shows the battery mass calculation for the mission.....	71
Table 8.7-The table shows the different types of solar cell types considered for the mission [21].....	71
Table 8. 8- The table shows the solar array sizing for the mission	72
Table 9. 1- The table shows the link margin calculations for the mission	75
Table 10. 1- The table shows the operating temperature ranges for different subsystem components.....	80
Table 10. 2- The table shows the thermal equilibrium temperature on the spacecraft around the asteroid for different surface finishes.	83
Table 10. 3- The table shows the thermal equilibrium temperature on the spacecraft around Earth for different surface finishes.....	83
Table 13. 1- The table details how space environment affects the spacecraft.....	92
Table 13. 2- The table shows how GCR and SEPs affect the spacecraft.....	93
Table 14. 1- The table shows the Mass budget for the mission	95
Table C. 1- ΔV Calculation for Mission Scenario 1 using Hohmann Transfer	103
Table C. 2- ΔV Calculation for Mission Scenario 1 using Patched Conics.....	104
Table C. 3- ΔV Calculation for Mission Scenario 2	105
Table C. 4- ΔV Calculation for Mission Scenario 3	107
Table C. 5- ΔV Calculation for Mission Scenario 4	108
Table C. 6- Optimised ΔV Calculation for Mission Scenario 4	110
Table C. 7- ΔV Calculations for Mission Scenario 5	111
Table C. 8 - ΔV Calculations for Mission Scenario 6	113
Table D. 1- Time of flight calculations for the mission.....	116

List of Equations

Equation 5. 1	34
Equation 5. 2	34
Equation 5. 3	34
Equation 5. 4	35
Equation 5. 5	35
Equation 5. 6	35
Equation 5. 7	35
Equation 5. 8	35
Equation 5. 9	35
Equation 5. 10	35
Equation 5. 11	36
Equation 5. 12	36
Equation 5. 13	36
Equation 5. 14	36
Equation 5. 15	36
Equation 5. 16	36
Equation 5. 17	36
Equation 5. 18	36
Equation 5. 19	37
Equation 5. 20	37
Equation 5. 21	40
Equation 5. 22	40
Equation 5. 23	40
Equation 5. 24	40
Equation 5. 25	40
Equation 6. 1	52
Equation 6. 2	52
Equation 6. 3	53
Equation 6. 4	53
Equation 6. 5	55
Equation 6. 6	55
Equation 6. 7	56
Equation 6. 8	56
Equation 6. 9	56
Equation 6. 10	56
Equation 6. 11	57
Equation 6. 12	57
Equation 8. 1	68
Equation 8. 2	68
Equation 8. 3	68
Equation 8. 4	68
Equation 8. 5	70
Equation 8. 6	70
Equation 8. 7	70
Equation 8. 8	72

Equation 8. 9.....	72
Equation 8. 10.....	72
Equation 8. 11.....	72
Equation 9. 1	74
Equation 9. 2	74
Equation 10. 1.....	81
Equation 10. 2.....	81
Equation 10. 3.....	81
Equation 10. 4.....	82
Equation 10. 5.....	82
Equation 10. 6.....	82
Equation 10. 7	82
Equation 10. 8.....	82

1 Introduction

It is not unknown that the once easily accessible minerals on planet Earth are depleting. The more expansive humanity is the more resources we need to sustain. Demand for minerals especially metals has increased dramatically over the last few years. The cost of extraction of minerals has greatly increased due to the decrease in ore grade quality [1] [2] [3] [4]. This forces us to look for other techniques and places to source the minerals as the current mining industry is becoming highly unsustainable leading to a myriad of problems such as [2] [3]:

- a) Production of highly toxic waste as a by-product of ore extraction
- b) Soil erosion due to deeper mines
- c) Ground water contamination due to acidic mine drainage
- d) Excessive energy consumption
- e) Loss of habitat and forest coverage

All these factors are proving detrimental to the home we can Earth due to severe ecological impacts. Hence, Mining in space seems to be the only step –forward to continue the technological progress and to restore the ecological balance on the planet.

Asteroid Mining can help in the following ways [3]:

- a) Expanding the presence and technology of Humanity by developing technologies capable of mining in low gravity conditions and the systems necessary to support that which potentially down the line could greatly help in colonization efforts of other planetary bodies like Mars
- b) Mining opportunities of valuable metals such as Platinum, which is expensive on Earth due to its scarcity but abundant on Asteroids [4] which could lead to a global technology renaissance.
- c) Raw material for future in-orbit fuelling stations for interplanetary and solar system exploration
- d) A positive environmental impact due to better technology and reduction in fossil fuel dependency
- e) Asteroid Mining throughput or return will be much greater than the investment cost of technology readiness.

Due to the critique and advantages mentioned above, this report explores the feasibility of a mining mission to a Near Earth asteroid with a resource return of 500 kg. Standard systems engineering principles are used to justify the design process and to explore a realistic mission analysis that allows Asteroid mining using current technology methods for a launch within the next decade.

1.1 Aims and Objectives for the Asteroid Resource Return Mission

Primary Objectives:

- Mining of 500 kg regolith ore of a Near Earth Asteroid and resource return to LEO with a launch window from 2027 to 2030

Secondary Objectives:

- Demonstration of the viability of mining an Asteroid
- Collection of Vital Data of Asteroid characteristics and mining feasibility

Political Objectives:

Being the 'first' stakeholder to mine asteroids to make up for the deficit on Earth and to serve as a framework for future mining missions.

1.2 Decomposition of Report Structure

Chapter 1 - Introduction: This section includes the introduction to Asteroid Mining and the missions that have flown to Near-Earth Asteroid and have planned for a sample return. This section also details the aims and objectives of the project. It includes how the project was managed, including the tools used by the team to track the progress, communicate and manage the documentation. It also, details the work package structure and finally, the challenges faced during the project and how it was resolved. Chapter 1 is captured by the team leader- Akanksha Maskeri.

Chapter 2 - Literature Review: This section includes the literature review of Near Earth Asteroid Missions and takes a closer look at Asteroid missions with sample return such as OSIRIS-REX and Hayabusa 1 and 2. The output of these missions establishes a framework for our project. Chapter 2 is captured by Team member- Lalithej Vyasam with inputs from the Team.

Chapter 3 - Requirements: This section discusses the requirements for the mission, including the scope of the mission and the depth into which it was feasible given the time and human resource limitations of the GDP. It discusses the critical requirements and how these were derived. Key mission drivers that had a large impact on the design solution and final design are addressed. Chapter 3 is captured by the team leader - Akanksha Maskeri.

Chapter 4 - Selection of Target asteroid: This section includes discussion on the selection criteria for the target asteroid and critiques the trade considerations for the final asteroid selection. Chapter 4 is captured by the team leader - Akanksha Maskeri with inputs from the Team.

Chapter 5 - Mission Analysis: This section includes definition and trade of mission concept architectures. Calculation of the ΔV requirements for the mission and various proximity operations. This section also includes discussion on orbital selection and mission analysis. Chapter 5 is captured by the team leader - Akanksha Maskeri with inputs from self and Team Member- Lalithej Vyasam.

Chapter 6 - Propulsion: This Section includes selection and trade of a Propulsion system suitable for the mission. It includes propellant budgeting, Lift-Off mass estimation for the mission and selection of launch vehicle based on the lift-off mass. PMD and pressurant tanks are also designed and a top-level feedline system architecture is developed. Chapter 6 is captured by the team leader - Akanksha Maskeri with inputs from self.

Chapter 7 – AOCS: This Section includes the definition of different satellite modes during different phases of the mission. Slew rates and de-tumbling rates and aerodynamic drag, solar radiation and gravity effects on torque of the satellite are calculated. Chapter 7 is captured by the Team Members - Abhijeeth Someshwar and Assistant team leader - Srinithya Nerella.

Chapter 8 – Electrical: This Section includes capturing power requirements of different sub-systems and calculation of various eclipse times that have a high constraint on the Spacecraft. Trade is performed to find the battery and Solar cells. Battery and solar array sizing is included. Chapter 8 is captured by the Team Members - Ria Matthew and Akash C.

Chapter 9 - Communications and OBDH: This Section includes the calculation of link budget required for nominal data transmission for the payloads using the Deep Space network by NASA and other high gain antennas. It includes the trade and configuration of the Communication sub-system and also touches upon the OBDH equipment required .Chapter 9 is captured by the Team Member - Kallu Sudarshan.

Chapter 10 –Thermal: This section includes the calculation of equilibrium temperatures of the spacecraft and Passive thermal control material selection and critique. Chapter 10 is captured by the Team Member - Kuljeet Kaur with inputs from self and team leader Akanksha Maskeri.

Chapter 11 - Structures: This section includes discussion of different materials used for spacecraft bus and structure. It includes orientation of different payloads within the spacecraft framework in compliance with the launcher fairing. Chapter 11 is captured by the Team Members – Malavika D S and Arun Pradeep.

Chapter 12 - Mining Operations: This section includes discussion and critique of different mining operational architecture and selection of mining method. Chapter 12 is captured by the Team Member – Keerthana Balakrishnan with inputs from team leader - Akanksha Maskeri and Team Member- Lalithej Vyasam and previous SSERD intern group – ‘Team Vulcans’ [5]

Chapter 13 - Space Environment: This section discusses the challenges faced by the spacecraft during interplanetary travel, the radiation and thermal constraints to which the spacecraft is exposed to. Chapter 13 is captured by Assistant team leader - Srinithya Nerella and Team Member – Spandana Chilukuri.

Chapter 14 – Mass Budget: This section captures the overall Mass budget of the spacecraft and its payloads. Chapter 14 is captured by the team leader - Akanksha Maskeri with inputs from the Team.

Chapter 15 - Conclusion and Future Work: This section discusses the outcomes of the project and the future work required to advance the project further. Chapter 16 is captured by team leader - Akanksha Maskeri with inputs from the Team.

1.3 Project Management

1.3.1 Project Management Role

The size of the project called for a dedicated project management work package. The role of the team leader had the responsibility of ensuring that the project ran smoothly and efficiently on a day to day basis considering the limited time constraints of 6 weeks. Day to day responsibilities included but not limited to:

- Setting deadlines for the group tasks including presentations, design output deadlines.
- Organising weekly internal meetings for the group and setting a time that was convenient for most all the members.
- Acting as appoint of contact via official channels i.e. Lyra if the members were unable to attend the meetings
- Managing the Chair and Secretary ROTA for official meetings and deciding to have a rotating system for Chairs and Secretaries of the meetings to give everyone equal opportunities to gain experience in those areas.
- To ensure smooth communication between all project members and to resolve any conflict within the project.
- The team leader was responsible for making a collective presentation for meetings with the mentors Rashika and Vishnuvardhan Shaktibala and for weekly general

meetings for SSERD. This role was taken up by other members of the group if the team leader wasn't available.

- The Final presentation for the internship review was the responsibility of the team leader to ensure the information provided by the team was consistent and had a good flow for a space mission design project.
- Constant communication when possible was kept with all team members to have a clear overview of all the sub-systems.

1.3.2 Project Timeline

The initial information given was the problem statement by SSERD and the mentors. The scope of the project was uncertain and it was upon the team to decide. The WBS was decided by the team leader and the mentors which was altered to meet the needs of the project.

The first 3 weeks were taken up by the 'project definition phase' where the establishment of project structure and the person in-charge was decided. The main focus was to decide the Target Asteroid for the project and this was done by extensive research on previous Asteroid Missions discussed in section 5 and trade study conducted which is discussed in Section 4. Once the Target Asteroid was selected and preliminary mission ΔV was found using Online Mission Analysis Tool by NASA SSD, the 'design phase' was started. The 5 week mark of the project concluded the design phase and the last week was utilised to document the project deliverables and the report review presentation. The end of the design phase was set a week before the submission of the project as to give everyone sufficient time to write their report and finalise their design without having to constantly update details due to an evolving design.

1.3.3 Project Management Tools

To effectively manage the team and the project, a number of tools were decided upon by SSERD. Lyra or Rocket Chat was used as a means of communication between all members of the team, the mentors and co-ordinators- Anisha and Prateek B. To share and upload relevant documents, reports and files, the Yandex platform was used. Since, the internship was an online internship all meetings and presentations were held using the Lyra online platform. Some informal ice-breaker sessions were held on Google Teams and Zoom. Google drive was used to share 'active' documents that multiple people could work on concurrently as Yandex did not have that capability.

1.3.4 Work Breakdown Structure

The WBS in Figure 1.1 gives an overview of the top-level work packages for this specific mission. The WBS is divided into 3 distinct sections i.e. Systems Engineering, Interplanetary and Asteroid Phase. Work packages were chosen based on the Team members' preference and workload capacity that they can handle as shown in Table 1.1. Majority of the workload was taken up by the team leader - Akanksha Maskeri handling Systems Engineering, Project management, Mission Analysis and Propulsion. Once, the final WBS structure was agreed upon it was re-checked to ensure that all members were happy with the WPs that they would be working on.

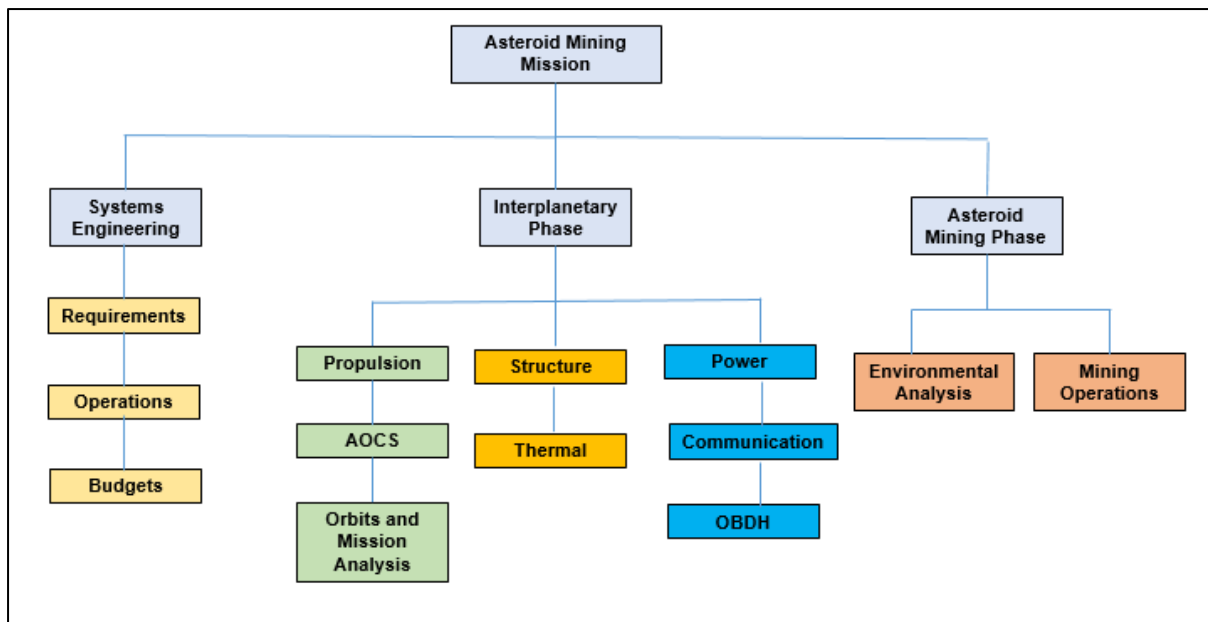


Figure 1. 1- The figure shows the Work Breakdown structure for the project

Table 1. 1- The table shows the team individual responsible the WPs for the project

Orbits	Lalithej Vyasam Akanksha Maskeri
Propulsion	Akanksha Maskeri
AOCS	Someshwar Abhijeeth Srinithya Nerella
Structures	Arun Pradeep Malavika D S
Thermal	Kuljeet Kaur
Power	Ria Matthews Akash C
Communication and OBDH	Kallu Sudarshan
Mining	Keerthana Balakrishnan
Environmental Analysis	Srinithya Nerella Spandana Chilukuri

1.3.5 Management Challenges

As with any project there were a number of times when unforeseen problems occurred and had to be dealt with. Due to the way the work packages were split the team leader had a number of technical roles in addition to management. As a result of this the technical parts of the project would come at a temporary price of keeping management tools up to date, simply due to the tight schedule that had to be set in order to meet deadlines. However, even with this measure implemented Yandex was not used to its full potential due to the reasons mentioned above and partly because members weren't encouraged enough to keep up to date with tasks on Yandex.

In order to make sure deliverables were met in time, deadlines were set with a considerable margin of a few days to make leeway where possible. Important deadline reminders were given via Lyra when relevant. It was necessary in some cases to message people on an individual basis to ensure relevant work was completed, both via official channels using the co-ordinators and secondary channels where response was not given via primary channel.

In a few cases where the crucial work was simply not completed for when it was needed it was necessary for other to complete the work instead. Individual meetings were held between the team leader and the respective parties involved in those cases to explain that such a situation will not occur again and in these cases the Co-ordinators and the mentors to ensure the project was not at a threat. There were occasions in particular, near the start and the end where certain individuals would not attend official and unofficial meetings. In order to minimize the impact of this on the project, the individuals were contacted through secondary channels and brought up to speed on what they had missed and what was expected of them. The co-ordinators were kept informed and would be resolved through official channels of SSERD.

At the 4th week mark of the internship, through the on-going design phase it was discovered that one of the sources used as the basis for the size of the target asteroid was misunderstood and therefore a significant part of the trade would be affected, changing the target asteroid and eventually the preliminary ΔV for the mission which would snow-ball into all other sub-system design. This knock-out effect would change the entire design process and hence it was acknowledged that it would be best to carry on with the current Target Asteroid. Similarly, the mining concept for the mission was chosen as a single spacecraft operation from the start of the internship without a trade study and it was later found that the Mother-daughter Spacecraft operation would be more favourable and suited for Asteroid Mining due to low failure modes. This change in operational mode would impact the overall design of the mission as considerations needed to be taken for all sub-systems and the biggest constraints then would be on mass, power and ΔV budgets. Hence, a top-level decision was taken not to change the mining operations acknowledging the risks that comes with it.

Environmental Factors such as Rain, Poor connectivity and Cyclones played a large role in the overall timely deliverables, an executive decision was made to extend the deadline by a week in interest of all the members involved so that they got enough time to finish their deliverables and document their work. The extension also gave time to re-check the sub-system budgets and it was found that the power sub-system was using the wrong eclipse times and this put a heavy constraint on the solar array size and battery mass which made the mission un-feasible. The team leader re-calculated the eclipse time and the battery mass and solar array size was corrected. A decision was made to make the change to these baseline budgets as they heavily constrained the placement of payloads fit within the payload fairing dimensions of the launcher within acceptable ranges.

2 Literature Review

2.1 Literature Review of previously flown Near Earth Asteroid Missions

There have been a few missions that enabled spacecrafts to collect samples from the asteroids and return to earth. Over the years, NASA, JAXA and other space agencies have targeted many asteroids in their spacecraft missions. Some of these missions were designed specifically to learn more about the physical characteristics of asteroids and comets while others were able to view and analyse asteroids on their way to other planetary destinations.

Table 2. 1- The table shows the previously flown Asteroid missions and their status

Target Body	Event		Mission Details		
	type	date	name	launch	status
16 Psyche	arrival	2026	Psyche	2022	pre-launch
101955 Bennu	sample-return	2023	OSIRIS-REx	2016-Sep-08	cruise
101955 Bennu	departure	2021-Aug	OSIRIS-REx	2016-Sep-08	cruise
162173 Ryugu	sample-return	2020-Dec	Hayabusa2	2014-Dec-03	cruise
162173 Ryugu	departure	2019-Dec	Hayabusa2	2014-Dec-03	cruise
101955 Bennu	arrival	2018-Aug	OSIRIS-REx	2016-Sep-08	cruise
162173 Ryugu	arrival	2018-Jun	Hayabusa2	2014-Dec-03	cruise
1 Ceres	arrival	2015-Mar	Dawn	2007-Sep-27	cruise
67P	landing	2014-Nov	Rosetta	2004-Mar-02	complete
67P	rendezvous	2014-Aug	Rosetta	2004-Mar-02	complete
4 Vesta	departure	2012-Aug	Dawn	2007-Sep-27	cruise
9P/Tempel 1	fly-by	2011-Feb-14	Stardust-NExT	1999-Feb-06	complete
103P/Hartley 2	fly-by	2010-Nov-04	EPOXI	2005-Jan-12	complete
21 Lutetia	fly-by	2010-Jul-10	Rosetta	2004-Mar-02	complete
25143 Itokawa	sample-return	2010-Jun-13	Hayabusa	2003-May-09	complete
2867 Steins	fly-by	2008-Sep-05	Rosetta	2004-Mar-02	complete
25143 Itokawa	departure	2007-Apr-25	Hayabusa	2003-May-09	complete
81P/Wild 2	sample-return	2006-Jan-15	Stardust	1999-Feb-06	complete
25143 Itokawa	arrival	2005-Sep-12	Hayabusa	2003-May-09	complete
9P/Tempel 1	impact/fly-by	2005-Jul-04	Deep Impact	2005-Jan-12	complete
81P/Wild 2	fly-by	2004-Jan-02	Stardust	1999-Feb-06	complete
5535 Annefrank	fly-by	2002-Nov-02	Stardust	1999-Feb-06	complete
19P/Borrelly	fly-by	2001-Sep-22	Deep Space 1	1998-Oct-24	complete
433 Eros	rendezvous	2000-Feb-14	NEAR	1996-Feb-17	complete
9969 Braille	fly-by	1999-Jun-28	Deep Space 1	1998-Oct-24	complete
253 Mathilde	fly-by	1997-Jun-27	NEAR	1996-Feb-17	complete
243 Ida	fly-by	1993-Aug-28	Galileo	1989-Oct-18	complete
951 Gaspra	fly-by	1991-Oct-29	Galileo	1989-Oct-18	complete
1P/Halley	fly-by	1986-Mar-14	Giotto	1985-Jul-02	complete
1P/Halley	fly-by	1986-Mar-11	Sakigake	1985-Jan-07	complete
1P/Halley	fly-by	1986-Mar-09	Vega 2	1984-Dec-21	complete
1P/Halley	fly-by	1986-Mar-08	Suisei	1985-Aug-18	complete
1P/Halley	fly-by	1986-Mar-06	Vega 1	1984-Dec-15	complete
21P	fly-by	1985-Sep-11	ISEE 3/ICE	1978-Aug-12	complete

Table 2.1 contains the list of all the asteroid related missions in chronological order. Based on the mission criteria, the asteroid missions are classified into flyby and rendezvous missions.

Flyby missions involve viewing and analysing the asteroid without a full scale interaction. These missions are usually served as an additional objective(s) for a different larger missions. A good example of such mission can be the Galileo mission in which the spacecraft flew by the asteroids 243 Ida and 951 Gaspra during its voyage to the Jupiter.

Rendezvous missions, on the other hand usually serve as the primary purpose in the asteroid missions. These missions are designed to reach the asteroid and interact with them even for a short period of time. Rendezvous missions can either involve the spacecraft

to orbit around the asteroid or landing missions as well. An example of such mission is the Rosetta mission which landed on the 67P/Churyumov-Gerasimenko asteroid.

Apart from the technical feasibility of these missions, it is also equally important to address the techno-economic feasibility of said missions. For instance, a techno economic feasibility of said missions has been carried out by Heina et al. (2018) [6] for mining asteroids for platinum and water considering many economic factors for the next decade.

The economic feasibility of asteroid mining, focusing on supplying water in space and returning platinum to earth under ideal conditions for determining lower bounds and tendencies is extensively studied. Sonter et al. (2012) [7] found that from a profitability perspective, the throughput rate and using smaller but multiple spacecraft per mission are key technical parameters for reaching break-even quickly.

Hence, the development of efficient mining processes and developing small spacecraft that are mass-produced seem to be key to economic viability, ignoring additional cost factors for reuse, and without taking in-space manufacturing into consideration. In the context of asteroid mining, sample return missions, which are in turn part of the rendezvous missions, play a pivotal role in the framework of such missions which will be discussed in the next section.

2.2 Literature Review of previously flown Near Earth Asteroid Missions that have a sample return

Sample-return missions usually bring back merely particles or a deposit of complex compounds such as sand and loose rocky material known as regolith. These samples may be obtained in a number of ways, some of which include soil and rock excavation or a collector array used for capturing particles of solar wind or the debris of comets.

To date, many samples of lunar rocks have been collected by robotic and crewed missions, the comet Wild 2 and the asteroids 25143 Itokawa and 101955 Bennu have been visited by robotic space crafts which returned samples to Earth, and samples of the solar winds have been returned by the robotic Genesis mission.

In addition to these, few missions like Hayabusa 2 and Psyche have been proposed to visit asteroids Ryugu and 16 Psyche respectively and collect samples from these bodies and send them back to Earth. In addition to these missions, a Mars Sample-Return (MSR) initiative has been proposed by NASA and ESA to collect rock and dust samples on Mars and then return them to Earth.

Sample collection necessarily does not include sample return missions. Some of the samples of extra-terrestrial bodies have been collected through various meteorites. Samples from a few identified non-terrestrial bodies have been collected by means other than sample-return missions. For instance, the samples from the Moon in the form of Lunar meteorites, samples from Mars in the form of Martian meteorites, and samples from Vesta in the form of Howardite-Eucrite-Diogenite (HED) meteorites.

However, the context of this research is limited to robotic sample return missions that are capable of autonomously collecting and sending the samples of the bodies back to the Earth. The following section contains the list of sample return missions, both ongoing and completed, in the context of small bodies like asteroids and comets.

Table 2. 2- The table shows the previously flown Asteroid sample return missions

Mission	Primary Objectives	Mission Firsts
OSIRIS Rex	1. Bennu Sample return and Analysis	First sample return mission
	2. Resource Identification	
	3. Comparison of asteroid data to ground-based observations	
NEAR	1. Orbit around 433 Eros	First orbit around an asteroid
	2. Soft landing on the asteroid	First landing on asteroid (Unplanned)
	3. Analysis of compositional details of Eros	
	4. Analysis of Mathilde during Flyby	
Stardust	1. Comet Rendezvous Asteroid Flyby	First observation of C-Type asteroid
	2. non-destructive capture of comet dust	Non destructive sample collection
	3. flyby of Wild 2 under low velocities	First Comet Impactor mission
Hayabusa2	1. Research on planetary evolution	
	2. Research on material evolution in the solar system	Exploration of C-type asteroid
	3. Demonstration of technology of deep space sample return exploration	Asteroid Impactor Rendezvous
	4. Demonstration of impactor technology	
Hayabusa	1. Deliver Pristine samples to Earth	Sample Return First Attempt
	2. Demonstration of fully autonomous exploration equipped with MINERVA	First craft designed to make physical contact with the surface of an asteroid
	3. Test Technologies of Ion Engine and deep space communication under low gravity	First landing on an asteroid (planned)

Table 2.2 provides a summary of a chronological order of asteroid landing and sample return missions including their objectives and their accomplishments and mission firsts. Apart from a general literature survey of Sample Return Missions, a more detailed survey of two missions OSIRIS-REx and Hayabusa is provided in the subsequent sections.

2.3 Literature Review of Key System Architecture Elements of OSIRIS-REX

OSIRIS-REx is the first NASA mission to return a sample of an asteroid to Earth [8] [9]. Navigation and flight dynamics for the mission to acquire and return a sample of 101955 Bennu asteroid establish many firsts for space exploration. These include relatively small orbital manoeuvres that are precise to 1 mm/s, close-up operations in a captured orbit about an asteroid that is small in size and mass, and planning and orbit phasing to revisit the same spot on Bennu in similar lighting conditions.

After preliminary surveys and close approach flyovers of Bennu, the sample site is scientifically characterized and selected. A robotic shock-absorbing arm with an attached sample collection head mounted on the main spacecraft bus acquires the sample, requiring navigation to Bennu's surface. A touch-and-go sample acquisition manoeuvre (TAGSAM) resulted in the retrieval of up to 1.4 kilograms of regolith. The flight activity concludes with a return cruise to Earth and delivery of the sample return capsule (SRC) for landing and sample recovery at the Utah Test and Training Range (UTTR).

The spacecraft (Lauretta (2017)) [10] consists of aluminium honeycomb structure sandwiched between graphite composite face sheets. The core of the structure is a 1.3-meter diameter cylinder that encloses the propellant tank of the spacecraft. Two decks, the forward and aft deck, are installed on the top and bottom of the central cylinder with the upper panel supporting the Sample Acquisition and Return Assembly (SARA), the science instruments, navigation equipment, and antennas. The deck houses the batteries, medium gain antenna, reaction wheels, and solar array gimbals. The high-gain antenna is centred on the +X axis of the spacecraft.

The spacecraft, as shown in Figure 2.1 hosts a total of 28 engines divided into four groups: a bank of four high-thrust main engines, six medium-thrust engines, 16 attitude control thrusters, and a pair of specialized low-thrust engines. All thrusters installed on the spacecraft are fed from a central propellant tank holding the hydrazine supply needed for the mission.

The spacecraft has solar panels affixed to the aft deck of the spacecraft. Covered with gallium-arsenide solar cells, the arrays deliver between 1,226 and 2,500 watts of electrical power depending on the spacecraft's distance from the sun, which varies over the course of the seven-year mission. The solar arrays are attached to the spacecraft structure with two-axis gimbals, allowing the arrays to be moved into a range of configurations depending on the mission phase.

The main purpose of the TAGCAMS suite of imagers is to aid in navigation around Bennu. They will also contribute significantly to the photo-documentation of Bennu. The purpose of TAGCAMS is to provide imagery during the mission to facilitate navigation to the target asteroid, acquisition of the asteroid sample, and confirmation of sample stowage. The cameras were designed and built by Malin Space Science Systems based on requirements developed by Lockheed Martin and the OSIRIS-REx project. All three of the cameras are mounted to the spacecraft nadir deck and provide images in the visible part of the spectrum, 400–700 nm.

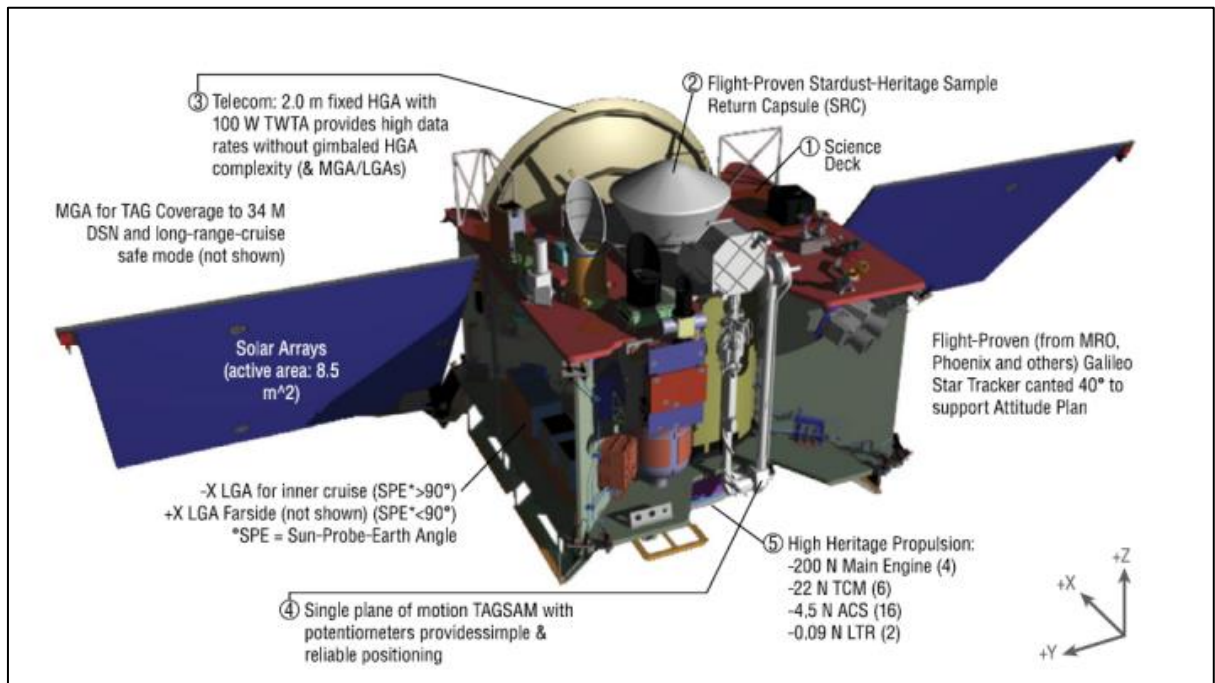


Figure 2. 1-The figure spacecraft module for OSIRIS-Rex [9] [8]

Two of the TAGCAMS cameras, NavCam 1 and NavCam 2, serve as fully redundant navigation cameras to support optical navigation and NFT. Their boresights are approximately aligned in the nadir direction with small angular offsets for operational convenience. The third TAGCAMS camera, StowCam, provides imagery to assist with and confirm proper stowage of the sample. Its boresight is pointed at the SRC located on the spacecraft deck. All three cameras have a 2592×1944 -pixel detector array that can

provide up to 12-bit pixel depth. All three cameras also share the same lens design which produces a camera field of view of roughly $44^\circ \times 32^\circ$ with a pixel scale of 0.28 mrad/pixel. The StowCam lens is focused to image features on the spacecraft deck, while both NavCam lens focus positions are optimized for imaging at infinity.

The timeline of OSIRIS-Rex is provided in Figure 2.2. About 55 minutes after launch on Sept. 8, 2016, from Cape Canaveral, Florida, and after a boost by the Centaur upper stage, OSIRIS-REx separated from its Atlas V rocket and began the deployment of solar arrays. At 17:30 UT Sept. 9, 2016, the spacecraft crossed the orbital path of the Moon at about 386,500 km and later an orbit around the Sun was deployed. On Sept. 19, 2016, the mission team activated all of its scientific instruments and spacecraft's trajectory



Figure 2. 2- The figure shows the operational timeline of OSIRIS-Rex [9] [8]

The spacecraft carries the following thrusters, attitude control system (ACS), the main engine (ME), low thrust reaction engine assembly (LTR) thrusters .This configuration provides significant redundancy for manoeuvres. On Dec. 28, 2016, the spacecraft conducted its first deep-space manoeuvre (DSM-1), firing the main engine to properly position it for an Earth gravity assist (EGA) in late 2017. A second firing, the first to use the spacecraft's attitude control system (ACS) thrusters, on Aug. 25, 2017, further sharpened its trajectory by changing the velocity by about 19 inches (47.9 centimetres) per second. About a month later, on Sept. 22, OSIRIS-REx passed Earth at a range of about 10,710 miles (17,237 kilometres) as part of a gravity-assist manoeuvre that tilted its orbit to match that of Bennu. During the encounter, the spacecraft took several high-resolution pictures of both Earth and the Moon. [11]

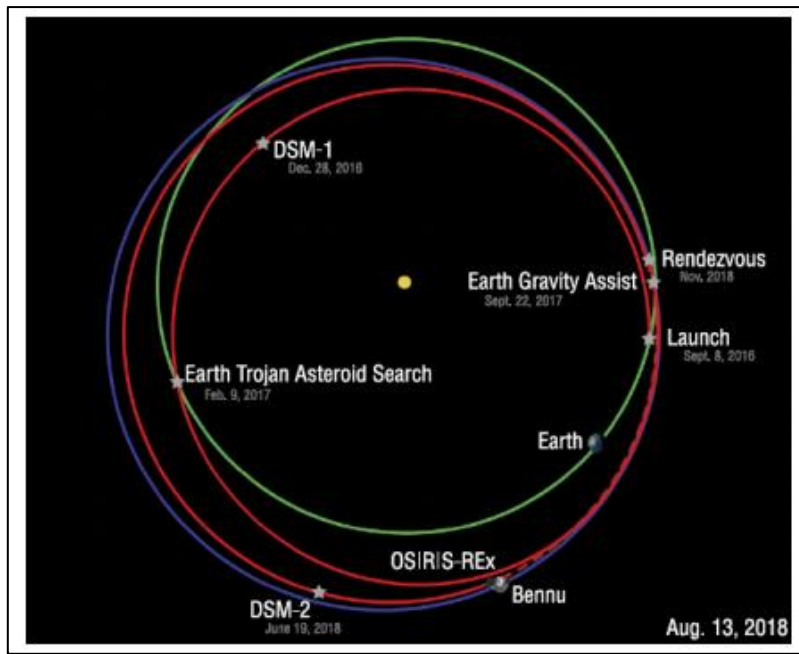


Figure 2. 3- The figure shows the mission orbits for the OSIRIS-Rex mission [8] [9]

The orbit diagram of OSIRIS-Rex is provided in Figure 2.3. The spacecraft got its first glimpse of Bennu in August 2018, sending back a grainy image taken at a distance of about 1.4 million miles (2.3 million kilometres). In early November, OSIRIS-REx sent back detailed images showing the asteroid's shape and some surface features. After arriving at Bennu on Dec. 3, 2018, OSIRIS-Rex carried out proximity operations as provided in figure. 2.4, mapped the asteroid in detail while the mission team searched for a safe sample collection site.

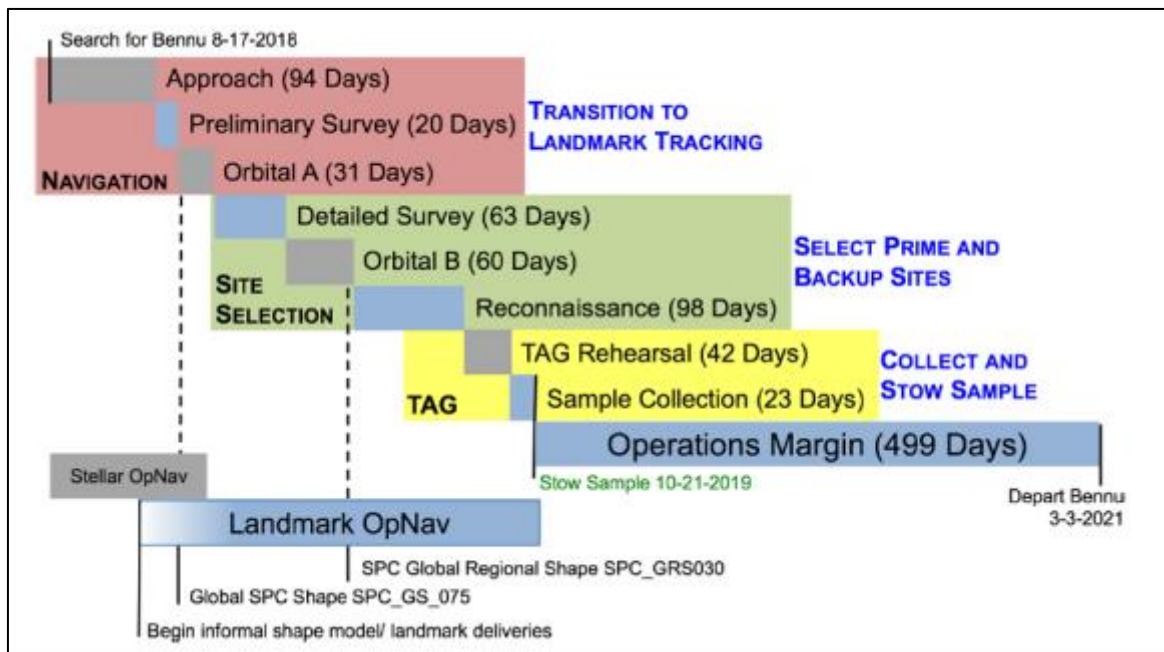


Figure 2. 4 - The figure shows the operational architecture for the OSIRIS-Rex mission [8] [9]

One of the biggest challenges was that Bennu has an extremely rocky surface with hazardous boulders. After a year, the mission team selected a sample site called "Nightingale" located in a northern crater 460 feet (140 meters) wide. The crater is thought to be relatively young, and the regolith, or rocks and dust, is freshly exposed to allow for a pristine sample of the asteroid, giving the team insight into history of Bennu.

2.4 Literature Review of Key System Architecture Elements of Hayabusa

Hayabusa is the sample return mission spacecraft developed by the Japan Aerospace Exploration Agency (JAXA) to return a sample of material from a small near-Earth asteroid named 25143 Itokawa to Earth. Hayabusa, formerly known as MUSES-C a.k.a Mu Space Engineering Spacecraft C, was launched on 9 May 2003 and performed a rendezvous with Itokawa in mid-September 2005. After arriving at Itokawa, the spacecraft performed a detailed study on various elements of the asteroid such as shape, spin, topography, color, composition and density in addition to the historical analysis as well. In November 2005, it landed on the asteroid and collected samples, which were then returned to Earth aboard the spacecraft on 13 June 2010.

Refs. Kuninaka et al. (2010) [11] and Alan M. Cassell (2011) [12] provide the summary of Hayabusa spacecraft. The spacecraft was launched in 2003 to a near Earth asteroid Itokawa, to which it accessed in 2005. The aim of the space mission was to retrieve surface material of the asteroid to Earth. Total launch mass of the spacecraft is 510 kg which includes hydrazine fuel of 67 kg. The solar cell paddles (SCP) can generate 2.6 kW electrical power at 1 AU from the Sun. The high gain antenna (HGA) is mounted on the upper surface of the body and the SCP and HGA have no rotational or tilt mechanisms.



Figure 2. 5- The figure shows the spacecraft module for the Hayabusa Mission [14] [15]

A schematic of the Hayabusa/MUSES – C spacecraft is shown in Figure 2.5. A novel μ 10 ion engine with 10 cm effective diameter was developed in order to dedicate to the Hayabusa space mission [15] as the ion engine system (IES). The main feature of this engine is microwave plasma generation without electrodes, which is exhaustive in nature.

The dry mass of IES is 59 kg which includes a gimbal and a propellant tank, filled with xenon propellant 66 kg. A single μ 10 engine is rated at 8 mN thrust, 3,000 sec Isp, and 350 W electrical power consumption so that the Hayabusa spacecraft is accelerated 4 m/s per a day by the maximum thrust 24 mN. The IES is mounted on the side panel perpendicular to the z-axis, on which the HGA aperture is aligned.

At high bit rate communication with 8 kbps, the spacecraft orientates the HGA towards Earth without IES firing. In cruise mode, the spacecraft orients the SCP face toward Sun in order to generate electrical power and rotates its attitude around the solar direction to steer the thrust direction of the IES. Three reaction wheels (RW) control the attitude of spacecraft.

Kuninaka et al. (2010) [11] present the flight chronology of the Hayabusa spacecraft on the total accumulated operational time of the ion engines and the remaining propellant is shown in figure 2.6. On May 9th, 2003, the M-V rocket launched the Hayabusa spacecraft into deep space. After test operations and parameter tuning, the delta-V manoeuvre was started in July.

In the first year, the spacecraft stayed on a 1-year Earth-synchronous orbit and changed its orbital eccentricity using IES manoeuvres to accumulate a relative velocity compared to Earth, which would then be converted into orbital energy at the moment of the Earth swing-by. The 1-year Earth-synchronous orbit supplies the spacecraft with enough solar energy, a moderate temperature environment, and enough time for acceleration for the electric propulsion to attain its maximal capabilities.

The relative position of the Hayabusa spacecraft in the rotational coordinate system, where Sun is located at the origin and Earth on the horizontal axis, is presented in figure 2.7. A manoeuvre by the IES gradually changed the orbit and finally achieved an orbit crossing Earth at the end of 2003.

The spacecraft passed through perihelion at a distance of 0.86 AU from Sun receiving its most severe solar radiation on February 23rd, 2004. Guidance towards the swing-by point was also executed using IES manoeuvres. Orbital determination indicated that the IES manoeuvres made the crossing point gradually approach Earth.

By the end of March 2004, the IES had generated a delta-V of 600 m/s while consuming 10 kg of propellant. On May 19th, 2004, Hayabusa passed through Earth at a point 4,000 km above the Pacific Ocean, and was input into the asteroid transfer orbit. On the transfer orbit to the asteroid, the IES continued to accelerate Hayabusa.

Three of four ITRs, supplied enough electric power, accelerated the spacecraft with their full capability until August 2004. From September 2004, the IES was throttled down in order to adapt to a reduction of solar power due to an increase in the solar distance. The IES generates a maximum thrust of 24 mN while consuming 1.1 kW of electrical power and a minimal thrust of 4.5 mN while consuming 250 W of electrical power.

On February 18th, 2005, Hayabusa reached the aphelion at a distance of 1.7 AU from Sun. On May 2005, two ITRs were turned on again because of a recovery in solar power.

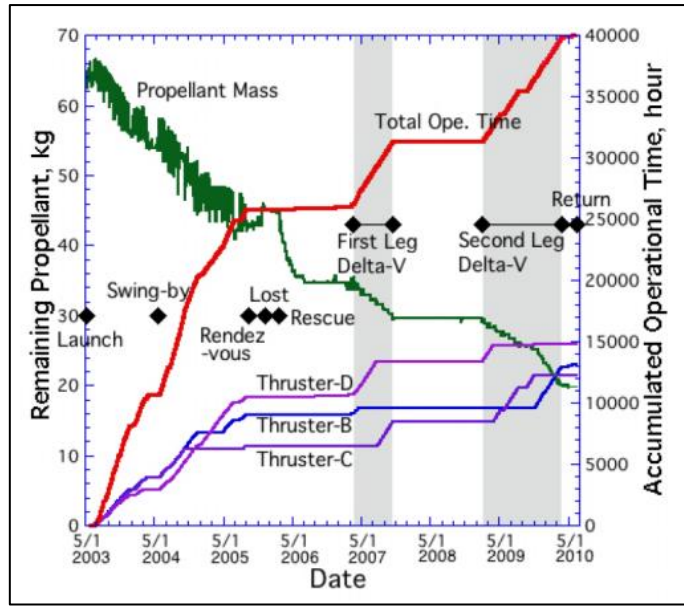


Figure 2.6- The figure shows the Hayabusa operational mission details [13] [12]

In July, Hayabusa was in the solar conjunction, and the delta-V manoeuvre by the IES was paused due to insufficient orbital determination. From August, three ITRs accelerated the Hayabusa again to reduce the distance to and relative velocity with respect to Itokawa.

On August 28th, 2005, the IES completed the outward journey and handed over the space manoeuvres of the Hayabusa spacecraft to the bipropellant thrusters at a distance 4,800 km from the target with an approach speed of 9 m/s. The Hayabusa sent Earth a complete picture of Itokawa. The total operational time was 25,800 hour unit, while consuming 22 kg of xenon propellant and generating a delta-V of 1,400 m/s.

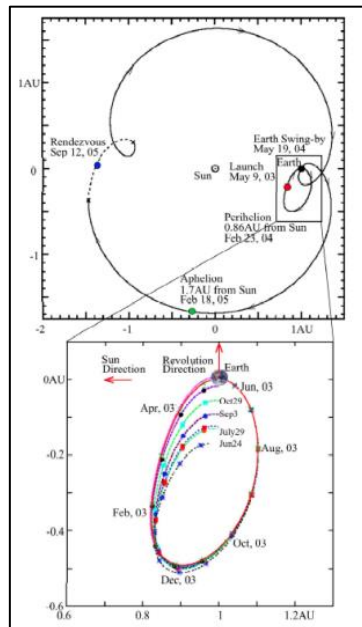


Figure 2.7- The figure shows the Hayabusa mission orbits [13]

2.5 Conclusions of Literature Review and Mission Drivers for our Mission

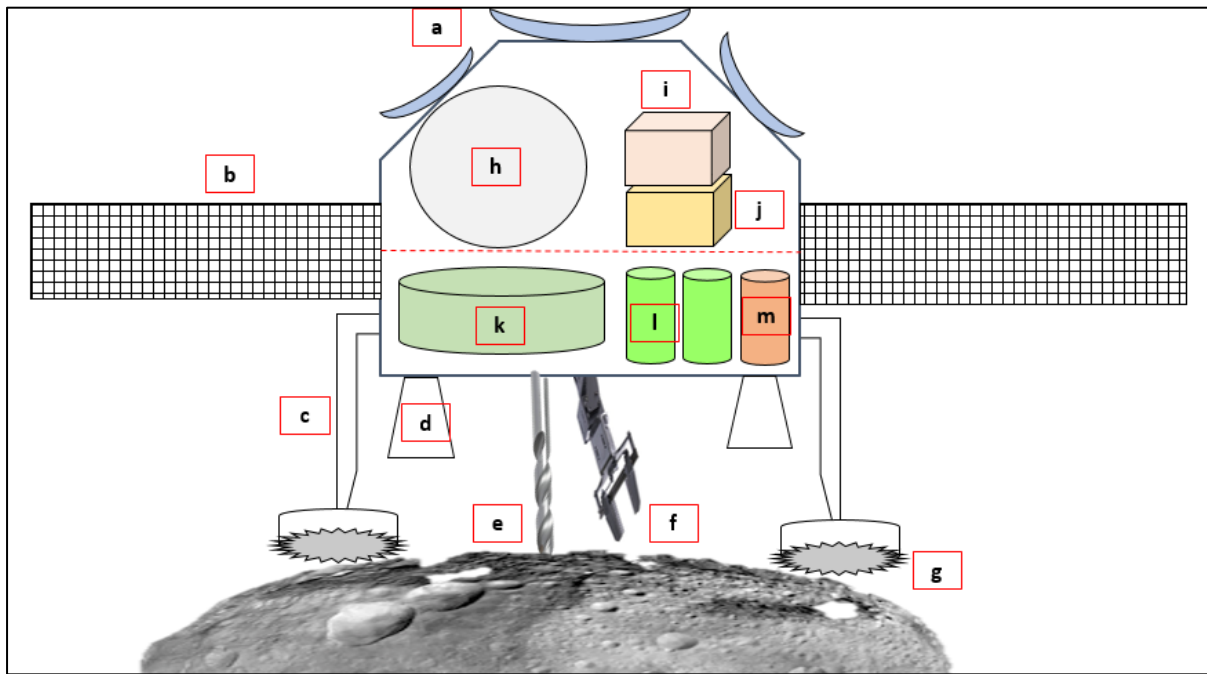


Figure 2. 8- The figure shows the system architectural elements derived from literature

Based on the literature of previously flown mission such as OSIRIS-Rex and Hayabusa missions [8] [9] [13] [12] [15] the Figure 2.8 was developed that shows the final spacecraft configuration based on the literature review in Section 2. It is found that the following spacecraft elements are essential for an asteroid mining mission justified through Section 2 which are designed and critiqued through the report.

- Communication system that includes antennas for uplink and downlink of essential payload data
- Solar panels to help power the spacecraft during sunlit times for nominal operations
- Landing legs to land on the asteroid
- Propulsion and AOCS thrusters(and other control mechanisms) for landing, proximity operations and mapping
- Mining mechanism
- Asteroid collection mechanism
- Mechanical anchor to mine in low gravity conditions
- Propellant and pressurant tanks
- Battery pack to store power for use during eclipse times for nominal operations
- Avionics and OBDH
- Storage space for asteroid regolith ore
- NAC and WAC cameras
- Spectrometers (X-ray and Infrared), thermal Imagers, laser altimeters and micro gravimeter.

3 Requirements for the Asteroid Mining Mission and Challenges

This project is unique in comparison to most asteroid sample return missions , in particular its scope as the constraint to return 500 kg of regolith ore has never been attempted before. At the start of the project we weren't given a specific mission statement and hence one was derived from the information provided. Instead the team was given a vision and an opportunity to work collaboratively to design a spacecraft and a mission capable of resource return that is feasible and possible from a systems engineering perspective. The top-level requirements that had to be met was:

1. Must mine a Near Earth Asteroid
2. Must mine an asteroid that has a high metallic content
3. The launch window shall be within 2027 to 2030
4. The asteroid must be mapped for environmental data for scientific value
5. The resource return shall be greater than 500 kg
6. The size of the Asteroid must be greater than 200 m
7. The delta V of the mission shall not be greater than 9km/s

If such a mission were to be carried out there would undoubtedly be extra considerations. Such a mission would likely involve multiple space agencies as well as private companies, partly due to very high cost and political considerations [3]. All these stakeholder parties would have their own set of requirements, but for the purpose of the project these were not considered due to 6 week time constraint and the uncertainty of conditions under which such a mission would take place.

The timeline of the mission was set to launch from 2027-2030 which is further discussed in Section 5 assuming there is relevant technologies available with a high TRL of 5 or greater.

4 Selection of Target Asteroid

4.1 Asteroid Classification

Asteroids are classified into three major groups, namely:

- a) **C-Type:** C-Type asteroids or Chondrites have a high compositional content of silicates, carbon and clay. [16] [17]
- b) **S-Type:** S- Type asteroid or Stony type have a high compositional content of silicates and Ni-Fe metals [16] [17]
- c) **M-Type:** M-Type asteroids have a high compositional content of metals and precious metals. [16] [17]

Asteroids are further sub- categorised into various classes such as A, B, C, M, O etc. [17] whose significance will be discussed in Section 4.2.

For this mission Near Earth asteroids were considered as they have orbits that reconnaissance close to Earth and have low ΔV requirement constraints. Near Earth asteroids were also considered as they have previously flown or to-be flown sample return and reconnaissance missions that would act as a baseline framework for our project. Some of these missions are OSIRIS-REX, Hayabusa 1 and 2, Rosetta etc. [14] [15] [8] [9] [17] Section 4.2 includes details of key element considerations for Asteroid Selection.

4.2 Key Trade Elements for Selection of Asteroid

SSERD gave the team a Mission statement that did not have any specific Asteroid constraint, so it was up to the team to select the Asteroid through standard systems engineering practices. It was decided that in order to select the Target Asteroid various trade elements had to be considered. This was important to establish early on in the project phase as it set a baseline for all other sub-systems with heavy constraints on Mission Analysis.

The key Tradeable elements considered were:

a) Composition of the Asteroid

The Composition of the Asteroid was considered important because the objective of the mission was to mine an Asteroid and have a resource return. In order for the mission to be successful, the commercial value of regolith ore brought back to LEO had to be hugely more profitable than the initial mission costs and this could only be achieved if the objective of mining a metallic asteroid was included. It was decided that focus and priority would be given to the metallic asteroids (M types and sub-categories) over other S and C type compositions.

b) Size of the Asteroid

The size of the Asteroid was considered important because asteroids under the size of 1 km had a high tumbling rate [10] and this would place very high constraints and complexity on the AOCS sub-system. So it was decided that asteroids with size ≥ 1 km would be preferable due to less spacecraft failure modes during landing and mining operations.

c) Preliminary ΔV requirements

The ΔV for the Target Asteroid was considered important because ΔV requirements would place very high constraints on Propulsion (Fuel requirements and Launch

Vehicle capabilities), Mission Analysis (Orbital selection), Power (Solar and battery sizing) and AOCS (Control requirements) sub-systems. It was decided that ΔV (km/s) lower than 9 km/s for the entire mission would be preferable.

d) Number of launch opportunities possible within the launch window of 2027 to 2030

The number of launches was considered important because the number of launches gave the team a range of low ΔV opportunities to choose from. In some cases of launch opportunities the ΔV would be low but the launch mass for those scenarios were not ideal. It was also considered as an asset from an operational standpoint where the launch could be pushed to the next best low ΔV opportunity in case of environmental issues during launch. It was decided the Asteroid missions with more than 2 launch opportunities would be ideal.

e) Inclination of the Asteroid

The inclination of the Asteroid from the ecliptic plane of Earth was considered important because it would place ΔV constraints on the Mission Analysis sub-system due to ΔV for inclination changes assuming an equatorial launch. It was decided that asteroids with low inclinations would be preferable.

4.3 Trade Analysis and Conclusion

In order to select the Target asteroid a trade study needed to be conducted. This report uses the AHP method of trade and uses the trade elements discussed in Section 4.2.

The first step was to create a rating system for the tradeable elements mentioned in Section 4.2 which is discussed as below:

a) Composition of Asteroid

Table 4. 1- The table shows rating system for Composition of Asteroid

Composition rating System	
X,Xc	10
O,Xk,Xe	9
M	8
S	7
Q,L,R	6
K	5
C	4
B	3
D	2
T	1

The rating system for composition of Asteroid was developed as shown in Table 4.1 on the basis of high metallic asteroids were more preferable over asteroids with higher carbon and rock content as the objective of the mission was to mine precious metals and minerals and was not focused on the planetary science. This rating

system considered the 3 main categories of asteroid (M, C and S) an also their sub categories.

b) Size of Asteroid

Table 4. 2- The table shows rating system of the size of Asteroid

Size Rating system(>200m)	
>1 km	10
900	9
800	8
700	7
600	6
500	5
400	4
300	3
200	2
<200 m	1

The rating system for size of Asteroid was developed as shown in the Table 4.2 on the basis that larger asteroids had lower tumbling rates [19] [10] and Yarkovsky affect and were more preferable over asteroids with smaller size as discussed in Section 4.2

c) Preliminary ΔV requirements

Table 4. 3- The table shows the rating system for the preliminary ΔV for the mission

ΔV (km/s) rating system	
4	10
4.5	9
5	8
5.5	7
6	6
6.5	5
7	4
7.5	3
8	2
8.5	1
9	0

The rating system for the preliminary ΔV requirements was developed as shown in Table 4.3 on the basis that lower ΔV requirements for the mission were favourable for reasons discussed in Section 4.2

d) Inclination

Table 4. 4- The table shows the rating system for the inclination of the asteroid wrt Earth ecliptic plane

i	Rating
1	10
2	9
3	8
4	7
5	6
6	5
7	4
8	3
9	2
10 or >	1

The rating system for the inclination ΔV requirements was developed as shown in Table 4.4 on the basis that lower inclination ΔV change requirements for the mission were favourable for reasons discussed in Section 4.2

The second step was to create a comprehensive list of Near Earth Asteroids. This trade considered 24 NEAs where some asteroids have pre-flown missions, some have to-be flown missions and some are un-named asteroids.

Data such as Asteroid composition, size of asteroid, ΔV for the mission, asteroid inclination wrt earth ecliptic plane and number of launches were compiled using various sources such as NASA SSD. [18]

Once the asteroids were categorised with their respective tradeable elements, weights were added to the trade elements that the team thought that had a higher constraint on the overall design of the mission.

For the first pass of trade, the trade element with the highest weight was given to Type of composition and size of asteroid as discussed in Section 4.2 and the lowest weight was given to the number of launch opportunities. The preliminary ΔV requirements was weighted average as all the asteroids with ΔV less than 9 km/s were chosen and did not impose a high constraint in the first pass of trade .

All the trade passes was normalised that as an equaliser when comparing different trade elements that were not implicitly related to each other.

Table 4.5 shows the first Pass of Trade and Table 4.6 shows its Normalisation Matrix

Table 4. 5- The table shows the prioritisation matrix of Trade Pass 1

Prioritisation Matrix	Type of asteroid Composition	Size>200m	$\Delta V(\text{km/s})$	i	Number of launches possible within 2027 to 2030
Bennu	4	2	7	5	7
Ryugu	4	4	9	6	7
Eros	7	10	4	1	1
Itokawa	7	1	9	10	7
Nereus	9	1	6	10	4
Didymos	9	4	6	8	2
Anteros	6	10	4	3	3
Seleucus	7	10	2	6	1
1989 ML	10	10	9	7	5
2001 CC 21	6	10	8	6	6
2011UW158	10	3	6	6	5
1992TC	9	6	2	4	1
2001SG10	9	2	2	7	2
2002DO3	9	2	2	8	6
2000CE59	6	6	3	1	4
1995BC2	9	10	3	6	1
2000RW37	4	3	2	1	1
1989UQ	3	9	8	10	3
1988XB	3	5	3	8	1
1997XF11	9	10	1	7	1
1996FG3	4	10	6	9	1
1999JV6	9	4	4	6	6
2005YU55	4	4	4	10	3
1992BF	10	3	6	4	5
Lucianotesi	10	2	2	1	4
SUM	177	141	118	150	87
Weights	0.05	0.05	0.2	0.3	0.4
ModSum	8.85	7.05	23.6	45	34.8

Table 4. 6- The table shows the normalisation matrix for Pass 1

Normalisation matrix						SUM(>2)
Bennu	0.452	0.284	0.297	0.111	0.201	1.34
Ryugu	0.452	0.567	0.381	0.133	0.201	1.74
Eros	0.791	1.418	0.169	0.022	0.029	2.43
Itokawa	0.791	0.142	0.381	0.222	0.201	1.74
Nereus	1.017	0.142	0.254	0.222	0.115	1.75
Didymos	1.017	0.567	0.254	0.178	0.057	2.07
Anteros	0.678	1.418	0.169	0.067	0.086	2.42
Seleucus	0.791	1.418	0.085	0.133	0.029	2.46
1989 ML	1.130	1.418	0.381	0.156	0.144	3.23
2001 CC 21	0.678	1.418	0.339	0.133	0.172	2.74
2011UW158	1.130	0.426	0.254	0.133	0.144	2.09
1992TC	1.017	0.851	0.085	0.089	0.029	2.07
2001SG10	1.017	0.284	0.085	0.156	0.057	1.60
2002DO3	1.017	0.284	0.085	0.178	0.172	1.74
2000CE59	0.678	0.851	0.127	0.022	0.115	1.79
1995BC2	1.017	1.418	0.127	0.133	0.029	2.72
2000RW37	0.452	0.426	0.085	0.022	0.029	1.01
1989UQ	0.339	1.277	0.339	0.222	0.086	2.26
1988XB	0.339	0.709	0.127	0.178	0.029	1.38
1997XF11	1.017	1.418	0.042	0.156	0.029	2.66
1996FG3	0.452	1.418	0.254	0.200	0.029	2.35
1999JV6	1.017	0.567	0.169	0.133	0.172	2.06
2005YU55	0.452	0.567	0.169	0.222	0.086	1.50
1992BF	1.130	0.426	0.254	0.089	0.144	2.04
Lucianotesi	1.130	0.284	0.085	0.022	0.115	1.64

For the second pass of trade, the outputs of the normalisation matrix of pass 1 was narrowed down and used as input to pass 2 of trade. The trade element weights remained the same as pass 1.

Table 4.7 shows the second Pass of Trade and Table 4.8 shows its Normalisation Matrix

Table 4. 7- The table shows the trade table for Pass 2

Prioritisation Matrix	Type of asteroid Composition	Size>200m	$\Delta V(\text{km/s})$	i	Number of launches possible within 2027 to 2030
Eros	7	10	4	1	1
Didymos	9	4	6	8	2
Anteros	6	10	4	3	3
Seleucus	7	10	2	6	1
1989 ML	10	10	9	7	5
2001 CC 21	6	10	8	6	6
2011UW158	10	3	6	6	5
1992TC	9	6	2	4	1
1995BC2	9	10	3	6	1
1989UQ	3	9	8	10	3
1997XF11	9	10	1	7	1
1996FG3	4	10	6	9	1
1999JV6	9	4	4	6	6
1992BF	10	3	6	4	5
SUM	108	109	69	83	41
Weights	0.05	0.05	0.2	0.3	0.4
ModSum	5.4	5.45	13.8	24.9	16.4

Table 4. 8- The table shows the normalisation matrix for Pass 2

Normalisation matrix						SUM(>3.5)
Eros	1.296	1.835	0.290	0.040	0.061	3.522
Didymos	1.667	0.734	0.435	0.321	0.122	3.279
Anteros	1.111	1.835	0.290	0.120	0.183	3.539
Seleucus	1.296	1.835	0.145	0.241	0.061	3.578
1989 ML	1.852	1.835	0.652	0.281	0.305	4.925
2001 CC 21	1.111	1.835	0.580	0.241	0.366	4.133
2011UW158	1.852	0.550	0.435	0.241	0.305	3.383
1992TC	1.667	1.101	0.145	0.161	0.061	3.134
1995BC2	1.667	1.835	0.217	0.241	0.061	4.021
1989UQ	0.556	1.651	0.580	0.402	0.183	3.371
1997XF11	1.667	1.835	0.072	0.281	0.061	3.916
1996FG3	0.741	1.835	0.435	0.361	0.061	3.433
1999JV6	1.667	0.734	0.290	0.241	0.366	3.297
1992BF	1.852	0.550	0.435	0.161	0.305	3.303

For the third and final pass of trade, the outputs of the normalisation matrix of pass 2 was narrowed down and used as input to pass 3 of trade. The trade element weights of Composition, Size and ΔV remained the same as pass 1. Number of launches was given the same priority as ΔV and the priority of inclination was reduced for a more refined trade model.

Table 4.9 shows the final Pass of Trade and Table 4.10 shows its Normalisation Matrix

Table 4. 9- The table shows the trade table for Final pass

Prioritisation Matrix	Type of asteroid Composition	Size>200m	ΔV (km/s)	i	Number of launches possible within 2027 to 2030
Eros	7	10	4	1	1
Anteros	6	10	4	3	3
Seleucus	7	10	2	6	1
1989 ML	10	10	9	7	5
2001 CC 21	6	10	8	6	6
1995BC2	9	10	3	6	1
1997XF11	9	10	1	7	1
1996FG3	4	10	6	9	1
SUM	58	80	37	45	19
Weights	0.05	0.05	0.2	0.5	0.2
ModSum	2.9	4	7.4	22.5	3.8

Table 4. 10- The table shows the normalisation matrix for Final pass

Normalisation matrix						SUM
Eros	2.414	2.500	0.541	0.044	0.263	5.762
Anteros	2.069	2.500	0.541	0.133	0.789	6.032
Seleucus	2.414	2.500	0.270	0.267	0.263	5.714
1989 ML	3.448	2.500	1.216	0.311	1.316	8.791
2001 CC 21	2.069	2.500	1.081	0.267	1.579	7.496
1995BC2	3.103	2.500	0.405	0.267	0.263	6.539
1997XF11	3.103	2.500	0.135	0.311	0.263	6.313
1996FG3	1.379	2.500	0.811	0.400	0.263	5.353

Table 4.11 shows that the Asteroid 1989ML is the front runner and is selected as the Target Asteroid for the Mission.

Table 4. 11- The table shows the Trade table with correct value of size of 1989ML

Prioritisation Matrix	Type of asteroid Composition	Size>200m	$\Delta V(\text{km/s})$	i	Number of launches possible within 2027 to 2030
Eros	7	10	4	1	1
Anteros	6	10	4	3	3
Seleucus	7	10	2	6	1
1989 ML	10	3	9	7	5
2001 CC 21	6	10	8	6	6
1995BC2	9	10	3	6	1
1997XF11	9	10	1	7	1
1996FG3	4	10	6	9	1
SUM	58	73	37	45	19
Weights	0.05	0.05	0.2	0.5	0.2
ModSum	2.9	3.65	7.4	22.5	3.8

Table 4. 12- The table shows the normalisation matrix for the correct value of size of 1989ML

Normalisation matrix						SUM
Eros	2.414	2.740	0.541	0.044	0.263	6.002
Anteros	2.069	2.740	0.541	0.133	0.789	6.272
Seleucus	2.414	2.740	0.270	0.267	0.263	5.954
1989 ML	3.448	0.822	1.216	0.311	1.316	7.113
2001 CC 21	2.069	2.740	1.081	0.267	1.579	7.735
1995BC2	3.103	2.740	0.405	0.267	0.263	6.778
1997XF11	3.103	2.740	0.135	0.311	0.263	6.553
1996FG3	1.379	2.740	0.811	0.400	0.263	5.593

Through the 4- week mark of the internship (Design Phase) it was found that the size of the Asteroid 1989ML was misjudged and that the size of the asteroid was ~300 m [19]and not the previously assumed value of 1.6 km [20]. This changed the front runner of the Trade as shown in Table 4.11 and Table 4.12 and would have knock out effect on the design of all sub-systems. An executive decision was made to continue with the selection of target asteroid as 1989ML but that this misjudgement be captured.

4.4 Properties of Target Asteroid and Preliminary Mission Analysis

As a natural flow down from Selection of Asteroid the next step is to analyse and characterise Asteroid 1989ML which feeds into different sub-systems and mission analysis.

NASA Solar system Dynamics (SSD) tool was used to find the preliminary ΔV requirements for the mission and different orbital elements. Space environment analysis of the asteroid is critiqued in Section 13 [18]. This repository of data sets a framework for designing the mission and its sub-system elements.

Figure 4.4.1 shows the orbital properties of the Target asteroid 1989ML. The semi-major axis, inclination and the period hold a significant importance as they are used in power and mission analysis calculations in section 5 and Section 8 respectively.

Orbital Elements at Epoch 2459000.5 (2020-May-31.0) TDB Reference: JPL 106 (heliocentric ecliptic J2000)			
Element	Value	Uncertainty (1-sigma)	Units
e	.1364029076489758	4.1185e-08	
a	1.272206355146454	5.0003e-09	au
q	1.098673709174972	5.3326e-08	au
i	4.378247099464627	4.5072e-06	deg
node	104.3401569726565	4.8591e-05	deg
peri	183.3544004215724	5.4412e-05	deg
M	188.5354318975914	2.9249e-05	deg
t _p	2459250.135679211705 (2021-Feb-04.63567921)	4.3325e-05	TDB
period	524.1248702912137 1.43	3.09e-06 8.46e-09	d yr
n	.6868592207806837	4.0495e-09	deg/d
Q	1.445739001117936	5.6823e-09	au

Figure 4. 1- The figure shows the Orbital properties of 1989ML from NASA SSD

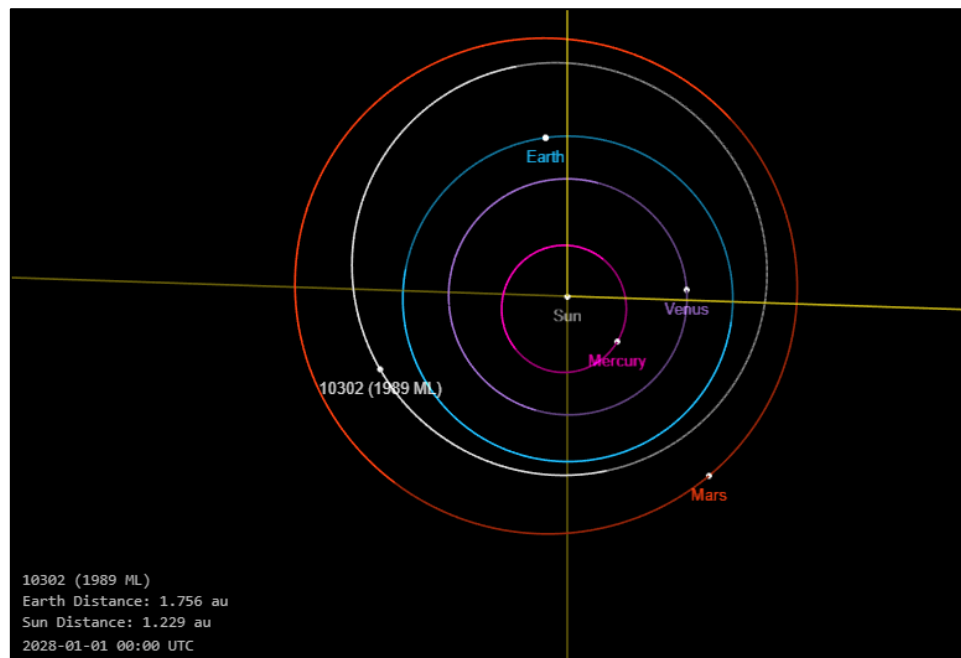


Figure 4. 2- The figure shows the orbital ephemeris position of 1989ML with respect to Earth and other planets

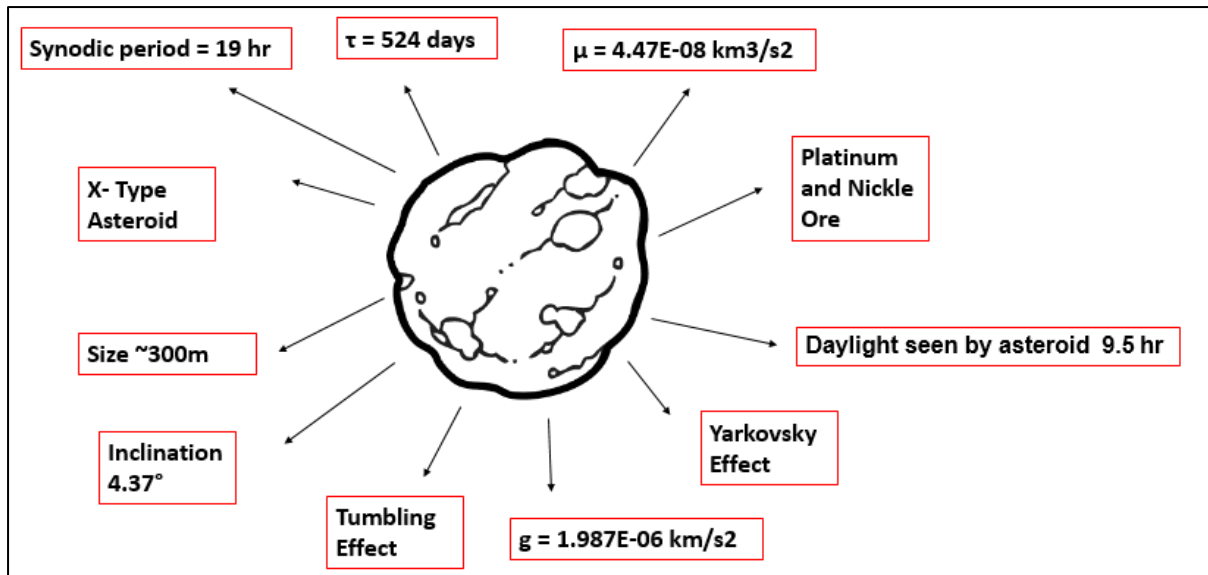


Figure 4. 3- The figure shows the asteroid environment data

Figure 4.3 shows the environmental data of the asteroid 1989ML. It captures the orbital properties of the Asteroid such as synodic rotation, period of asteroid around the sun, daylight and eclipse times as seen by a spacecraft if it is parked at 10km altitude from the asteroid, the gravity conditions of the asteroid and gravitational parameter. These elements are fed into Mission Analysis in section 5 and Power sub-system in section 8.

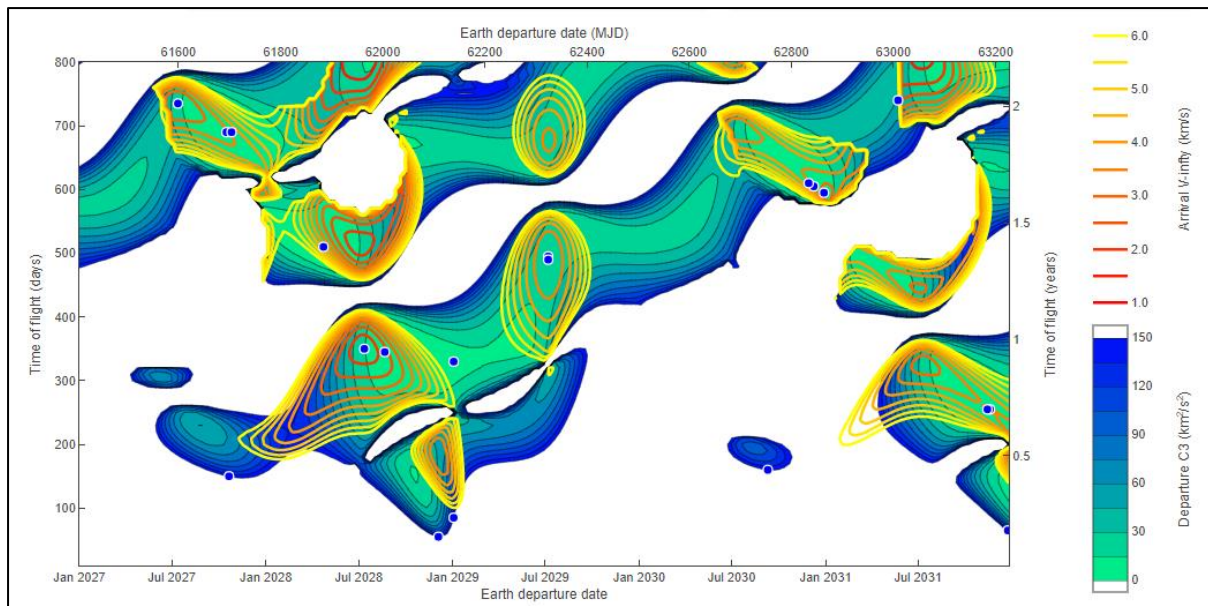


Figure 4. 4- The figure shows the pork-chop plot for the launch window 2027 to 2030

Id	Departure date		Arrival date		TOF (days)	C3 (km ² /s ²)	V _∞ dep. (km/s)	V _∞ arr. (km/s)	Total ΔV (km/s)	Phase angle (deg)	Dist. Earth (au)	Approach angle (deg)	SEP angle (deg)	DLA (deg)
	(cal)	▲ (MJD)	(cal)	△ (MJD)										
27	2026-07-08	61229	2028-01-14	61784	555	24.13	4.9	3.8	8.7	169.1	1.683	71.8	44.9	-23.0
28	2026-07-13	61234	2028-01-24	61794	560	23.74	4.9	3.8	8.7	168.3	1.637	72.1	46.0	-21.2
31	2027-07-13	61599	2029-07-17	62334	735	19.70	4.4	2.5	6.9	85.8	1.115	174.1	65.6	-5.6
76	2027-10-16	61694	2029-09-05	62384	690	0.93	1.0	3.4	4.4	105.1	1.147	135.7	61.1	1.1
6	2027-10-21	61699	2028-03-19	61849	150	147.88	12.2	13.4	25.6	26.4	1.471	117.0	48.8	-17.8
77	2027-10-26	61704	2029-09-15	62394	690	0.78	0.9	3.6	4.5	115.6	1.154	133.1	60.7	23.1
68	2028-04-23	61884	2029-09-15	62394	510	2.48	1.6	4.2	5.8	42.3	1.154	116.0	60.7	-23.0
36	2028-07-12	61964	2029-06-27	62314	350	16.06	4.0	1.7	5.7	82.0	1.087	173.1	69.2	-11.1
59	2028-08-21	62004	2029-08-01	62349	345	4.97	2.2	2.3	4.5	100.5	1.128	136.6	63.7	-18.9
7	2028-12-04	62109	2029-01-28	62164	55	147.04	12.1	18.9	31.0	11.8	0.463	81.4	165.7	26.1

Figure 4. 5- The figure shows the different launch opportunities and preliminary ΔV calculations for 2027 to 2030

Id	Departure date		Arrival date		TOF (days)	C3 (km ² /s ²)	V _∞ dep. (km/s)	V _∞ arr. (km/s)	Total ΔV (km/s)	Phase angle (deg)	Dist. Earth (au)	Approach angle (deg)	SEP angle (deg)	DLA (deg)
	(cal)	▲ (MJD)	(cal)	△ (MJD)										
50	2029-01-03	62139	2029-11-29	62469	330	8.88	3.0	7.2	10.2	168.2	1.335	108.3	58.6	46.0
1	2029-01-03	62139	2029-03-29	62224	85	149.65	12.2	7.6	19.8	32.8	0.738	129.2	103.4	33.3
30	2029-07-07	62324	2030-11-09	62814	490	20.05	4.5	3.1	7.5	174.6	2.173	76.8	15.4	-26.6
29	2029-07-07	62324	2030-11-14	62819	495	20.09	4.5	3.1	7.5	174.4	2.155	76.8	16.1	-25.5
2	2030-09-10	62754	2031-02-17	62914	160	149.28	12.2	12.3	24.5	46.8	1.922	136.5	24.3	-6.9
72	2030-11-29	62834	2032-07-31	63444	610	1.57	1.3	3.5	4.8	83.3	0.398	144.9	91.3	-10.0
69	2030-12-09	62844	2032-08-05	63449	605	1.82	1.4	3.3	4.7	86.7	0.402	148.8	91.1	2.1
61	2030-12-29	62864	2032-08-15	63459	595	4.51	2.1	2.8	5.0	92.7	0.413	166.3	91.2	27.5
21	2031-05-23	63009	2033-06-01	63749	740	46.30	6.8	2.4	9.2	52.7	2.134	130.8	35.3	8.7
80	2031-11-14	63184	2032-07-26	63439	255	0.48	0.7	3.5	4.2	100.7	0.394	139.2	91.5	4.3

Figure 4. 6- The figure shows the different launch opportunities and preliminary ΔV calculations for 2027 to 2030

Once the Target asteroid was fixed, the next step was to calculate the preliminary ΔV required by the mission as a baseline for future mission analysis work. The preliminary ΔV values were found using the NASA SSD tool which gives the different ΔV options during the launch window of 2027 to 2030. Figure 4.4 shows the pork chop plot of the mission opportunities from 2027 to 2030 and potential ΔV and launch dates that have a ΔV less than 9km/s . Figures 4.5 and 4.6 show the feasible departure and arrival date to the asteroid within the launch window. It is to be noted that this tool does not calculate the ΔV requirements for the entire mission but only till asteroid rendezvous. An initial assumption was made that the return ΔV was the same as that of the rendezvous mission and this value is refined in Section 5

ΔV of 4.4 km/s was considered as the first constraint for the entire mission until further mission analysis calculations were done.

Id	Atlas V (401) (kg)		Atlas V (421) (kg)		Atlas V (531) (kg)		Atlas V (551) (kg)		Falcon 9 (kg)		Falcon Heavy (kg)		Delta IV-H (kg)		SLS 1B (kg)		SLS 2 (kg)	
	Flyby	Rdzs	Flyby	Rdzs	Flyby	Rdzs	Flyby	Rdzs	Flyby	Rdzs	Flyby	Rdzs	Flyby	Rdzs	Flyby	Rdzs	Flyby	Rdzs
27	1670	495	2790	830	2995	890	3800	1130	-	-	6925	2065	6460	1925	13585	4050	36080	10765
28	1690	500	2815	835	3020	895	3830	1135	-	-	6995	2075	6510	1930	13695	4070	36300	10785
31	1895	860	3090	1400	3305	1500	4165	1890	-	-	7770	3525	7035	3190	14925	6770	38700	17550
76	2975	1000	4570	1540	4855	1635	6005	2025	3205	1080	12185	4110	10015	3380	22295	7520	51610	17415
6	-	-	-	-	-	-	-	-	-	-	-	-	-	-	-	-	-	
77	2985	945	4585	1455	4865	1545	6020	1910	3220	1020	12225	3880	10040	3190	22365	7100	51725	16430
68	2875	750	4440	1160	4715	1235	5835	1530	3035	795	11785	3085	9735	2550	21565	5650	50425	13210
36	2085	1210	3355	1945	3580	2075	4490	2605	-	-	8515	4940	7545	4375	16130	9360	40965	23770
59	2720	1305	4225	2030	4490	2160	5570	2680	2765	1330	11145	5360	9290	4465	20445	9830	48565	23355
7	-	-	-	-	-	-	-	-	-	-	-	-	-	-	-	-	-	

Figure 4. 7- The figure shows the different Lift-Off mass capabilities by launchers for the launch window from 2027 to 2030

Id	Atlas V (401) (kg)		Atlas V (421) (kg)		Atlas V (531) (kg)		Atlas V (551) (kg)		Falcon 9 (kg)		Falcon Heavy (kg)		Delta IV-H (kg)		SLS 1B (kg)		SLS 2 (kg)	
	Flyby	Rdzs	Flyby	Rdzs	Flyby	Rdzs	Flyby	Rdzs	Flyby	Rdzs	Flyby	Rdzs	Flyby	Rdzs	Flyby	Rdzs	Flyby	Rdzs
50	2490	250	3905	395	4160	420	5170	520	2340	235	10135	1025	8645	875	18805	1905	45765	4640
1	-	-	-	-	-	-	-	-	-	-	-	-	-	-	-	-	-	
30	1875	705	3065	1155	3280	1235	4135	1560	-	-	7700	2905	6985	2635	14815	5590	38480	14520
29	1875	705	3060	1155	3275	1235	4130	1560	-	-	7690	2900	6980	2635	14800	5585	38460	14520
2	-	-	-	-	-	-	-	-	-	-	-	-	-	-	-	-	-	
72	2935	950	4515	1465	4795	1555	5935	1925	3135	1015	12020	3905	9900	3215	21990	7140	51115	16600
69	2920	1005	4495	1555	4775	1650	5905	2040	3110	1075	11955	4135	9855	3405	21870	7560	50925	17605
61	2750	1110	4265	1720	4530	1830	5620	2270	2815	1135	11265	4550	9370	3785	20650	8340	48905	19760
21	755	345	1565	720	1730	795	2310	1060	-	-	3495	1605	4110	1885	8440	3875	25165	11560
80	3000	985	4610	1515	4895	1610	6050	1990	3255	1070	12305	4045	10095	3320	22510	7400	51960	17090

Figure 4. 8- The figure shows the different Lift-Off mass capabilities by launchers for the launch window from 2027 to 2030

Figure 4.7 and Figure 4.8 shows the launch capabilities of different launch vehicles for the asteroid rendezvous mission. For the Mission ID 76 with ΔV of 4.4km/s rendezvous, the maximum lift-off mass is 17 tonnes for SLS-2 and the minimum is 1 tonne for Atlas 5. So typically we need to design our mission such that the lift-off mass s with the abovementioned range.

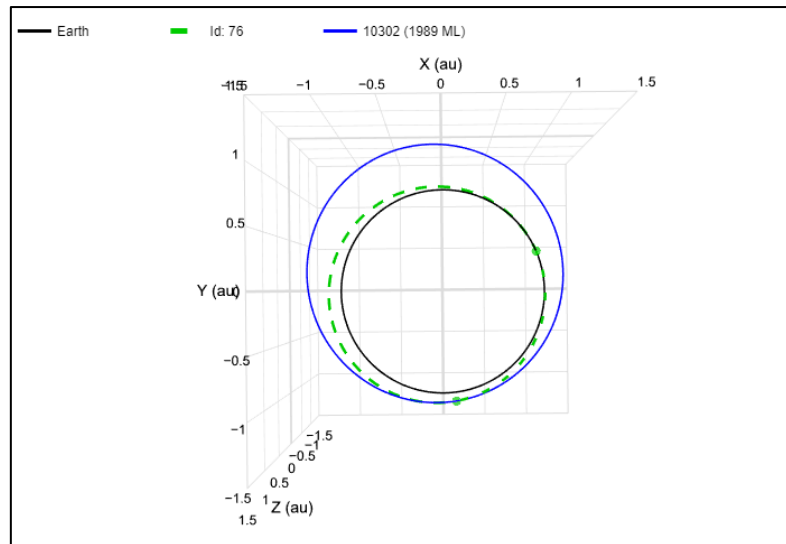


Figure 4. 9- The figure shows the orbital diagram for the direct transfer to Asteroid rendezvous found using the NASA SSD tool

Figure 4.9 shows the orbital diagram of a direct transfer of the spacecraft from Earth to the Target Asteroid 1989ML. Figure 4.10 and 4.11 and 4.12 shows that the maximum lif-off mass that can be delivered to the asteroid is during the launch opportunity of July 2028. Checking the ΔV requirements required for a 2028 launch is Mission ID 36 with a ΔV of 5.6 km/s.

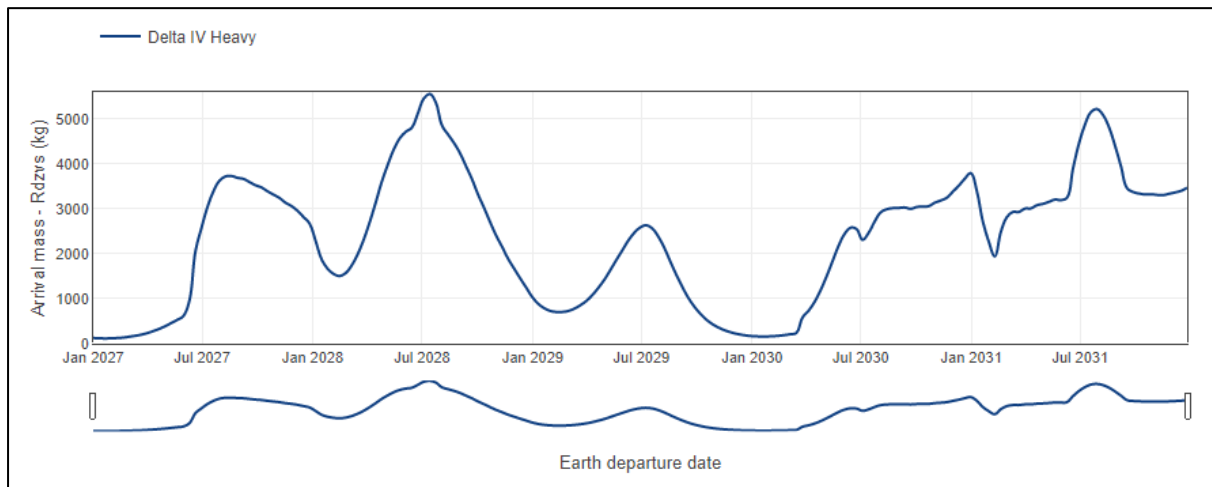


Figure 4. 10- The figure shows the range of Lift-Off mass for Delta 4 Heavy launcher

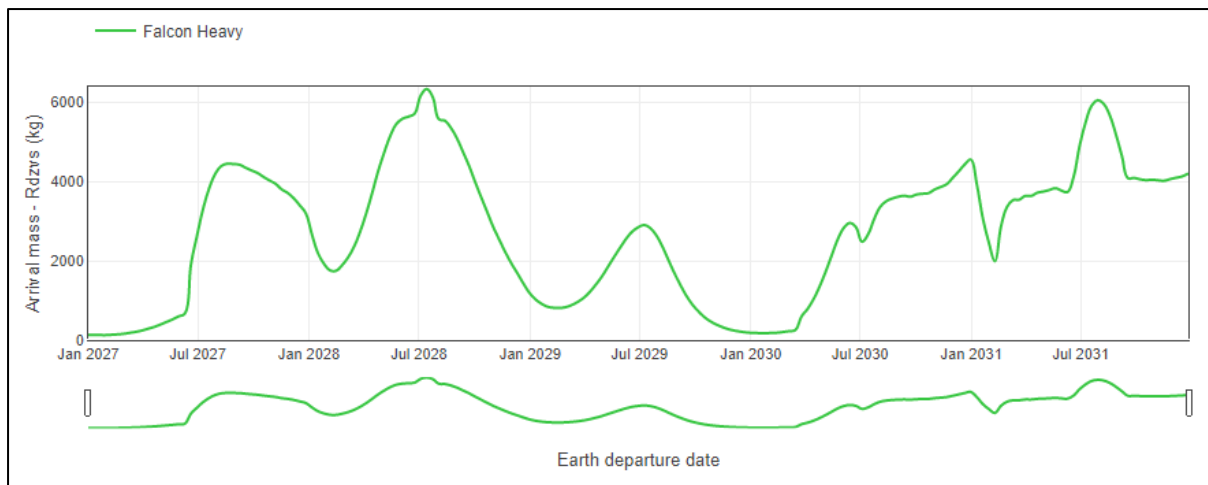


Figure 4. 11- The figure shows the range of Lift-Off mass for Falcon heavy launcher

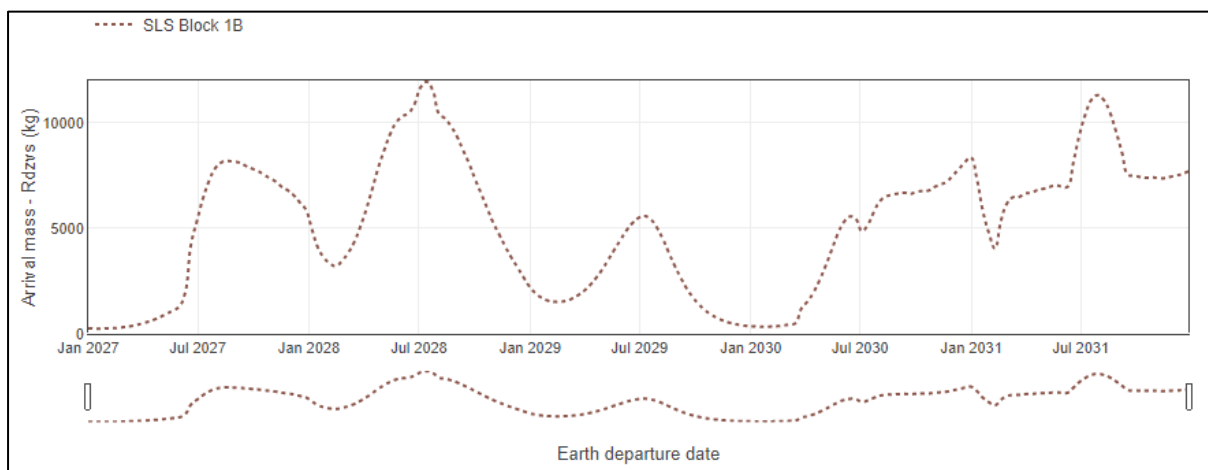


Figure 4. 12- The figure shows the range of Lift-Off mass for SLS Block 1 launcher

To conclude Chapter 4 gives us the target asteroid which is 1989ML; gives us the preliminary ΔV requirements of 4.4 km/s or 5.6 km/s for maximum lift-off mass of ~7 tonnes and a launch date of 2028 for maximum lift-off mass and minimum ΔV in km/s. The launcher capable of launching the required mass discussed in Section 14, for the given launch window is chosen as SLS Block 1 launcher and is most feasible.

5 Mission Analysis

5.1 Introduction

Mission Analysis capture the ΔV requirements for the mission and dictates the mission concept

The first was establishing the key steps in the mission sequence and the as many steps were considered as possible given the 6 week time frame of the internship.

- a) Earth Departure
- b) "Mission architecture Concepts" different possible combinations of interplanetary manoeuvres that would constitute the full mission from LEO to MO and back to LEO
- c) Asteroid Rendezvous and Capture
- d) Asteroid Mining and Departure
- e) Earth Arrival

5.2 Alternative Mission Architecture Concepts

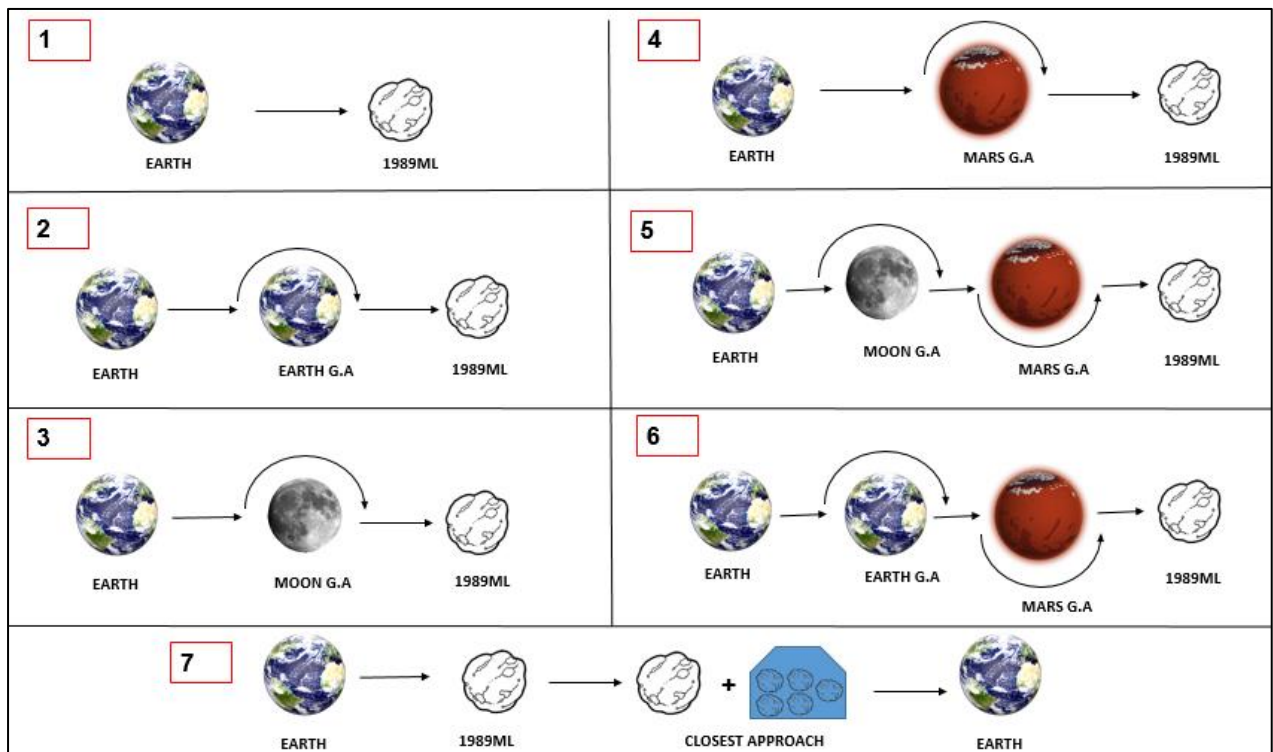


Figure 5. 1- The figure shows the different Mission Architectures that are considered for the Mission

After identification of the preliminary ΔV requirements for the asteroid rendezvous mission using NASA SSD for a direct transfer, we moved to defining "Mission Concepts". Mission Concepts are Concepts of Operations which segments the mission in a sequence and in which order. 7 different mission concepts were considered.

Concept 7 was considered to be high risk as the closest approach of the asteroid to earth was 2035, 2038 and having the spacecraft tethered to the asteroid had high risk factors that we could not calculate and hence was rejected.

Another decision regards Asteroid capture was made such that the excess hyperbolic velocity at the Asteroid is shed off such that the C3 relative energy to Asteroid becomes negative and the spacecraft is captured in the sphere of influence. This manoeuvre needed to be propulsive which involves flipping the spacecraft into the opposite direction to its velocity vector. A propulsive method was chosen because a) the sphere of influence of the asteroid is very small and b) other methods like aero braking/capture cannot be used as it has no atmosphere. This has a moderate risk factor involved and comes at a ΔV cost.

Some of the systems assumptions made in order to calculate the ΔV for the mission are:

1. All orbits are considered Keplerian about one body at a given time.
2. All orbital calculations are heliocentric
3. All planetary planes are considered coplanar
4. The launch is considered to be equatorial launch
5. Inclination of the asteroid is only considered and with the equatorial ecliptic plane of Earth
6. Earth parking orbit is considered at 10,000 km and asteroid parking orbit is considered at 10km. This is a preliminary assumption.

5.3 Selection of Mission Concept using ΔV Constraint for the Asteroid Mining Mission

Starting from these assumptions Patched conics method is used for estimation of ΔV requirements for the mission.

Initial ΔV requirements were calculated for a direct impulsive transfer to the asteroid which set a baseline to improve upon. This value was 5.53 km/s which checked out with the values from NASA SSD for the launch opportunity between 2027 and 2030. In minimize the ΔV requirements a planetary flyby was considered.

To establish the ΔV values hyperbolic escape velocities were calculated for the entire mission using the equations mentioned below and first level estimations of ΔV required for the mission were calculated using:

$$V_{\text{Planet}} = \sqrt{\frac{\mu_{\text{Sun}}}{\text{Distance of Planet from Sun}}}$$

Equation 5. 1

$$V_{\text{PlanetParking}} = \sqrt{2\mu_{\text{Sun}} \times \frac{1}{\text{Distance of Planet from Sun}} - \frac{1}{\text{Distance of Planet from Sun} + \text{Distance of FlyBy Planet from Sun}}}$$

Equation 5. 2

$$V_{\text{o}} \text{ Planet Departure} = V_{\text{Planet}} - V_{\text{PlanetParking}}$$

Equation 5. 3

$$V_{FlyByPlanet} = \sqrt{\frac{\mu_{Sun}}{Distance\ of\ FlyBy\ planet\ from\ Sun}}$$

Equation 5. 4

$$V_{Approach\ of\ FlyBy\ Planet} = \sqrt{2\mu_{Sun} \times \left(\frac{\frac{1}{Distance\ of\ FlyBy\ Planet\ from\ Sun}}{\frac{1}{Distance\ of\ Planet\ from\ Sun} + \frac{1}{Distance\ of\ FlyBy\ Planet\ from\ Sun}} - \right)}$$

Equation 5. 5

$$V_{\infty\ FlyBy\ Planet\ Approach} = V_{FlyByPlanet} - V_{Approach}$$

Equation 5. 6

$$Eccentricity\ of\ Arrival\ Trajectory\ at\ FlyBy\ Planet = 1 + \frac{FlyBy\ altitude \times V_{\infty\ FlyBy\ Planet\ Approach}^2}{\mu_{FlyBy\ Planet}}$$

Equation 5. 7

$$Deflection\ angle\ caused\ by\ FlyBy = 2 \times \sin^{-1} \frac{1}{Eccentricity}$$

Equation 5. 8

$$\Delta V_{FlyBy} = 2 \times V_{\infty\ FlyBy\ Planet\ Approach} \times \sin \frac{Deflection\ angle}{2}$$

Equation 5. 9

$$V_{\infty\ FlyBy\ Planet\ Approach} = V_{\infty\ FlyBy\ Planet\ Departure}$$

Equation 5. 10

$$VAsteroid = \sqrt{\frac{\mu Sun}{Distance of Asteroid from Sun}}$$

Equation 5. 11

$$VApproach of Asteroid = \sqrt{2\mu Sun \times \left(\frac{1}{Distance of Asteroid from Sun} - \frac{1}{Distance of Asteroid from Sun + Distance of FlyBy planet from Sun} \right)}$$

Equation 5. 12

$$V\infty Asteroid Approach = VAsteroid - VApproach of Asteroid$$

Equation 5. 13

$$\Delta V Total to Asteroid = \Delta V FlyBy Planet Departure - \Delta V Asteroid Capture$$

Equation 5. 14

$$VAsteroidParking = \sqrt{2\mu Sun \times \left(\frac{1}{Distance of Asteroid from Sun} - \frac{1}{Distance of Planet from Sun + Distance of Asteroid from Sun} \right)}$$

Equation 5. 15

$$V\infty Asteroid Departure = VAsteroid - VAsteroidParking$$

Equation 5. 16

$$VPlanetParkingNew = \sqrt{2\mu Sun \times \left(\frac{1}{Distance of Planet from Sun} - \frac{1}{Distance of Planet from Sun + Distance of Asteroid from Sun} \right)}$$

Equation 5. 17

$$V\infty Earth Arrival = VPlanet - VPlanetParkingNew$$

Equation 5. 18

$$\Delta V_{\text{Total to Earth}} = \Delta V_{\text{Asteroid Departure}} - \Delta V_{\text{Earth Arrival}}$$

Equation 5. 19

$$\Delta V_{\text{Total Mission}} = \Delta V_{\text{to Asteroid}} + \Delta V_{\text{to Earth}} - \Delta V_{\text{FlyBy}}$$

Equation 5. 20

ΔV requirements for all mission concepts were calculated as shown in Appendix X and the mission concept number 4 was chosen which included Earth Departure> Mars Flyby> Asteroid Rendezvous>Asteroid departure > Earth Arrival.

The V_∞ for Earth departure and Mars Approach were calculated using the equations (5-3) and (5-6). The V_∞ for Mars Approach and Mars departure was the same with respect to the Planet's frame of reference but changed with respect to the heliocentric frame of reference. The flyby increased the spacecraft's velocity and the approach angle for the fly-by is as shown below:

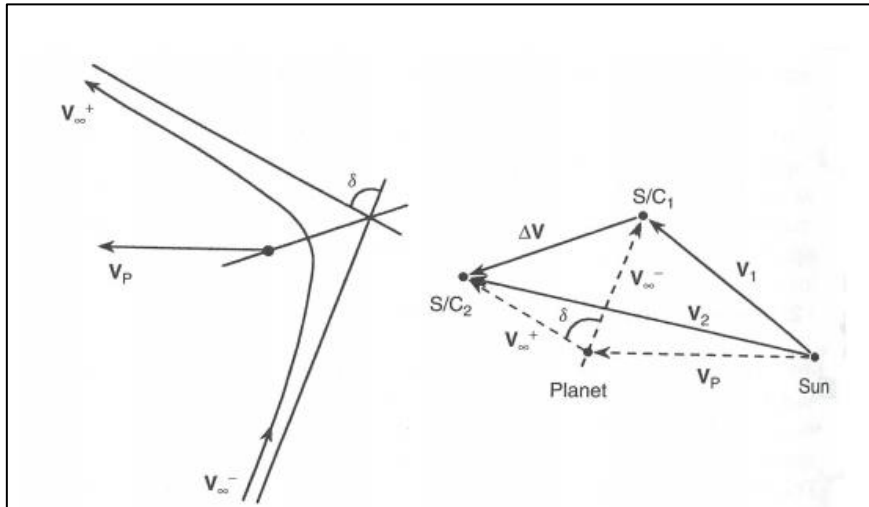


Figure 5. 2- The figure shows the Fly-By approach angle for a planet

Table 5.2 shows the deflection angle of the spacecraft due to the mars gravity well/sphere of influence and the ΔV reduction that the fly-by would offer. After the flyby sequence of operations the spacecraft starts the asteroid approach manoeuvre. The V_∞ for Mars departure and asteroid arrival are calculated using the equations (5-10) and (5-13). Once the spacecraft approaches the asteroid, the spacecraft then gets captured into the asteroids sphere of influence. The sphere of influence of the asteroid from earth and mars are calculated as shown below. The spacecraft is parked around the asteroid with a parking orbit of 10km. This helps the spacecraft orient itself wrt the asteroid and change its frame of reference from heliocentric to asteroid-centric. The ΔV required for asteroid capture and parking are shown in table 5.1

Table 5. 1- The table shows the ΔV calculation for the Mission using patched conics

True ΔV Calculation using Mars Gravity Assist				
Patched Conic Method				
μ_{Sun}	1.33E+20	m^3/s^2		
Earth distance from Sun	1	AU	1.50E+11	m
Mars distance from Sun	1.45	AU	2.17E+11	m
1989ML distance from Sun	1.1	AU	1.65E+11	m
Earth radius	6371	km		
Asteroid radius	0.15	km		
μ_{Earth}	3.99E+05	km^3/s^2		
μ_{1989ML}	4.47E-08	km^3/s^2		
μ_{Mars}	4.28E+04	km^3/s^2		
Earth parking	16371	km		
M fly-by altitude	50000	km		
Heliocentric Earth Departure				
V_{Earth}	29.78	km/s		
V_{parking}	32.40	km/s		
$V^\infty_{\text{Earth Departure}}$	2.62	km/s		
V_{Mars}	24.73	km/s		
V_{approach}	22.35	km/s		
$V^\infty_{\text{Mars Approach}}$	2.39	km/s		
Eccentricity of Arrival Trajectory at Mars				
eMars		7.65		
Deflection Angle				
δ	0.262158416	rad	15.02057	deg
$\Delta V_{\text{fly-by}}$	4.49	km/s		

Table 5. 2- The table shows the ΔV calculation for the Mission using patched conics

Heliocentric Mars Departure		
V ∞ Mars Departure	2.39	km/s
V1989ML	28.40	km/s
VAapproach	30.28	km/s
V ∞ Asteroid Approach	1.89	km/s
ΔV Mars Hyperbolic Departure		
Vparking around Mars	2.72	km/s
Vcircular around Mars	0.93	km/s
$\Delta V1$	1.80	km/s
ΔV Asteroid Arrival Hyperbolic Capture		
Asteroid Parking distance	10.15	km
VcircularAsteroid	0.00006637	km/s
VparkingAsteroid	1.89	km/s
$\Delta V2$	1.89	km/s
$\Delta V_{\text{total to asteroid}}$	3.68	km/s
Heliocentric Earth Arrival		
V1989ML	28.40	km/s
VApproach	27.71	km/s
V ∞ Asteroid departure	0.68	km/s
VEarth	29.78	km/s
VParking	30.48	km/s
V ∞ Earth Arrival	0.70	km/s
ΔV Asteroid Hyperbolic Departure		
Asteroid Parking	10.15	km
VcircularAsteroid	0.00006637	km/s
VparkingAsteroid	0.68	km/s
$\Delta V1$	0.68	km/s
ΔV Earth Hyperbolic Arrival		
VParking	7.01	km/s
VCircular	4.93	km/s
$\Delta V2$	2.08	km/s
$\Delta V_{\text{total to Earth}}$	2.76	km/s
$\Delta V_{\text{total mission}}$	1.95	km/s

The inclination changes are not captured and is included as a part of future work. Proximity operations begin after the asteroid phase to get closer to the asteroid and capture the asteroid properties and to select a landing site. The ΔV for proximity operations is calculated in Section 5.4. Once the proximity operations are completed the spacecraft lands for mining operations. It is noted that the mining does not happen in one phase and the spacecraft completes this in multiple phases for which the ΔV is not calculated and is a part of future work. Detailed mining operations are mentioned in Section 12

Even if these calculations are somewhat flawed in their ΔV assumptions they were able to show the preliminary ΔV requirements that realistically could be achieved by using Liquid propulsion techniques discussed in Section 6

5.4 ΔV Budget for Proximity Operations

The ΔV budget for proximity operations gives us an estimation of the ΔV required for the first order of approximations of the mapping of the asteroid. Proximity operations is a set of multiple operations such as mapping, de-orbiting manoeuvres and rehearsal manoeuvres for landing on the asteroid. As a part of first order of approximations only asteroid mapping manoeuvres are considered. To calculate this equation show below are used.

$$\text{Area of mapping Camera Coverage} = \text{Spacecraft Altitude} \times \tan \frac{\text{Field Of View}}{2}$$

Equation 5. 21

$$\text{Surface Area of Asteroid} = 4\pi \times \text{Radius of asteroid}^2$$

Equation 5. 22

$$\text{Number of Passes required} = \frac{\text{Surface area of Asteroid}}{\text{Area of mapping camera coverage}}$$

Equation 5. 23

$$\sum_{\text{Transfer orbit} = 10}^{0.5} \text{Total } \Delta V = \sqrt{\mu_{\text{Asteroid}} \left(\frac{1}{\text{Transfer orbit}} - \left(\frac{2}{\text{Transfer Orbit}} - \frac{2}{\text{Transfer Orbit} + \text{Transfer Orbit New}} \right) \right)}$$

Equation 5. 24

$$\Delta V \text{ expendable in each phase} = \frac{\text{Total } \Delta V}{\text{Number of phases}}$$

Equation 5. 25

NAC and WAC cameras are used for mapping operations for our mission. The field of view for the cameras are found to be 4° and 21° and using equation (5-20) coverage area of the camera is found. The NAC and WAC are chosen based on the OSIRIS-Rex mission [9] .

The assumptions made here are that the spacecraft deorbits from a parking orbit of 10 km to 5km, 2km, 1 km and 500m gradually before landing.

Table 5. 3- The table shows the ΔV calculation for proximity operations

Proximity Operations			
Asteroid centre fixed co-od sys			
μ_{asteroid}	4.47E-08	km ³ /s ²	
Sidereal Orbital period around the sun	524	days	
Synodic rotation	19	h	

Table 5. 4- The table shows the number of passes required for proximity operations for NAC

Mapping Operations	NAC							
FOV	4	deg	4	deg	4	deg	4	deg
h	5	km	2	km	1	km	0.5	km
Area of coverage	0.175	km	0.070	km	0.035	km	0.017	km
radius of asteroid	0.15	km	0.15	km	0.15	km	0.15	km
SA of asteroid	0.283	km ²						
Number of passes required	1.62	passes	4.05	passes	8.10	passes	16.19	passes
	~2	passes	~4	passes	~8	passes	~16	passes

Using equation (5-22) the number of passes are found to be ~34 passes as shown in table 5.4 and the ΔV for those passes are found using standard Hohmann transfer equations.

Table 5. 5- The table shows the number of passes required for proximity operations for WAC

Mapping Operations	WAC			
FOV	21	deg	21	deg
h	2	km	0.5	km
Area of coverage	0.371	km	0.093	km
radius of asteroid	0.15	km	0.15	km
SA of asteroid	0.283	km ²	0.283	km ²
Number of passes required	0.76	passes	3.05	passes
	~1	passes	~3	passes

Table 5. 6- The table shows the total number of passes for proximity operations for the mission

Total number of orbits to Map	33.77169285		passes
	~34		passes

Table 5. 7- The table shows the ΔV requirements for different parking orbits

Transfer Orbit	10.15	km	5.15	km	km	2.15	km	1.15	km
v1	7E-05	km/s	9E-05	km/s	km/s	0.0001	km/s	0.00019719	km/s
v2	5E-05	km/s	8E-05	km/s	km/s	0.0001	km/s	0.000168	km/s
ΔV	1E-05	km/s	1E-05	km/s	km/s	2E-05	km/s	2.96107E-05	km/s

The total ΔV required for proximity operations is found to be 13.38 cm/s and the total ΔV expendable per pass is around 0.405 cm/s considering a circular orbit around the asteroid. The ΔV for proximity operations is fairly the same order of magnitude as the proximity operations as that of OSIRIS REX [10] [9] [8]

Table 5. 8- The table shows the ΔV requirements for proximity operations

Number of passes	34	
ΔV per pass	0.405	cm/s
Total proximity ΔV	9E-05	km/s
	8.917	cm/s
50% margin	1E-04	km/s
	13.38	cm/s

Table 5. 9- The table shows the ΔV expendable in each phase

FOV (deg)	4	4	4	4	21	deg
H (km)	5	2	1	0.5	2	km
Number of passes	2	4	8	16	1	passes
ΔV Expendable in each phase (cm/s)	0.81	1.62	3.24	6.49	0.41	cm/s

5.5 Critique and Concept of Operations for Selected Mission Architecture

Once the ΔV budget is found for the mission we can capture the detailed Concept of operations for the mission as shown in table 5.10. The ΔV calculations in Section 5 are first order of operations using the Patched conics method and need to be further investigated using a simulation tool such as STK. The ΔV budget changes If the parking orbits around earth and the asteroid are changed and also the fly-by altitude around mars is changed.

The second order of approximation after calculating the ΔV budget was to optimise the flyby altitude around mars for the same ΔV reduction caused by the planets SOI. This optimisation is done by finding the ΔV reduction at corresponding fly-by altitudes. The trend is plotted as shown in Figure 5.9 and the maximum is found.

The fly-by altitude values are optimised for the same preliminary ΔV calculated in section 5.5 and the final optimised fly-by altitude is found to be 31,897 km or 47,497 km rather than the previously assumed 50,000km.

Table 5. 10- The table shows the operational elements for our mission [8] [9]

Based on Mission Analysis of Osiris - REX (Direct derivation of mission Phases)		
Earth Departure	Launch	Launch from Earth Parking Orbit Geocentric Frame of Reference
	Gravity Assist	Mars Gravity Assist Heliocentric Frame of reference
	Cruise	Interplanetary cruise from Earth to Mars Fly-by ; Mars to Asteroid Heliocentric Frame of reference
Destination Rendezvous	Asteroid Approach and Arrival	Hyperbolic trajectory V_∞ ; To locate 1989ML visually and to survey for any potential hazard; Collect spectral imagery to generate detailed shape of model, Change Co-ordinate system to Asteroid Centric and Evaluate its spin state
	Preliminary Asteroid Survey	Estimate Mass, refine spin state and refine Asteroid model
	Injection into Asteroids Orbit	10 km from asteroid
	Detailed Asteroid Survey	Viewing angles, use spectrometer to map chemical composition, high resolution images , identify possible mining sites, hazard map
	Sample Site Selection	Refine mining site selection, slews between north and south pole , trade based on safety, scientific value and high ore value, 5 to 1km
	Reconnaissance	Flyovers over mining sites , assess for further suitability, topography , Autonomous Nav System needed to navigate surface of asteroid during collection, further reduction in flyover range 500m high resolution imagery
	Rehearsal	Leaving its orbit, reaching a checkpoint to approach sample site, checks controllability and manoeuvrability
	Mining Operation	Collection of regolith through mining, short bursts of time, multiple times, after set time spin the spacecraft to check ore weight collected (at the end or between each mining operation) Comes at a fuel cost
Destination Departure	Cruise	Hyperbolic trajectory V_∞ ; Change of co-ordinate systems back to star-based ; Asteroid to Earth
Earth Return	Insertion to LEO or Cis-Lunar	Change of Co-ordinate system to Geocentric and Spacecraft insertion into LEO or GEO

Table 5.10 shows the different operational elements for different phases of the mission whereas Table 5.11 shows the different operational modes of different sub-systems for the mission. The table is colour coded as Red, Green and Yellow which indicates that the sub-system is either inactive, active or on standby respectively. Table 5.10 is a direct derivative of the OSIRIS-Rex mission and this was chosen because both the mission have a lot of similarities in terms of the concept of asteroid mining and resource return. [8] [9]

Table 5. 11- The table shows the operational modes of sub-systems for different phases of the mission

Phase of mission		Propulsion	AOCS	Orbits	Structure	Thermal	Payload	Power	Communication	OBDH	EA	Mining
Earth Departure	Launch											
	GA											
Asteroid Rendezvous		Preliminary Asteroid Survey	Asteroid Approach	Cruise								
Earth Return	Asteroid Departure		Proximity Operations									
Insertion to LEO or Cis-Lunar	Cruise	Launch	Mining Operation	Rehearsal	Reconnaissance	Sample Site Selection	Detailed Asteroid Survey	Injection into Asteroid Orbit				

Mission concept of operations can be summarised by the following figures (Figure 5.3 to Figure 5.6): It is to be noted that all these manoeuvres are impulsive manoeuvres.

- Earth Departure
- Mars Approach
- Mars Fly-by
- Asteroid Approach
- Asteroid Arrival
- Proximity Operations
- Mining Operations
- Asteroid Departure
- Earth Arrival

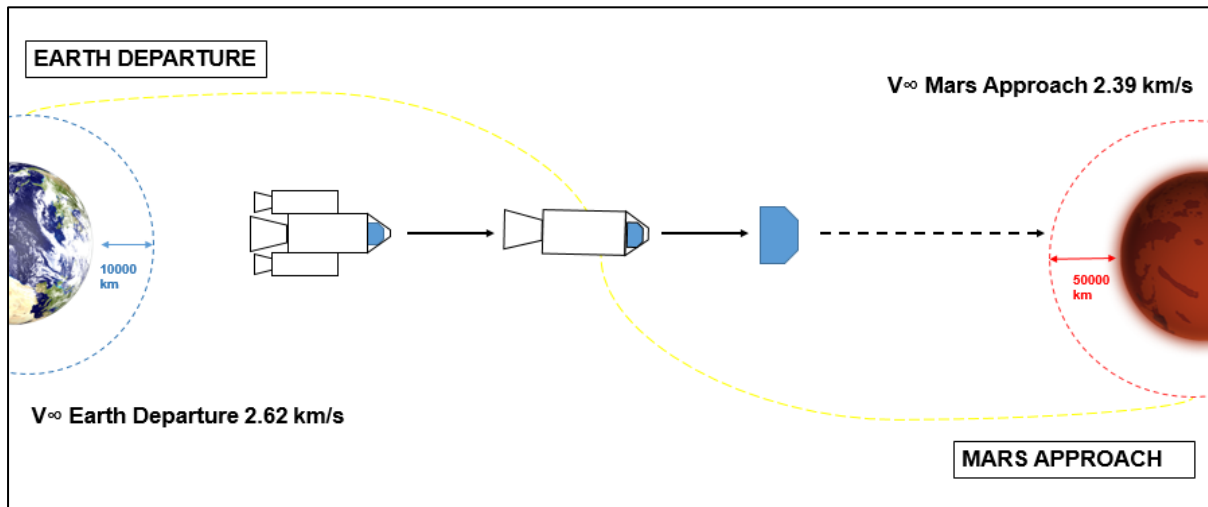


Figure 5. 3- The figure shows the interplanetary transfer of the Spacecraft using a hyperbolic trajectory from Earth Departure to Mars Approach.

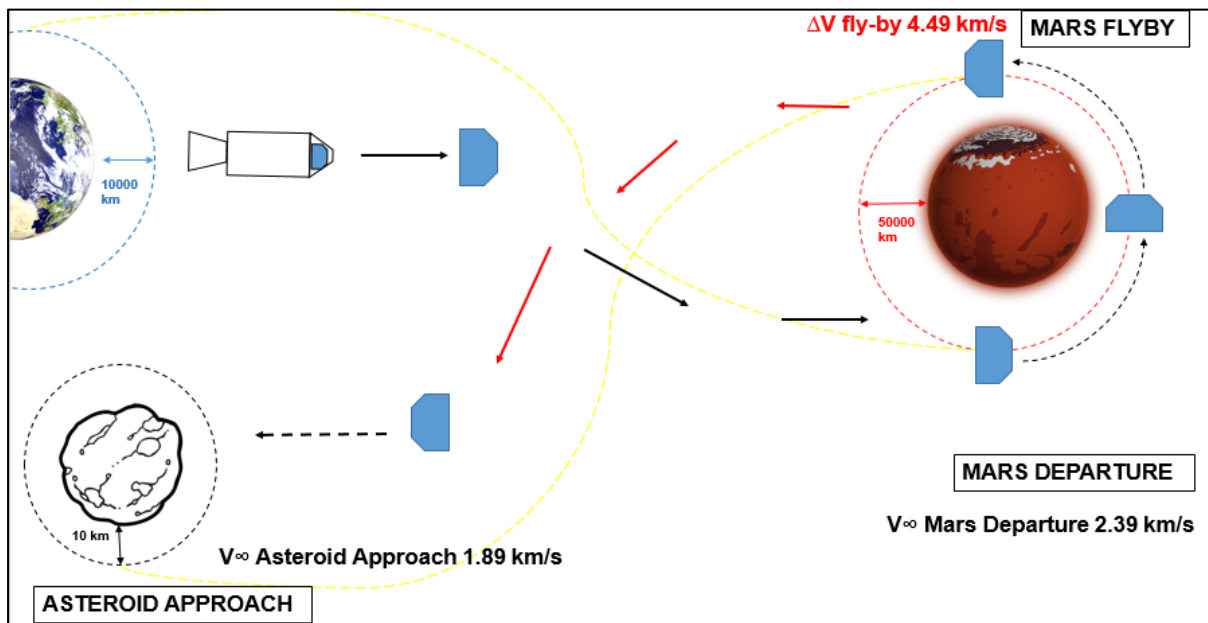


Figure 5. 4- The figure shows the Martian Fly-By of the Spacecraft which then takes a hyperbolic trajectory to the asteroid 1989ML from Mars departure to Asteroid Approach

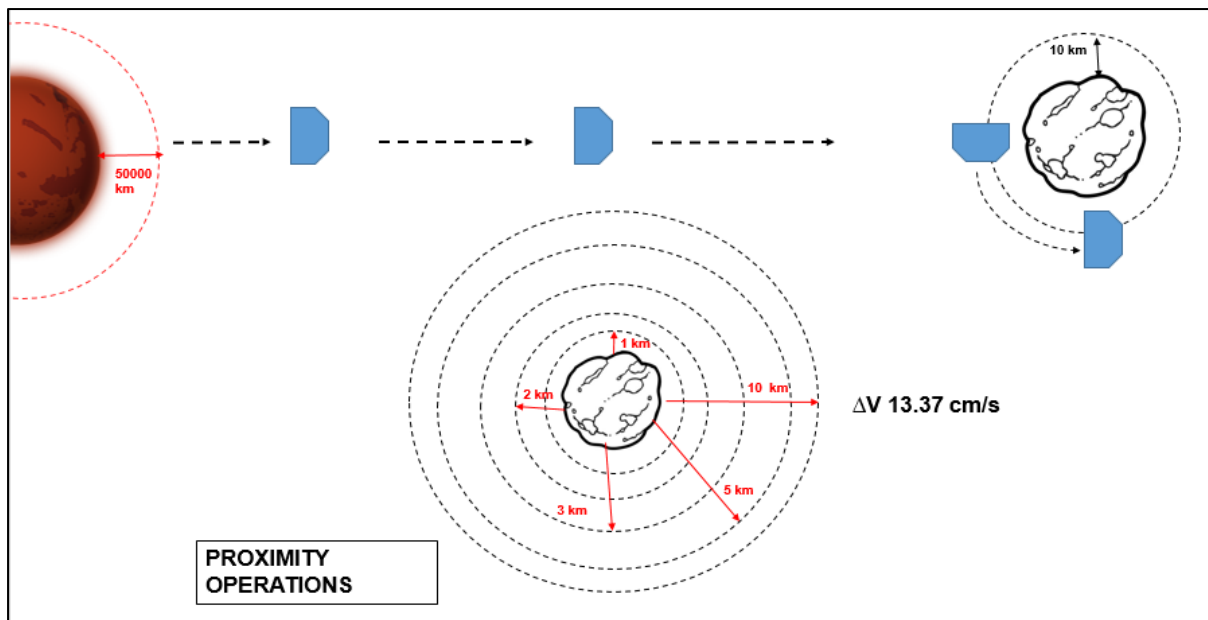


Figure 5. 5- The figure shows the Inter-Asteroid phase i.e. Proximity Operations performed by spacecraft (Mapping manoeuvres)

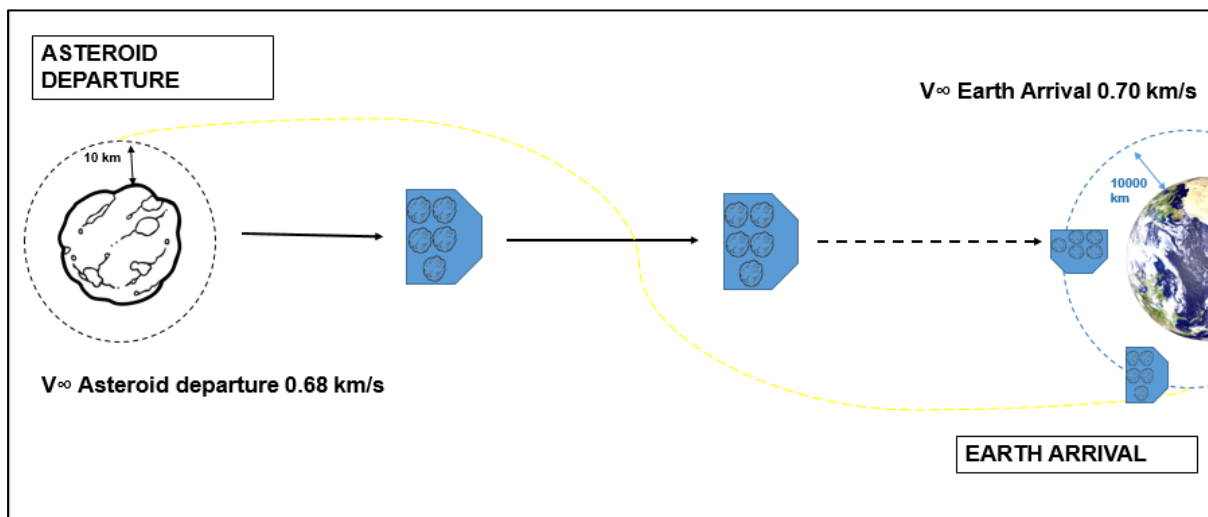


Figure 5. 6- The figure shows the interplanetary phase of the spacecraft which takes a hyperbolic trajectory from Asteroid departure to Earth Arrival

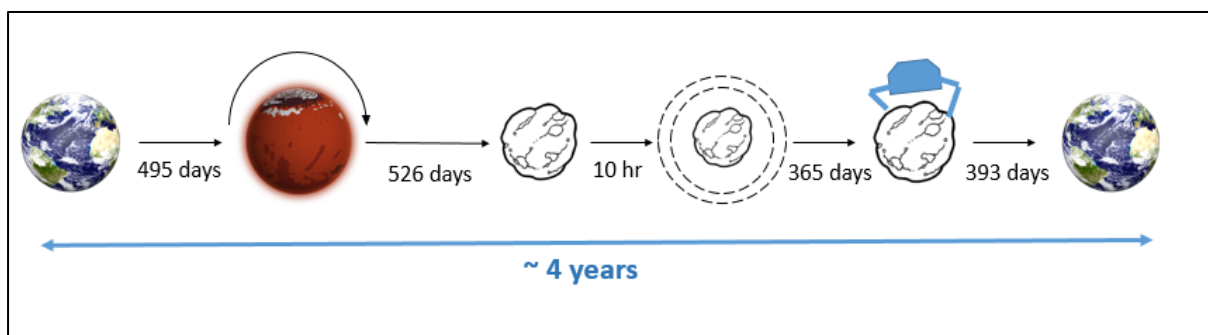


Figure 5. 7- The figure shows the overview of the mission timeline

The preliminary mission time calculated is ~4 years as shown in Appendix D

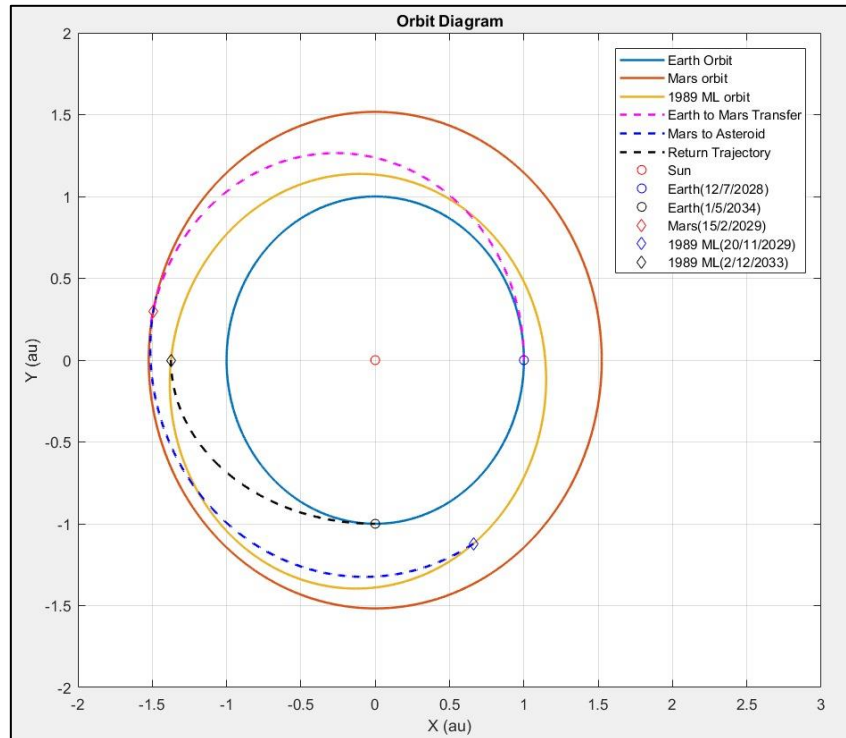


Figure 5. 8- The figure shows the orbit diagram for the mission

The orbital diagram for the mission is shown in Figure 5.8 which is estimated using MATLAB in Appendix C.

Table 5.12 and Figure 5.9 show the ΔV reduction to Mars Flyby altitude trend for the mission. The fly-by altitude is optimised using this data by considering the maxima of the curve for maximum reduction in ΔV due to the Martian gravity well.

Table 5. 12- The table shows the ΔV for different fly-by altitudes

Flyby altitude (km)	ΔV Flyby(km/s)
1000	3.66
5000	3.39
10000	1.32
15000	2.90
20000	0.70
25000	3.43
30000	4.03
40000	1.51
45000	4.44
50000	4.49
55000	2.79
60000	0.52
65000	1.56
70000	3.14

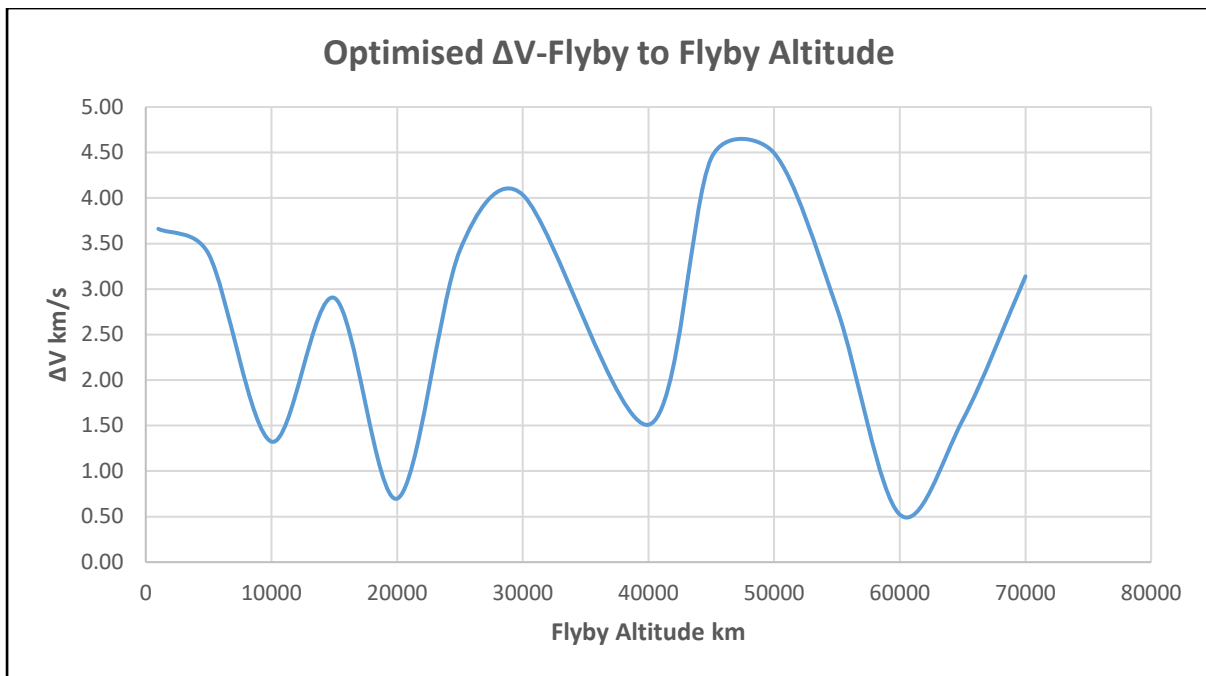


Figure 5. 9- The figure shows the plot between ΔV and the flyby altitude to find the optimal flyby altitude

Table 5. 13- The table shows the optimal flyby altitude

Flyby alt (km)	e	δ (rad)	ΔV (km/s)	Final Mission ΔV
47497.74146	7.32E+00	2.74E-01	4.77318	1.61
61174.05837	9.14E+00	2.19E-01	2.2E-06	6.39
31897.55217	5.24E+00	3.84E-01	4.77318	1.61

The total ΔV for the mission is 1.61 km/s with a ΔV of 4.49 km/s reduction due to the Martian fly-by with a fly-by altitude of either 47,497 km or 31,897 km. The spacecraft is parked at an altitude of 10km around the asteroid and is slowly deorbited to around 1km prior landing for proximity operations with a ΔV of 13.38 cm/s with a 50% margin.

To conclude, the total ΔV of the mission is 1.61 km/s if the spacecraft performs a fly-by manoeuvre at 31,897 km.

6 Propulsion Sub-System

6.1 Introduction

This Chapter discusses the propulsion system used for the mission using the ΔV requirements from Mission Analysis. Having established the ΔV required from the equations in Section 5, lift off mass of the spacecraft is found for the mission. This preliminarily helps us in selecting a launcher that is capable of launching the spacecraft to the Target Asteroid. Further launcher propulsion study needs to be conducted that isn't part of this report.

The estimation of requirements are summarized as follows:

1. The Propulsion system of the spacecraft shall have sufficient propellant to perform high impulsive burns to change trajectories and for autonomous or assisted landing on the Asteroid during Proximity operations and Mining Phase.
2. The launcher selected shall be able to launch the given spacecraft into Orbit from whereon which the spacecraft propulsion system including staging will take over.

Some of the system assumptions made were:

- a) Payload: The initial payload mass was estimated at 2048 kg before mining. Asteroid regolith Resource mass is 500 kg.
- b) 340 s ISP: This value is standard for a Hydrazine and Nitrogen-Tetroxide liquid propulsion engine.
- c) The storage container for the asteroid regolith was considered to be a cube with dimensions of 0.61m

6.2 Trade Of Different propulsion systems for the Mission

Different propulsion systems were considered for the mission such as: Liquid propulsion system, Cryogenic propulsion system, Electric propulsion system, solar electric propulsion and nuclear propulsion. At this stage, a top-level analysis was performed to evaluate the advantages and disadvantages of each. This report focuses on the liquid propulsion and electric propulsion options.

Other propulsion methods were not considered because of reasons stated below:

- a) Solar Electric Propulsion although has low specific mass in the order of 10-20 kg/kW it is highly dependent on the solar flux from the Sun and at the distance of 1.45 AU its specific power decreases. This kind of propulsive method cannot be used during an eclipse which restricts the trajectory design. Solar cells suffer degradation due to ionising radiation of Van Allen belts and since it is low thrust trajectory, the orbits can only be raised slowly.
- b) Nuclear Propulsion although can provide high thrust and is independent of Eclipse conditions was not considered because of reactor waste heat. Where the reactors have a limited efficiency in converting heat to electricity, which includes inclusion of large radiators which is not feasible due to high volumes that cannot be accommodated within the payload fairing of the launcher. This propulsive method also needs higher dry mass and requires additional radiation and thermal shielding increasing the complexity and mass of the spacecraft system.

- c) Cryogenic Propulsion systems are complex and not desirable for long-duration missions such as this, due to boil-off effects of the propellants. Furthermore, if the system is pressure-fed, then the pressurizing gas must also be cooled to cryogenic temperatures to pressure the propellant tanks.

A note to both systems (Liquid propulsion systems and Electric propulsion systems) is their difference in terms of the trajectory design to impulsive transfers: liquid propulsion systems can provide impulsive transfers whereas electric propulsion systems need low trajectory manoeuvres which use long arcs to minimize both propellant and power requirements. This results in long ToFs which is not desirable.

Some of the common advantages and disadvantages deriving from the propulsive elements are reported here. Their dissimilarities are listed as below:

Advantages of Electric propulsion	Advantages of Liquid propulsion
<p>ISP: Electric propellants are in the order of 3000-8000 s and can leverage on the efficiency of engines to require a limited amount of propellant, therefore raising Payload Fraction and reducing Mass ratio.</p> <p>Flexibility in outbound/inbound departure dates: low thrust trajectories considerably expand transfer opportunities due to the ability of performing long thrusting arcs.</p> <p>Easier handling of propellants: in comparison to LH₂, the heavy ion propellants of Electric propulsion</p>	<p>Long trajectory geometries: due to the long arcs required for achieving efficiency and realistic power levels, TOF is severely longer and might not fit within the Mission timeline for Electric Propulsion which is not the case with Liquid propulsion</p> <p>Propellant availability: no Electric propellant is produced globally on the scale required for the Mission (while Chemical leverage the commonality to Launchers' propellants).</p> <p>Thrust: Electric Propulsion systems although have High ISPs have very low thrust outputs. Liquid Propulsion systems have high thrust outputs.</p> <p>Complexity : The Complexity of electric propulsion is higher than that of regular liquid propellants and have a higher failure mode as it does not have space heritage for long term missions and is currently used only for AOCS purposes</p> <p>Power: Power required for Electric propulsion is much higher than that required for Liquid propulsion systems and Higher power requirements leads to higher overall dry mass of spacecraft</p>

Since the disadvantages of electric propulsion outweigh the advantages, it was decided that the mission will use Liquid propulsion system. This decision was also made based on the fact that previously flown missions such as OSIRIS Rex also used liquid propulsion systems for impulsive burns, manoeuvring and AOCS [8] [9]. Hayabusa used Ion thrusters for their propulsion system [14] [15] but the sample return was <1g and the mission timeline was around 6 years which is longer than our mission timeline and hence electric propulsion wasn't preferred. Electric and other propulsion systems may be explored as a part of future work. It is noted that there wasn't a time constraint for the mission, yet liquid propulsion was chosen for reasons listed in Section 6.2. Electric propulsion can be explored as part of future work.

6.3 Selection of Propellant and Preliminary Propellant Budget

Once the Liquid propulsion system was chosen the next step in the process was to choose if Monopropellant system or Bipropellant system was best suited for the mission. Solid rocket motors were not considered as they do not have throttleability and manoeuvrability capabilities and this was important for the mission as precision manoeuvres were required for low gravity environments of the Asteroid and mining operations.

The advantages and disadvantages of monopropellant and bipropellant systems are listed below:

Advantages of Monopropellants	Advantages of Bi-propellants
<p>Complexity: Monopropellant systems are less complex compared to bi-propellant systems and are mainly used for AOCS.</p> <p>Cost : Monopropellants are more affordable than bi-propellants</p> <p>Reliability : Monopropellants are more reliable than Bi-propellant systems</p>	<p>Performance: Monopropellant systems have lower performance than bi-propellant</p> <p>ISP: The bi-propellant systems have higher ISP values and have higher Thrust outputs.</p>

Mainly for the reasons listed above, a bi-propellant system was chosen for the mission with propellants Hydrazine and Nitrogen-Tetroxide. Monopropellant systems can also be considered as it was chosen for the OSIRIS Rex mission which used only Hydrazine [9]. OSIRIS Rex had a sample return of 60g but our mission has a minimum requirement of 500kg resources return. Hence the payload mass fraction for the chosen bi-propellant was higher than monopropellant system.

$$M_f = M_{propellant} + M_{dry}$$

Equation 6. 1

$$\Delta V = ISP \times \ln \frac{M_0}{M_{final}}$$

Equation 6. 2

$$M_{fuel} = M_f - M_0$$

Equation 6. 3

$$V \text{ of regolith Container} = l \times b \times h$$

Equation 6. 4

Table 6. 1- The table shows preliminary fuel calculations for Asteroid rendezvous

InterAsteroid Phase				
Nitrogen Tetroxide	ISP	3335.4	m/s	
Hydrazine				
ΔV	3620	m/s		
Instrument mass	22.64	kg		
density of Al₂O₃	2.2	g/cm ³		
	2200	kg/m ³		
m of ore	500	kg		
density of Pt	2145	kg/m ³		
V of Pt ore	0.2331	m ³		
I,b,h	0.615433	m		
t	0.01	m		
R	0.625433	m		
V of storing shell	0.011548	m ³		
m of shell	25.40641	kg		
Total payload mass= Instrument mass + Shell mass + dry mass(33% of M_f)	48.04641	2000	2048.046	kg
M₀	6063.05	kg		
M_{fuel}	4015	kg		

Table 6. 2- The table shows preliminary fuel calculations for Earth rendezvous

Post Mining Phase			
Nitrogen Tetroxide	ISP	3335.4	m/s
Hydrazine			
ΔV	2760	km/s	
Instrument mass	22.64	kg	
Ore mass	500	kg	
Total Payload mass	2548.04	kg	
M_0	5828.81	kg	
M_{fuel}	3280.77	kg	

Table 6.1 uses equations (6-1) to (6-4) to calculate the fuel required for the spacecraft from earth to asteroid assuming a direct transfer which is found to be ~4 tonnes. Table 6.2 calculates the fuel required for the spacecraft from Asteroid to Earth post mining which is found to be ~3.2 Tonnes. It is to be noted that these are preliminary values of propellant requirements and the final propellant required is calculated in Section 6.4 for the entire mission.

6.4 Launch mass of the Spacecraft for the Mission and Selection of Launch Vehicle

Once the preliminary propellant mass is calculated the next step is to calculate the lift-off mass i.e the total mass of propellant required for the mission with an assumption of dry mass of around 2 tonnes for initial payload mass of ~100 kg. [21]

A stage separation study must be conducted to estimate the optimal number of stages required for this mission to ensure fuel requirements are minimized. This may be done by taking valid assumptions on the dry mass per stage, and estimating the fuel requirements using the ideal rocket equation [21]. Delta – V requirements are split equally between the number of stages, and the results are shown in the following figure.

It is seen the optimal number of stages is 3. The final stage of the mission will also be responsible for the return journey to planet earth.

Table 6. 3- The table shows the fuel calculations for different stage separations

No Separation			Stage Separations					
			S3		S2		S1	
$M_{payload}$	100	kg	100	kg	1292.3	kg	3004.3	kg
M_{dry}	2000	kg	800	kg	800	kg	800	kg
M_{total}	2100	kg	900	kg	2092.3	kg	3804.3	kg
ISP	3335.4	m/s	3335.4	m/s	3335.4	m/s	3335.4	m/s
ΔV	3620	m/s	1206.7	m/s	1206.7	m/s	1206.7	m/s
M_0	6216.9	kg	1292.3	kg	3004.3	kg	5462.5	kg
M_{fuel}	4116.9	kg	392.29	kg	912.0	kg	1658.2	kg

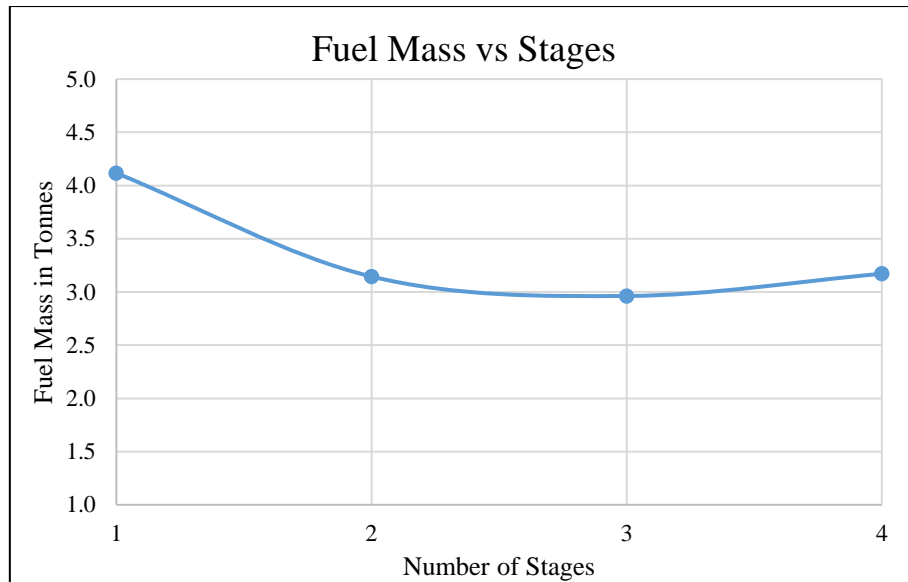


Figure 6. 1- The figure shows the plot for Fuel mass vs Number of Stages

The next step is to refine the total propellant required for the mission which is calculated in Table 6.4 using the ΔV for mission as 1.6 km/s. The total fuel required for the mission is found to be 4.62 tonnes. It is noted that there are heavy fuel constraints for the return journey as the spacecraft is carrying 500 kg of regolith ore. The fuel required to reach the asteroid is 1.273 tonnes for a dry mass of 2000kg and the spacecraft mass of around 100 kg.

Table 6. 4- The table shows the Total fuel required for the entire mission

Mission	ISP	DV	M0	MF	MPROP
Asteroid to Earth	3335.4	2760	5947.663	2600	3347.663
Earth to Asteroid and back	3335.4	1610	12068.53	7447.663	4620.864

6.5 Fuel Tank design

As a flow-down from the total propellant required for the mission, the next step would be to calculate the amount of oxidiser and fuel required for a bi-propellant system which is calculated using the equations (6-5) to (6-10)

$$Fuel\ mass = \frac{Total\ propellant\ mass}{1 + Mixture\ ratio}$$

Equation 6. 5

$$Fuel\ Volume = \frac{Fuel\ Mass}{Fuel\ density}$$

Equation 6. 6

$$\text{Oxidiser mass} = \text{Fuel mass} \times \text{Mixture ratio}$$

Equation 6. 7

$$\text{Oxidiser Volume} = \frac{\text{Oxidiser Mass}}{\text{Oxidiser density}}$$

Equation 6. 8

$$\text{Thickness of Tank} = \frac{\text{Maximum Operating Pressure} \times \text{Volume of Fuel or Oxidiser}}{2 \times \text{UTS of Tank Material or Hoops stress for thin walled pressure vessels}}$$

Equation 6. 9

$$\text{Radius of Tank} = \sqrt[3]{\frac{3 \times \text{Volume of Propellant}}{4\pi}}$$

Equation 6. 10

Table 6. 5- The table shows the Calculation of Fuel and oxidiser mass for the mission

Total Fuel	4620.864462	kg
Mixture ratio and Mass of ox/Fuel		
0.9		
ox		fuel
2188.83	kg	2432.03
Density of Ox/ Fuel (kg/m3)		
Density of Hydrazine	1.021	g/cm3
Density of N2O4	1.442	g/cm3
Volume Calculation of ox/Fuel(m3)		
ox		fuel
1.517	m3	2.382
Radius Calculation of PMD Tank in m		
0.712	m	0.828
Thickness Calculation of PMD Tank		
UTS / σTitanium	950	Mpa
Pressure (P1)	22	Bar
ox		fuel
0.00175	m	0.00275
0.175	cm	0.275

Table 6.5 shows the amount of oxidiser and propellant fuel required for the mission assuming a mixture ratio of 0.9 [22]. The amount of oxidiser required for the mission is 2.18 Tonnes and the amount of fuel required is 2.43 tonnes which is calculated using then equations (6-5) and

(6-7). Titanium tanks of 2310 litres and 2500 litres (customised) for the propellants the Northrop Grumman data sheets. [23]. The tanks are assumed to be spherical while developing the structure of the spacecraft but can be cylinders with rounded tops and bottoms. These tanks are pressure fed using a pressurant which is discussed in Section 6.6.

6.6 Pressurant Tank design

The tanks are pressurised using Helium as a pressurant because an inert gaseous pressure fed system prevents cavitation of the propellants and maintains the desired tank pressure during low gravity operations without any of the propellants resettling back into the tanks. Furthermore, Helium is ideal as it remains in its gaseous state even at low temperatures such as 273K

$$\text{Volume of pressurant tank} = \frac{\text{Volume of Propellant} \times \text{Pressure of Propellant tank}}{\text{Pressure of pressurant tank}}$$

Equation 6. 11

$$\text{Mass of pressurant fluid} = \frac{\text{Volume of Pressurant tank} \times \text{Pressure of pressurant tank}}{\text{Temperature} \times \text{Gas Constant}}$$

Equation 6. 12

Table 6. 6- The table shows the mass of Helium pressurant required for the mission

Pressure Calculation of Pressurant Tank					
Volume of ox/Fuel (V1)					
Ox/Fuel					
4620.86			l		
Pressure (P1)	20.7	Bar	2070000	Pa	N
Pressure (P2)	350	Bar	35000000	Pa	N
Pressure of Pressurant Helium(V2) Calculation using Boyle's Law (P1V1=P2V2)					
Volume of Tank(V2)	273.2911267	l	0.27329	m3	
Mass of Pressurant Helium Calculation using PV=mRT (288K)					
Mass of Helium	15.99			kg	

Using the equations (6-11) and (6-12) , the Ideal gas law and the Boyles law the mass of Helium required to pressure the Propellants is ~16 kg which is pressured at 350 Bar.

6.7 Conclusions

To conclude the summary of propulsion system for our mission is:

- 1 titanium Fuel tank of Hydrazine propellant having capacity of 2500 litres with a nominal operating pressure of ~20 Bar.
- 1 titanium Oxidiser tank of Nitrogen Tetroxide Oxidiser of 2310 litres with a nominal operating pressure of ~20 Bar

- c) 1 titanium Pressurant tank of gaseous Helium pressurant which is pressured at 350 Bar [24]
- d) Feed system components (Selection and design as a part of future work)
- e) A selection of thrusters were selected by finding the thrust required for the mission using similar Thrust to weight Ratios. As shown in Table 6.7. It is noted that this is a preliminary calculation and a concrete value needs to be decided upon through rigorous AOCS design.
- f) The thrust required for the mission is ~15kN as shown in Table 6.7
- g) The spacecraft reaches the Asteroid with 3 stage separations and the final spacecraft module return to earth with 500kg of regolith ore. Figure 6.2 shows the fuel requirements for separate stages.
- h) The spacecraft has a thrust to weight ratio of 2.20
- i) The effective ISP for the mission is 296.27 s

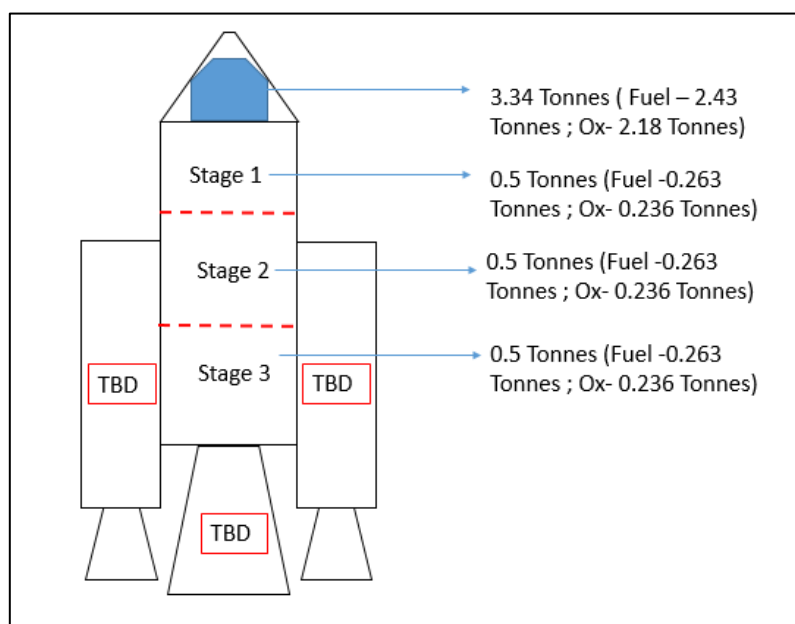


Figure 6. 2- The figure shows the different stages for the mission

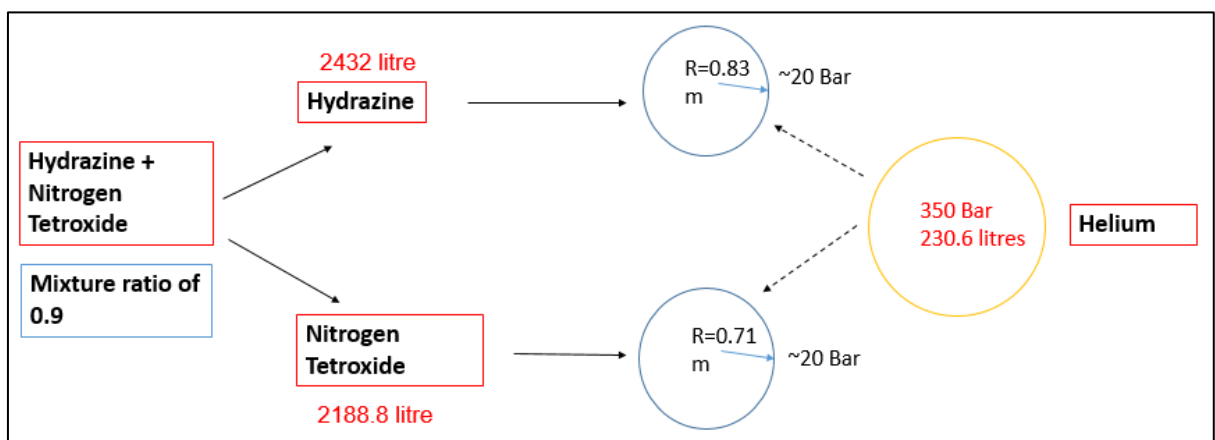


Figure 6. 3- The figure shows the Propulsion system and its components for the mission

Table 6. 7- The table shows the Effective ISP and Net Thrust required for the mission

Number	Thrust	Total Thrust		Flow rate				
2	4000	8000		2.8	kg/s			
8	890	7120		2.4	kg/s			
10	22	220		0.074	kg/s			
8	4	32		0.0145	kg/s			
4	0.09	0.36		0.0002	kg/s			
Net Thrust		15372.36		Net Flow Rate	5.29	kg/s		
Effective ISP	2906.42			m/s				
	296.27			s				

7 AOCS Sub-System

7.1 Introduction

The Interplanetary Trajectory phases of the Mission ,proximity and mining operations in low gravity conditions will have constraints upon the ability of the spacecraft to set and maintain correct attitude and know where they are in space and how they are oriented. These tasks are taken care of by the Attitude and Orbit Control System and by the Navigation System. These are very well known and implemented systems in the space industry, and their use in interplanetary missions to Asteroids and other planets is also well documented. [9] For this reason and given the level of development of industry-standard architectures, as well as the systems-level approach of this study, an in-depth analysis of this system was not performed. However, the need for mining in low-gravity conditions significantly increases the capability that it would need to have. The Attitude and Orbit Control System WP is aimed at determining what type of equipment would be needed to allow station-keeping, proximity and mining operations and verify if they present any relevant impact on the Mission Architecture.

The estimation of requirements, given the scope of this WP, rested mostly on similarity to proposed concepts in similar Mission profiles involving Rendezvous and tagging of Osiris rex [9] [8] and Interplanetary Trajectories to Planets. They are not reported here in detailed form but are instead summarized as follows:

1. The AOCS & Navigation System of the spacecraft shall have sufficient control authority to perform autonomous or assisted landing on the Asteroid during Proximity operations and Mining Phase.
2. The AOCS & Navigation System shall be capable of correctly orienting the spacecraft for the Main Impulsive Manoeuvres
3. The AOCS & Navigation System shall be capable of performing Midcourse Corrections and Attitude Control, as well as positional and attitude determination, during the Deep Space transit.
4. The AOCS shall be capable of performing the station-keeping of the spacecraft both in Earth Orbit and Asteroid orbit.

7.2 Initial Design Options

The initial design options for the System were conducted to address three issues:

1. Definition & Selection of Stabilisation Methods
2. Selection of Attitude Determination Sensors
3. Selection of Attitude Control Actuators

These three steps were designed for three different scenarios: one considering the spacecraft orbiting Earth or Asteroid, one considering the spacecraft during its Deep Space transit and one considering the Mars Flyby scenario. These phases of the mission have different disturbance torques, positional references and employable technologies, as well as in the type of manoeuvres the spacecraft needs to implement in the context of each. These different design points are listed below which is based on the International Handbook of Space Technology [25] [21]

- a) Spacecraft orbit Attitude Determination and Control around Earth and Asteroid

Table 7. 1- The table shows the different stabilisation methods considered for the Asteroid phase of the mission

Stabilisation Methods	
Design Point 1	Bias Momentum Stabilisation
Design Point 2	Dual Spin Stabilisation
Design Point 3	Zero Momentum Stabilisation
Design Point 4	Zero Momentum Stabilisation (thrusters only)
Sensors	
Design Point 1	Sun Sensors
Design Point 2	Star & Planet Sensors
Design Point 3	Earth & Horizon Sensors
Design Point 4	Magnetometers
Design Point 5	Rate Gyros & Accelerometers (IMUs)
Design Point 6	GPS attitude determination
Actuators	
Design Point 1	Control Moment Gyros
Design Point 2	Magnetotorquers
Design Point 3	Thrusters

- a) Spacecraft Attitude Determination and control in Interplanetary/Interasteroid cruise phase

Table 7. 2- The table shows the different stabilisation methods considered for interplanetary phase of mission

Stabilisation Methods	
Design Point 1	Spin Stabilisation
Design Point 2	Dual Spin Stabilisation
Design Point 3	Zero Momentum Stabilisation
Design Point 4	Zero Momentum Stabilisation (thrusters only)
Sensors	
Design Point 1	Sun Sensors
Design Point 2	Star & Planet Sensors
Design Point 3	Rate Gyros & Accelerometers (IMUs)
Actuators	
Design Point 1	Control Moment Gyros (CMGs)
Design Point 2	Thrusters

7.3 Spacecraft Modes

This section discusses the different operational modes of the spacecraft with respect to the different phases on the Mission as discussed in ConOps in Section 5. The different spacecraft modes gives us an understanding of the state of the spacecraft at a given time and what actions needs to be taken by AOCS to either maintain that state of operation or change that state of operation and that can be categorised as:

a) **Detumbling mode:**

After launch the spacecraft has a pre-requisite attitude with a large angular velocity. AOCS systems detumble to orient the spacecraft as necessary and to reduce the angular velocities for a 3-axis stabilisation. This mode is active during Earth departure phase.

b) **3-axis Stabilisation/Control mode:**

This mode is initiated if the spacecraft drifts, slews or jitters due to disturbing torques such as but not limited to solar radiation pressure, gravity gradient, drag, magnetic fields and sets off course its orbital trajectory. The spacecraft is stabilised in all 3 directional axes either by using thrusters or reaction wheels. The mode is initiated in all phases of the mission if the spacecraft is not stabilised and is disturbed by torques. The frames of reference for orientation change from geocentric to heliocentric to asteroid-centric through the different phases of mission.

c) **Safe/Contingency Mode:**

The safe mode is a low-power state mode of the spacecraft where there is insufficient power available to perform a given task. This is the least power demanding mode and no active monitoring of the attitude takes place in this mode. This mode is entered if there is any attitude destabilisation of the spacecraft. This mode is initiated during eclipse times in all phases of the mission.

d) **Standby Mode:**

This is a power raising mode where no operations are performed i.e no payload is active. The sun sensors, reaction wheels and other IMUs are active during this phase. The spacecraft points towards the sun. This mode is initiated during sun-lit periods of the orbit in all phases of the Mission.

e) **Operations Mode:**

The spacecraft enters this mode when power, OBDH and attitude requirements are met, on completion it enters safe mode and power raising mode to charge the batteries. The sensors are ON and the thrusters and reaction wheels are available for attitude corrections. This mode is initiated when the spacecraft performs proximity, mapping, and mining operations.

f) **Communications Mode:**

The spacecraft dumps the data acquired from the payloads to the ground station. In this mode all payload instruments are powered OFF and or in standby mode. AOCS thrusters, Reaction wheels and sensors available to point the spacecraft towards Earth for a direct line of sight. This mode is initiated when the spacecraft downlinks housekeeping and other payload data to the ground station when it is in direct line of sight.

7.4 Satellite Control Configuration and Conclusion

a) Earth and Asteroid orbit Attitude and Control

Zero Momentum Stabilisation, enabled only via thrusters, was selected due mainly to:

1. **Precision:** although not as performant as Zero Moment Stabilisation implemented with Reaction wheels, thrusters have proven their ability to reach a degree of precision sufficient to satisfy the needs of the most taxing task of the Mission, proximity operations and landing on an asteroid for mining.
2. **Low Complexity:** the absence of Reaction wheels and other rotating mechanisms makes this system the most reliable, a relevant characteristic given the long duration of a mission involving multiple manoeuvres.
3. **Capability of performing Subtle Trajectory Correction Manoeuvres** alongside the Main Propulsion System

Table 7. 3- The table shows the final AOCS configuration for mission for Asteroid phase of mission

Stabilisation method	3- axis Stabilisation (thrusters only)
Sensors	Sun Sensors Star & Planets Sensors
Actuators	Thrusters

b) Interplanetary cruise Attitude determination and control

Zero Momentum Stabilisation, enabled via thrusters and reaction wheels, was selected due mainly because the combination of thrusters and reaction wheels provides a complete 3-axis stabilization of the spacecraft where the thrusters are used for impulsive attitude corrections and the reaction wheels are used for pointing and attitude control of the 3-axes. [21]

Table 7. 4- The table shows the Work Breakdown structure for the project for interplanetary phase of mission

Stabilisation method	Zero Momentum Stabilisation /3-axis stabilisation
Sensors	Sun Sensors Star & Planets Sensors
Actuators	Reaction wheels and thrusters

Sun sensors and Star sensors are selected for Attitude Determination, as it was done for the OSIRIS Rex and Hayabusa missions [9], and are both employed for redundancy. Sun sensors are chosen to understand the orientation of spacecraft wrt Sun for a heliocentric cruise during sun-lit phase of mission whereas star sensors are used to find the orientation of spacecraft wrt to different constellations during eclipse phase of mission.

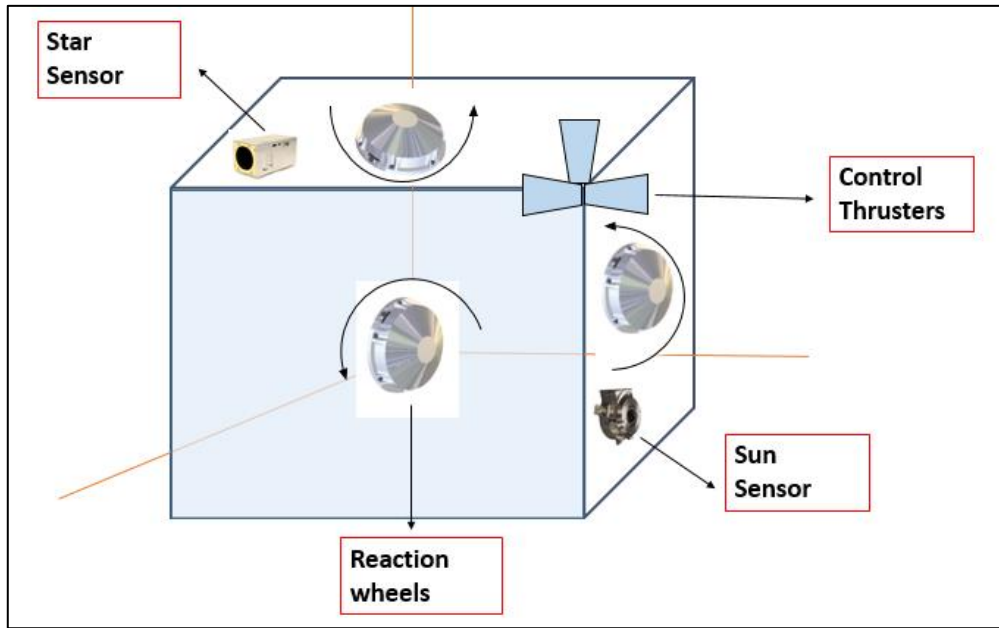


Figure 7. 1- The figure shows the AOCS configuration for the spacecraft

The final AOCS sub-system configuration is as shown in Figure 7.1 which includes:

- 4 reaction wheels (3 for each axis of the spacecraft and 1 redundant) which is similar to OSIRIS Rex and Hayabusa [9] [15]
- 1 Star sensor
- 1 Sun Sensor
- A Combination of thrusters shown in Table 6.7 used both for attitude control and propulsive needs (Note that the total thrust required was calculated using the Thrust to weight ratio of a spacecraft – Soyuz MS that weighs similar to the spacecraft for our mission which is ~7 tonnes. The thrust to weight ratio of the Soyuz spacecraft is 2.02 [26] [27] and using that the total thrust for the mission is around 14kN. This needs to be further refined and is considered a part of future work as the assumption is part of preliminary calculations and the thrust to weight ratio may not be relevant to the mission and needs to be explored)
- A set of NAC and WAC cameras used for mapping and proximity navigation similar to OSIRIS Rex [9] [8]
- 1 LIDAR for navigation similar to OSIRIS Rex [9] [8] used for landing, obstacle avoidance etc.

Table 7. 5- The table shows the preliminary selection of thrusters for the mission

Number	Thrust	Total Thrust	
2	4000	8000	N
8	890	7120	N
10	22	220	N
8	4	32	N
4	0.09	0.36	N
Net Thrust		15372.36	N

It is to be noted that the total thrust and the number of thrusters are a preliminary calculation and further investigation needs to be done. The spacecraft has a Thrust to weight ratio of 2.20 with a net Thrust of 15kN. This is further discussed in propulsion sub-system, Section 6.

8 Electrical Power Sub-System

8.1 Introduction

Electric power for spacecraft is the most fundamental requirement for the satellite payload. Its failure leads to mission failure as the payloads are power driven. The power system will be responsible for providing power to each subsystem to perform the required nominal operations. This section discusses the power sub-system architecture and its elements and calculates the relevant budgets.

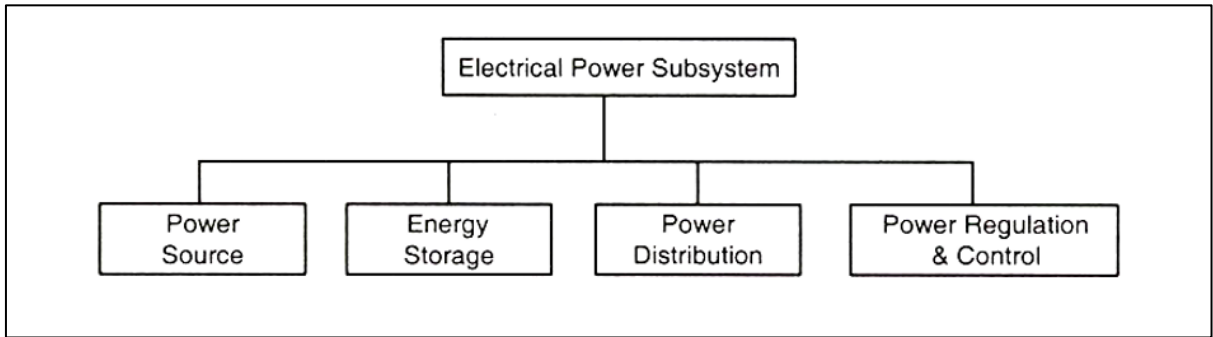


Figure 8. 1- The figure shows the architecture elements of EPS

The Figure 8.1 shows the architecture elements of the Electrical power sub-system. Power source and energy storage elements are designed in Section 8.4 and Section 8.3 respectively. The other elements are part of future work due to time constraints.

Table 8. 1- The table shows the different options for power generation for space crafts [21]

Power source	Principle	Typical performance	Remarks
Solar Photovoltaic	Cells convert incident solar radiation into electrical power	26-100W/kg ~0.2-25kW	Most commonly-used primary power source for spacecraft
Solar Thermal Dynamic	Brayton, Stirling, or Rankine cycle converts heat to electrical power	9-15W/kg 5-300kW	Solar concentrator used as heat source
Radio-Isotope	Radioisotope decay used as heat source	5-20W/kg 0.2-10kW	Application to deep space missions
Nuclear Reactor	Controlled nuclear fission as heat source	2-40W/kg 5-300kW	As above But safety issues
Fuel Cells	Chemical energy converted to electricity	275W/kg 0.2-50kW	Hydrogen-oxygen cells used on Shuttle

Table 8. 2- The table shows the trade table for different power generation for space crafts

Type of power source	Power range (kw)	Density (w/kg)	Cost	Manoeuvrability	Degradation	Sensitivity	Fuel	Safety	Σ
Solar	4	1	4	3	2	1	4	4	23
RTG	4	2	3	4	3	1	4	2	23
Nuclear reactor	3	3	2	4	3	4	1	2	22
Fuel cells	2	4	1	4	3	4	2	2	22

Table below shows the primary sources of power for a spacecraft. For our mission Solar Photovoltaic or Solar array cells is chosen because of the dissimilarities listed below:

Advantages of RTG	Advantages of Solar Photovoltaic
<p>Sunlight Independent: RTGs are not dependent on sunlight for power generation and uses radioactive decay for power generation</p> <p>Power density : They have higher power densities compared to Solar array/battery</p>	<p>Time: Power output doesn't exponentially decrease with time like the RTG</p> <p>Radiation/Thermal: Does not require constant radiation shielding and cooling</p> <p>Cost: Is more affordable than the RTG</p> <p>Switching Capability: Can be turned ON/OFF as desired</p>

The top-level requirements for the sub-system are:

- EPS shall supply , control and distribute power to relevant spacecraft subsystems
- EPS shall support power requirements for average and peak loads
- EPS shall house batteries to store the required power during eclipse times
- EPS shall use solar arrays for power generation during sunlit times of the mission

Table 8.3- The table shows the different selection of batteries considered for the mission [21]

	Energy density W h/kg	Storage life	Storage temp. deg C
Silver zinc	60-130	5 yr (dry)	0-30
Lithium sulphur dioxide	130-350	10 yr	0-50
Lithium carbon monofluoride	500-800	2 yr	0-10
Lithium thionyl chloride	175-440	5 yr	0-30

Table 8.3 shows the different sources of battery for a spacecraft. For our mission Lithium ion batteries are chosen as they have high energy densities ie high performance over long mission durations

8.2 Calculation of Eclipse time for the mission

In order to calculate the power budget of the spacecraft, the eclipse times were necessary for which certain assumptions were made and those are:

- a) The attitude of the spacecraft was considered to be 10km around the Asteroid
- b) The attitude of the spacecraft around Earth was 10,000km
- c) The orbit was considered a circular orbit hence the eccentricity was zero
- d) The eclipse time was calculated using the Equations (x-x) to(x-x) . These values can be refined using STK which is part of future mission analysis work package.

$$\tau_{spacecraft} = 2\pi \sqrt{\frac{(Radius\ of\ Asteroid + Parking\ orbit\ altitude)^3}{\mu_{Asteroid}}}$$

Equation 8. 1

$$\rho = \sin^{-1} \left(\frac{Radius\ of\ asteroid}{Radius\ of\ Asteroid + Parking\ Orbit\ Altitude} \right)$$

Equation 8. 2

$$Teclipse\ Spacecraft = \frac{2 \times \rho \times \tau_{spacecraft}}{360^\circ}$$

Equation 8. 3

$$Tsunlit\ Spacecraft = \tau_{spacecraft} - Teclipse\ Spacecraft$$

Equation 8. 4

The power sub-system was designed for the eclipse time that had a higher constraint and it was found that the eclipse time around the Asteroid was much greater than that of around the Earth and hence the system was designed for that. It is to be noted that the cruise conditions aren't considered as there was no way to find the eclipse times for cruise without having to use STK.

Table 8. 4- The table shows the eclipse calculation for the spacecraft at 10 km parking orbit from the Asteroid

Calculation of Eclipse time around Asteroid		
Sidereal Orbital period around the sun	524	days
Synodic period	19	hr
Daylight seen by asteroid	9.5	hr
R _a	0.15	km
H	10	km
ρ	0.847	deg
μ1989ML	4.47E-08	km ³ /s ²
T	9.61E+05	s
Teclipse for sat	4519.98	s
	75.33	min
	1.25555135	hr
Tsunlit for Sat	9.56E+05	s
	2.66E+02	hr

Table 8. 5- The table shows the eclipse calculation for the spacecraft around a 10000 km parking orbit around Earth

Calculation of Eclipse time around Earth(10k ~geo)		
R _e	6378	km
H	10000	km
ρ	22.919	deg
μEarth	3.96E+05	km ³ /s ²
T	2.09E+04	s
Teclipse for sat	2664.66	s
	44.41	min
	0.74018256	hr
Tsunlit for Sat	1.83E+04	s
	5.07E+00	hr

Table 8.4 shows the eclipse time of the spacecraft around the satellite which is 75 minutes.

8.3 Battery Sizing

Batteries have been used extensively for the secondary power system, providing power during periods when the primary one is not available. As a backup for a solar array this means that the batteries must provide power during eclipses, and that the array must recharge the batteries in sunlight. Following standard systems engineering practise from

'The elements of spacecraft engineering' and 'the new SMAD' [21] [28] Section 8.1 calculates the battery mass required for our mission.

The battery selection involves battery sizing and other considerations such as:

- a) Selecting the battery type
- b) Estimating battery mass
- c) Determining the number of fuel cells in a battery(part of future work)

a) Selection of Battery:

The available batteries that have space heritage are: Nickle-cadmium, Nickle-Hydrogen and Lithium-ion.

Lithium ion batteries are chosen over the other because they can be recharged and discharged multiple times and have a higher energy density. It has a low-discharge rate which makes it more power and energy efficient.

b) Estimation of Battery Mass:

The battery mass is estimated using the equations below for a Night time load of 300W (minimal usage of payload instruments). The total battery mass required is found to be 23.45 kg for an eclipse time of 75min.

$$\text{Battery energy drain}(W - \text{Hr}) = \frac{\text{Eclipse time load} \times \text{Eclipse time}}{\text{Battery discharge efficiency}}$$

Equation 8. 5

$$\text{Battery capacity (W - Hr)} = \frac{\text{Battery Energy Drain}}{\text{Depth of discharge}}$$

Equation 8. 6

$$\text{Battery mass (kg)} = \frac{\text{Battery capacity}}{\text{Battery specific energy}}$$

Equation 8. 7

Table 8. 6- The table shows the battery mass calculation for the mission

Battery sizing		
T eclipse	75.00	min
Eclipse (night-time) load Pn	300	W
Eclipse time Lnl	1.25	Hr
Battery discharge efficiency	0.96	
Battery energy drain Ebm	390.63	W-Hr
Number of cycles	12000	$\sim 1.2 \times 10^4$ cycles
Acceptable depth of discharge	20	%
Battery Capacity required	1953.13	W-Hr
Typical Li-ion battery specific energy	100	W-Hr/kg $\sim 70\text{--}110$ W-Hr/kg
Mass required	19.5313	kg
Margin (20 %)	23.4375	kg

8.4 Solar Array Sizing

Solar Arrays have been used extensively as the primary power system, providing power during sunlit parts of the spacecraft trajectories. Solar arrays not only help power the spacecraft for nominal payload operations but also charge the battery to prepare for the eclipse duration. Following standard systems engineering practise from ‘The elements of spacecraft engineering’ and ‘The new SMAD’ Section 8.1 calculates the solar array area required for our mission.

The solar array selection involves array sizing and other considerations such as:

- a) Selecting the type of Solar array
- b) Estimating the solar array size

a) Solar array Selection:

Table 8.7-The table shows the different types of solar cell types considered for the mission [21]

Cell type	Typical efficiency	Remarks
Silicon (Si)	15-22 %	Lowest cost, mature technology
Thin-sheet amorphous silicon	8 %	For flexible “blanket” arrays
GaAs triple-junction	30 %	V efficient cell produced by Emcore
Ultra and NeXt triple-junction GaAs	28.3-29.9 %	Produced by Spectrolab

Table 8.7 shows the different solar array cells available and for our mission Gallium Arsenide solar cells were selected because of high efficiency compared to the other variants.

b) **Estimation of Solar Array size:**

The solar array size is estimated using the equations below for a day time load of 938W (maximum usage of payload and mining instruments). The total solar array size required to sufficiently power all sub-system components is found to be 9.23 m² for an eclipse time of 75min and sunlit time of 266 hours.

The power requirements for the mission are captured in the figure shown below which is then used to calculate the solar array required.

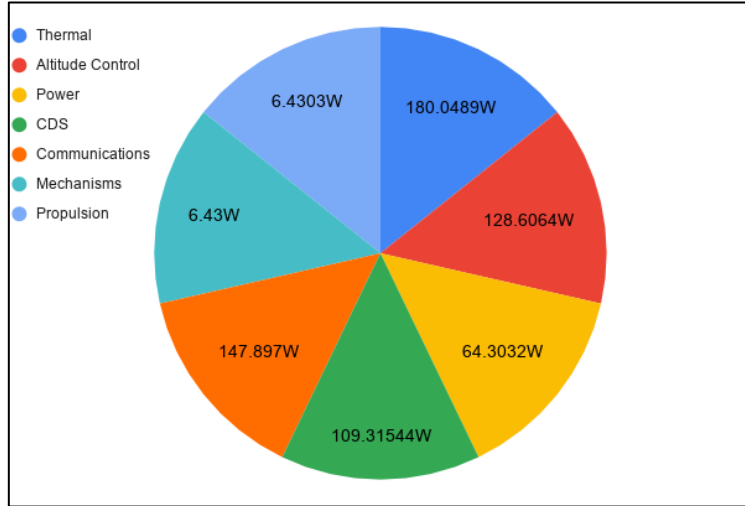


Figure 8. 2- The figure shows the power distribution between different sub-systems

$$\text{Power needed to recharge battery} = \frac{\text{Battery energy drain}}{\text{battery charge efficiency} \times \text{Length of shortest day}}$$

Equation 8. 8

$$\text{Total Power required from solar array} = \frac{\text{Power needed to recharge battery} + \text{Power load during sunlit time}}{\text{Efficiency}}$$

Equation 8. 9

$$\begin{aligned} \text{EOL array specific power} \\ &= \text{Solar cell Efficiency} \times \text{Inherent degradation factor} \times \text{Lifetime degradation factor} \\ &\quad \times \text{Cosine factor loss} \times \text{Solar Flux} \end{aligned}$$

Equation 8. 10

$$\text{Solar array required} = \frac{\text{Total power required from array}}{\text{EOL array specific power}}$$

Equation 8. 11

Table 8. 8- The table shows the solar array sizing for the mission

Solar Array Sizing		
Battery charge efficiency	0.7	
Length of shortest day Lds	266.00	Hr
Power Needed to recharge battery Pc	2.10	W
Power for load in Sunlight Pdl	983	W
Total Power required from array Psa	1094.55	W
Solar cell efficiency	19	%
Inherent Degradation factor	0.77	
Lifetime degradation	2.75	% GaS cells
Mission Lifetime	5	years
Lifetime degradation factor	0.87	
Cosine loss factor	0.98	
solar flux	1418	W/m ²
EOL array specific power	177.71	W/m ²
Array area required	6.1591	m ²
	61590.94	cm ²
Array area required(50% margin)	9.2386	m ²
	92386.40492	cm ²
Area of 1 solar panel	100	cm ²
Number of Solar Panels	923.86	

8.5 Electrical Power System Conclusion

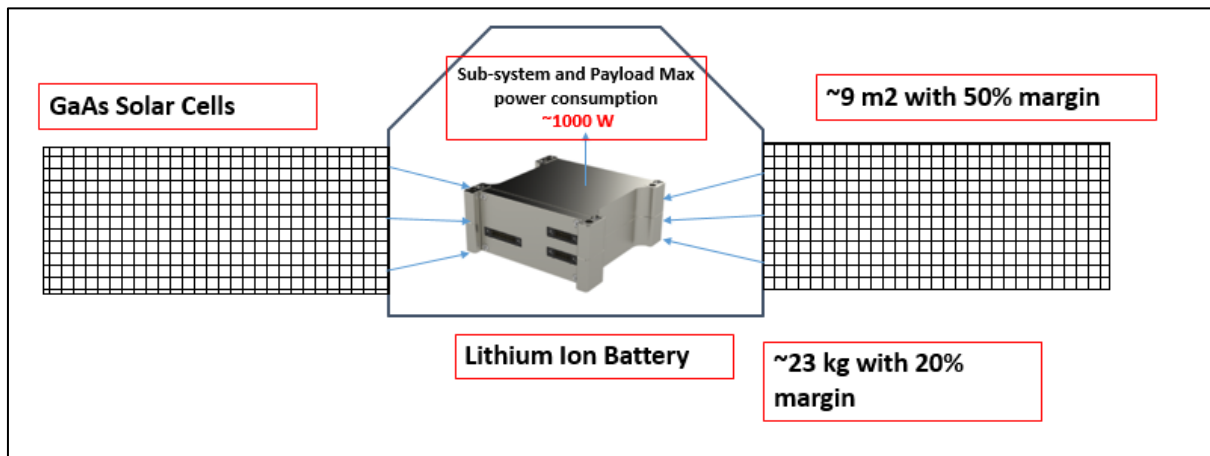


Figure 8. 3- The figure shows the power system configuration for the mission

To conclude, EPS can be summed as Gallium Arsenide Solar Cells of area 9m² and Lithium Ion Batteries of ~23 kg to power the payload needs for the mission.

9 Communications and On-Board Data Handling Sub-System

9.1 Introduction

The communication system helps downlink and uplink data to and from the ground station to the Spacecraft. It is important to select the correct radio frequency band to transmit the data over and the antennae with which the data is transmitted. Orbital parameters determine the data transmission times as the spacecraft needs to be in line of sight with earth for communication.

The main subsystem elements of the communication subsystem is :

- a) Tx/Rx Antennae
- b) Transmitter module
- c) Receiver module
- d) Diplexer

The objective of this sub-system relevant to the report is to:

1. Select a frequency channel for data transmission
2. Select a modulation method for the Data
3. Component selection based on traditional communication architectures
4. Design a link budget discussed in Section 9.2 that relates the transmitted power to the quality of the signal obtained at the receiver.
5. Discuss the OBDH subsystem architecture and elements

9.2 Link Budget

Link budget characterises the transmitted power, gains and losses of the communication system which enables us to calculate the strength of the received signal over a distance. A positive link margin is desired which indicates a communication system is feasible.

The link margin for the mission is calculated using the formula (9-1) and (9-2)

$$\frac{Eb}{N0} = \frac{P \times Ls \times Ll \times Gt \times Gr}{kB \times Ts \times R}$$

Equation 9. 1

$$\frac{Eb}{N0} = P + Ls + Ll + Gt + Gr - 10 \log_{10} kb - 10 \log_{10} Ts - 10 \log_{10} R$$

Equation 9. 2

P= Transmitter power

Ls= Free space propagation loss

Ll=other losses

Gt= Transmitter gain

Gr= Receiver gain

kb= Boltzmann constant (1.38E-23 W/K,Hz)

Ts= System noise temperature

R= Data rate in bits per second

Table 9.1 shows the link budget calculation using modulation index as 78 and bit error rate of 1E-5

Table 9. 1- The table shows the link margin calculations for the mission

	X band uplink	X band downlink
Maximum orbital distance	1	1
Signal frequency [GHz]	7.42	8.45
Data rate [kbps]	10	375
Transmit	DSN BWG Antennas	Spacecraft HGA
Antenna Diameter [m]	34	2
Pointing Accuracy [°]	n/a	0.3
Antenna beam-width [°]	2.1	1.24
Power [W]	2000	80
Antenna gain [dB]	68.3	42.5
Antenna efficiency	65	70
EIRP [dBW]	128.6	91.98
Losses	-3	-0.79
Pointing [dB]	-279.11	-274.35
Space [dB]	-0.2	-0.4
Atm. Attenuation [dB]	-0.2	-0.4
Implementation [dB]	-2	-1
cable loss[dB]	-1	-0.6
Total Loss [dB]	-285.31	277.14
Receive	DSN BWG Antennas	Spacecraft HGA
Antenna diameter, m	34	2
Antenna efficiency	n/a	62
G/T, dB/K	n/a	53.9
Antenna gain [dB]	78.52	43.08
Power, dB	-133.51	-110.56
Energy per bit [dB]	-191.35	-182.79
System noise temp, K	290	540
Noise density [dB]	-203.98	-201.27
Received Eb/N0 [dB]	12.62	28.82
Required Eb/N0 [dB]]	7.6	10
Link margin [dB]	5.02	18.82

9.3 OBDH and Flight Software Architecture

Flight software is the heart of the space flight computer. These have no direct user interface, therefore all interactions between operators and flight system occurs between downlink and uplink transmissions. There are different types of software and it should be considered while designing the subsystem such as:

- a) Operating system software
- b) Command and Data handling Software
- c) Control system software
- d) Payload management software

The Command and Data Handling Architecture Components selected for the mission were:

- a) 1 RAD on board computer
- b) Spacewire data bus
- c) Interface Cards
- d) Interface board
- e) Mass memory

It is to be noted that the above mentioned components and architectural elements are just placeholders selected due to time constraints of the internship and further study needs to be performed.

9.4 Communications Architecture for our Mission and conclusion

Spacecraft communication takes place through different channels such as C, S, X and Ka bands. By referring to the previous missions it was found that X band, S band and Ka band have been used most of the time due to the availability of larger band width.

The frequency allocation different band channels are:

- a) S band - 1.55GHz to 3.5 GHz
- b) X band - 6.2GHz to 10.9GHz
- c) Ka band - 10.9GHz to 36GHz (*all the values from Elements of Spacecraft design)

Since high data rates and less noise interference were desirable parameters, X band was chosen for the mission. X- Band provides better data rates than S band. It is also less sensitive to ionospheric delays.

Communication system involves modulation which is the process of imposing an input signal onto a carrier wave to produce a new signal. There are different modulation techniques for transmitting the digital data such as:

- a) FSK (Incoherent)
Carrier frequency is toggled, less complex, Modulation index of 0.3
- b) FSK (coherent)
Carrier frequency is changed using a phase shift, has less S/N ratio
- c) GMSK
Binary data is rounded off using Gaussian techniques and then converted to FSK
- d) PSK
Carrier phase is changed by 90°, Good BER performance
- e) BPSK
Carrier is modulated by +1 or -1, Doppler sensitive
- f) QPSK
Good spectral efficiency, Phase change every 2 bits

g) OQPSK

Phase is delayed by 1 bit

QPSK or Quadrature Phase Shift Keying is chosen for the mission as it allows the signal to carry twice as much information as ordinary PSK using the same bandwidth. This modulation technique has a very good noise immunity. For the same bit error rate it uses half the bandwidth as BPSK and has a low error probability.

Using Traditional Space Communication elements the relevant sub-system components were found:

a) HGA

High gain parabolic antenna is chosen as the main antenna for communication purposes. HGA is also used in OSIRIS Rex. The antenna has an aperture of 2m. It is used when high data rate is required and will be activated when narrow beam is required. It has a Gain of 42.35 dB and has a RCP polarisation

b) MGA

This Horn antenna is used when high data rates is not necessary or when HGA cannot maintain nadir pointing during spacecraft manoeuvres. It has a gain of 18.9dB and a aperture diameter of 0.4m. It also uses a RCP polarisation

c) LGA

Quadrifilar Helix antenna, a type of LGA is used when high data rates is not necessary or when HGA cannot maintain nadir pointing during spacecraft manoeuvres. It is used for low gain applications during cruise phase of mission. The antenna has an aperture diameter of 0.04 m and a gain of 8.76 dB, it uses RCP polarisation.

d) X Band Transponder

SDST X -band Transponder will interface to the data bus to receive data for transmission and telemetry and commands. This helps in navigation, detecting the spacecraft speed and distance from Earth.

e) X Band Diplexer

f) X Band switching cables

g) X Band connector cables

h) X Band TWTA

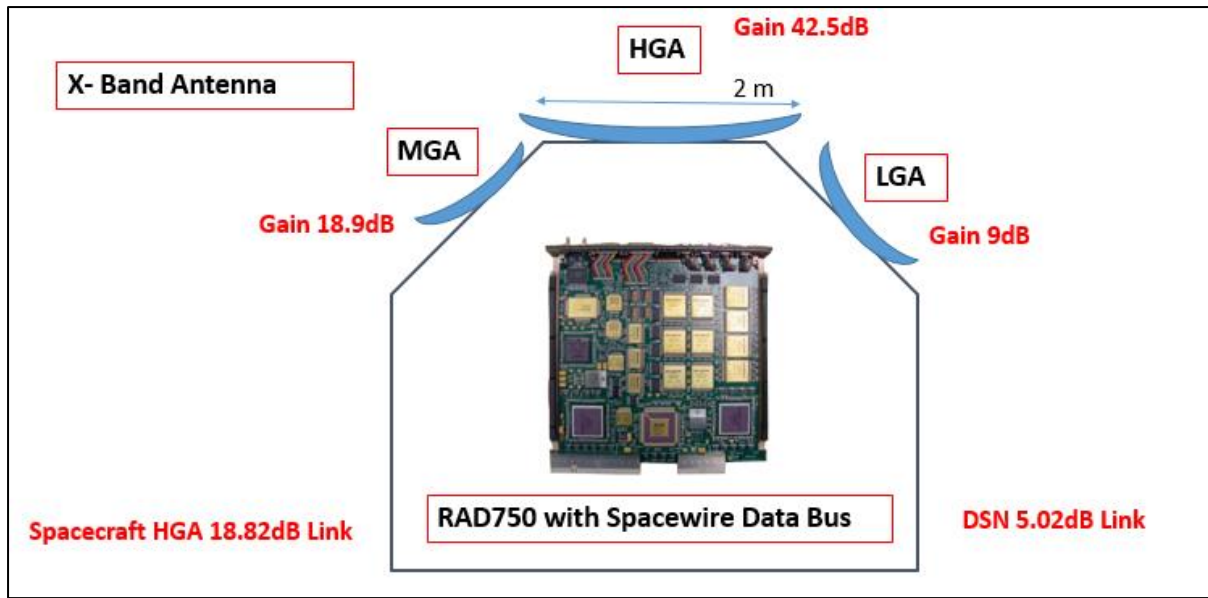


Figure 9. 1- The figure shows the final Communication configuration for the mission

Figure 9.1 shows the Final communications subsystem elements of the spacecraft. The link margin for the system is 18.82 dB with a 5dB downlink margin. The system uses X Band and DSN pathways for communication purposes.

100W wave tube amplifier will ensure the downlink signals have the strength to meet the derived requirement of a 5dB downlink margin. They produce larger output power at higher efficiency. The Amplifiers are located on the back of the High gain Antenna which boosts the power of the spacecraft's radio signals so that they can be captured in DSN.

DSN also known as Deep Space network is used to communicate with Earth which supports both X and Ka band. It also supports RCP and LCP polarizations of the antennae.

RAD 750 is chosen as the on-board computer due to radiation resistance but more detailed work such as data budget needs to be worked on in the future .OBDH Work package and was only discussed and not captured and is part of future work.

10 Thermal Sub-System

10.1 Introduction

Spacecraft thermal control is another integral part to mission success. The process of thermal control for a spacecraft involves managing the energy entering and leaving the spacecraft to ensure that the components of the spacecraft remain within an acceptable temperature range. Spacecraft perform optimally and have longer working lives when the temperature of their components remains within these boundaries, often near the temperature at which they were fabricated.

The thermal control system on a spacecraft generally uses two basic approaches for temperature management:

- a) Passive control
- b) Active control

Many space craft thermal control systems use a combination of passive and active control, though the passive control methods make up the majority of the system with supplemental active control methods for equipment with small temperature tolerances. Space missions most commonly employ passive control methods, though these methods may need more surface area or assistance from deployable systems to radiate heat away. Some active thermal control systems can be more compact, but most are often heavy and power intensive. [21]

The report focuses on passive thermal control techniques as it is less complex and due to time constraints of the internship. Future work may include exploring active thermal control techniques.

Passive thermal control techniques include:

- a) Material property selection
- b) Insulation systems to ensure that temperatures remain within acceptable limits.
Techniques including the use of multilayer insulation (MLI) and thermal coatings have a long heritage, but may require modifications for use.

10.2 Selection of Multilayer Insulation

Insulation systems are designed to minimize heat exchange in the vacuum of space. Thermal insulation acts as a barrier to radiation and prevents excess heat dissipation.

MLI blankets are the most common insulation, though single layer barriers are sometimes used where lesser degrees of insulation are required because they are lighter and less expensive.

MLI is composed of layers of low-emittance films. A simple MLI blanket consists of layers of about $\frac{1}{4}$ mm thick embossed Kapton or Mylar sheets that each have vacuum deposited aluminium finish on one side. [29] The embossing of the sheets causes them to only touch at a few points, which minimizes conduction between the sheets. The sheets are only aluminized on one side so that the sheet material acts as a low conductivity spacer. A more complex and higher performance construction consists of sheets that are metalized with aluminium or gold on both sides and silk or Dacron net between the sheets acting as the low conductivity spacer.

An outer cover encloses the stack to form the MLI blanket, which is held together with non-metallic thread, intermittent taping along the edges, or non-metallic snap buttons. The outer cover can be made from Teflon, aluminized Kapton, black Kapton, or Beta cloth, which is a Teflon coated glass fabric. The blanket assembly is typically secured by bonding or using Velcro strips. Grounding straps are added to reduce the electrostatic charge on the insulation during orbit.

Hence to conclude the abovementioned material – Kapton is used as an MLI for the spacecraft.

10.3 Preliminary Thermal Analysis

In this Analysis, the variances in temperature of spacecraft with respect to external thermal environment and outer and inner heat sources were taken in account.

Table 10.1 shows the different temperature ranges of spacecraft sub-system components:

Table 10. 1- The table shows the operating temperature ranges for different subsystem components

Sub-system	Components	Temperature Ranges	
		Min Operating Temp in °C	Max. Operating Temp in °C
Propulsion	Tanks and Lines	7	55
	Thrusters	7	65
Payload	Cameras	-30	40
	NAC	-36	19
	WAC	-36	19
	Solar Arrays	-150	100
	Infrared Spectrometers	-40	60
	Thermal IR Imager	-73	166
	Laser Altimeter	10	40
Communication	SDST X band Transponder	-40	60
	X band Diplexer	-30	85
	X band Switching Cables	-55	85
	X band Cables	-35	85
Thermal Control	Multi-Layer Insulation	-160	250
	Heaters, Heat Pipes	-35	60
	Radiators	-95	60

From table 10.1 we understand that the spacecraft temperature should not exceed 19°C or 292K. The temperature of the spacecraft should also not fall below 10°C or 283K.

Using the equations below the equilibrium temperature of the spacecraft is found for different Surface materials. The equilibrium temperatures are found for the spacecraft near the Asteroid and near Earth and the MLI material is chosen for the scenario that has a higher constraint.

In order to calculate the thermal load on the spacecraft some of the assumptions made are:

- a) The spacecraft is assumed to be a cube of sides 4m. The actual spacecraft dimensions are $4 \times 4 \times 5$ m excluding the solar panels as discussed in Section 8
- b) For the Asteroid scenario the IR flux calculations is excluded as a reliable source for IR flux of Asteroid was not found.
- c) The view factors are 0.8 and 0.2
- d) The heat transfer within the spacecraft is assumed to be 1000W which occurs through radiation and conduction. Convection is ignored for simplicity.

$$A_{sc} \times \varepsilon \times \sigma \times T^4 = \alpha \times ((A_s \times J_s) + (F_a \times A_e \times J_a)) + (\varepsilon \times F_e \times A_e \times J_e) + Q_{total}$$

Equation 10. 1

The above equation is the thermal balance equation and all the other equations are derived from it.

A_{sc} = Total Spacecraft Area

σ = Boltzmann Constant

J_s = Solar flux

A_e = Area of spacecraft that sees the Planet or Asteroid

ε = IR emissivity

J_e = Thermal flux

T = Spacecraft surface temperature

α = Solar absorptivity

A_s = Area of spacecraft normal to Sun

F_a = View factor for Albedo

J_a = Albedo flux

F_e = View Factor for thermal radiation

Q = Total spacecraft power dissipation

$$\text{Heat input flux from Sun} = \text{Area of Spacecraft facing Sun} \times \text{Solar Flux} \times \text{Solar absorptivity}$$

Equation 10. 2

$$\text{Albedo input (Planet or Asteroid facing)} = \text{Area of spacecraft facing Planet or Asteroid} \times \text{Albedo Flux} \times \text{View factor} \times \text{Solar absorptivity}$$

Equation 10. 3

Albedo input (side facing)

$$= \text{Area of spacecraft side facing} \times \text{Albedo Flux} \times \text{View factor} \times \text{Solar absorptivity}$$

Equation 10. 4

IR input (Planet or asteroid facing)

$$= \text{Area of spacecraft facing Planet or Asteroid} \times \text{IR flux} \times \text{View Factor} \\ \times \text{Infrared Emissivity}$$

Equation 10. 5

$$\text{IR input (side facing)} = \text{Area of spacecraft side facing} \times \text{IR flux} \times \text{View Factor} \times \text{Infrared Emissivity}$$

Equation 10. 6

$$\text{Total heat input} = \text{Internal Power heat} + \text{Sun input} + \text{Albedo} + \text{IR}$$

Equation 10. 7

$$\text{Spacecraft Temperature (Kelvin)} = \left(\frac{\text{Total heat input}}{\text{Total Area of spacecraft} \times \text{IR Emissivity} \times \text{Boltzman Constant}} \right)^{\frac{1}{4}}$$

Equation 10. 8

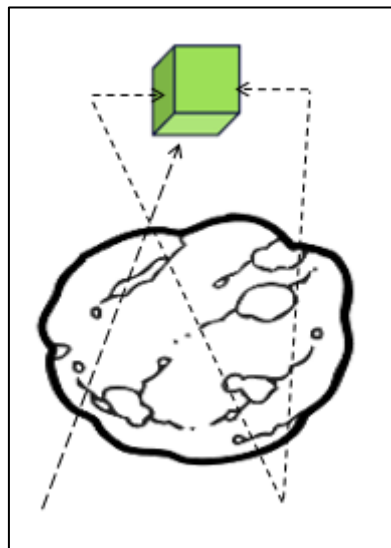


Figure 10. 1- The figure shows the Asteroid albedo directions on the spacecraft

Table 10. 2- The table shows the thermal equilibrium temperature on the spacecraft around the asteroid for different surface finishes.

spacecraft area values m ²				fluxes (W/m ²)		view factors		surface properties		heat inputs from external fluxes (W)					Spacecraft temperature /Kelvin	Surface finish	
Asc	Asun	Aasteroid	Asides	Solar flux Js	Albedo flux Ja	F(asteroid face)	F(4 side faces)	Internal heat Qtotal W	Solar absorptivity	Infrared emissivity	Boltzmann constant (W/m ² K4)	Sun input	Albedo input (Asteroid face)	Albedo input (side faces)	Total input (RHS of eqn)	Spacecraft temperature /Kelvin	Surface finish
96	16	16	64	1373	274.6	0.8	0.2	1000	0.2	0.9	5.67E-08	4393.6	703.0	703.0	6799.6	193.0	White-painted
96	16	16	64	1373	274.6	0.8	0.2	1000	0.6	0.9	5.67E-08	13180.8	2108.9	2108.9	18398.7	247.6	White paint - EOL
96	16	16	64	1373	274.6	0.8	0.2	1000	0.08	0.8	5.67E-08	1757.4	281.2	281.2	3319.8	166.2	OSR
96	16	16	64	1373	274.6	0.8	0.2	1000	0.21	0.8	5.67E-08	4613.3	738.1	738.1	7089.5	200.9	OSR - EOL
96	16	16	64	1373	274.6	0.8	0.2	1000	0.25	0.02	5.67E-08	5492	878.72	878.72	8249.44	524.67	Gold-Kapton
96	16	16	64	1373	274.6	0.8	0.2	1000	0.3	0.6	5.67E-08	6590.4	1054.464	1054.464	9699.328	233.44	MLI -Kapton

Using the above equations table 10.2 shows the different spacecraft equilibrium temperatures and based on our constraints the most suitable surface finishes for Asteroid scenario is MLI-Kapton.

Similarly table 10.3 shows the equilibrium conditions for Earth scenario and the most suitable surface finish is MLI Kapton.

Surface finishes like the white paint can be used but they have a very short EOL compared to Kapton and hence for ~ 4 year mission Kapton is best suited for reliability and durability.

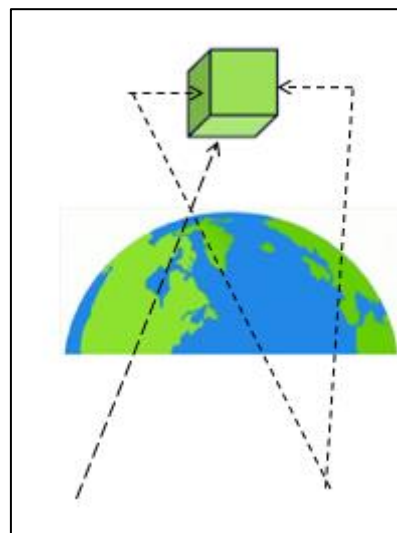


Figure 10. 2- The figure shows the Earth albedo directions on the spacecraft

Table 10. 3- The table shows the thermal equilibrium temperature on the spacecraft around Earth for different surface finishes.

spacecraft area values m ²				fluxes (W/m ²)		view factors		surface properties		heat inputs from external fluxes (W)					Spacecraft temperature /Kelvin	Surface finish				
Asc	Asun	Aearth	Asides	Solar flux Js	Albedo flux Ja	Earth IR flux Je	F(earth face)	F(4 side faces)	Internal heat Qtotal W	Solar absorptivity	Infrared emissivity	Boltzmann constant (W/m ² K4)	Sun input	Albedo input (Earth face)	Albedo input (side faces)	Earth IR input (Earth face)	Earth IR input (side faces)	Total input (RHS of eqn)	Spacecraft temperature /Kelvin	Surface finish
96	16	16	64	1418	482.12	237	0.8	0.2	1000	0.2	0.9	5.67E-08	4537.6	1234.2	1234.2	2730.2	2730.2	13466.5	229.0	White-painted
96	16	16	64	1418	482.12	237	0.8	0.2	1000	0.6	0.9	5.67E-08	13612.8	3702.7	3702.7	2730.2	2730.2	27478.6	273.7	White paint - EOL
96	16	16	64	1418	482.12	237	0.8	0.2	1000	0.08	0.8	5.67E-08	1815.0	493.7	493.7	2426.9	2426.9	8656.2	211.2	OSR
96	16	16	64	1418	482.12	237	0.8	0.2	1000	0.21	0.8	5.67E-08	4764.5	1295.9	1295.9	2426.9	2426.9	13210.1	234.7	OSR - EOL
96	16	16	64	1418	482.12	237	0.8	0.2	1000	0.25	0.02	5.67E-08	5672	1542.784	1542.784	60.672	60.672	9878.912	548.85	Gold-Kapton
96	16	16	64	1418	482.12	237	0.8	0.2	1000	0.3	0.6	5.67E-08	6806.4	1851.3408	1851.3408	1820.16	1820.16	15149.4	260.97	MLI -Kapton

11 Structures Sub-System

11.1 Introduction

Structure is the system framework that holds various payloads and system components together, it provide support for all load environments from prelaunch through launch and includes on orbit-loads. To be successful, the structure must survive all environments without detrimental deformations

The design needs to meet several demands such as:

1. The spacecraft needs to be highly reliable for environments that cannot be simulated on Earth or that which cannot be fully modelled analytically for combined mechanical and thermal loads.
2. It has to accommodate payloads within the spacecraft boundaries.
3. It has to be weight efficient by using materials such as composites to reduce mass.

A summary of typical structural design of the previous asteroid mission were taken to account. A basic CAD model is designed.

11.2 Orientation of Payloads within the Spacecraft

There are different constrains on the arrangement which are:

- a) Field of view for instruments, antennas, radiators, solar panels
 - b) Nadir pointing
 - c) Sun vector
- a) Field Of View
Much of the equipment of the on-board requires a certain field of view .Most scientific instruments all antennas, all motors, all solar panels and most electronics require a view of space. The high-grain antenna was fixed to the top of the bus; direct mounting to the bus provided maximum pointing stability for the antenna. The 10-sided bus body is an excellent arrangement from number of viewpoints, the electronics is installed in each of the 10 boxes .one side of each has a clear view of space for heat rejection
- b) Nadir Pointing
Nadir pointing is a special and common field of view requirement; the entire nadir face was dedicated to the mounting of earth-sensing instruments
The spacecraft bus equipment was mounted above the instrument ring and between two rotating solar panels.
- c) Sun Vector
The solar panel axis must be perpendicular to the sun vector .The sun vector is strictly prohibited from the field of view of light sensitive instruments such as camera, star scanners, horizon sensors and spectrometers.
The instrument can be designed to protect against sunlight, the preferred approach is to designate sun free faces and mount the instruments accordingly

There are several equipment items that need to be mounted together:

1. It's desirable for the telecommunications system to be installed as close to the antennas as possible to minimize cable losses.
2. Batteries are another heavy components, Multiple batteries must be installed side by side and with the power control equipment in order to save cable mass and complexity

3. The attitude control sensors and gyros need to be attached to a common, very rigid structure.
4. Communication system mounted on a high plate just below high gain antenna
5. It's desirable to mount propulsion equipment on or near tanks and to configure the system as separable module so that hazardous operations can be accomplished remotely.

11.3 Material Selection

An important factor that must be considered when designing a structure for space is the type of materials the structure will utilize. Choosing the proper materials will provide the optimal operational environment for the structure

The desirable properties for materials needed in space is:

a) **Dimensional stability:**

An object that is continually moving in and out of the sun's direct heat is in constant temperature flux, which can cause it to expand and contract. As a result, scientists consider a material's ability to maintain its size and shape despite temperature changes

b) **Environment stability:**

Structures in space also need to be able to withstand its uniquely harsh environment. In space this means that the material can remain stable in despite the presence of radiation and the vacuum of space.

c) **Strength and Stiffness:**

When an object is in orbit around the Earth it will be subjected to forces that will tear apart weaker structures. The material must maintain its integrity and not break or bend under immense forces

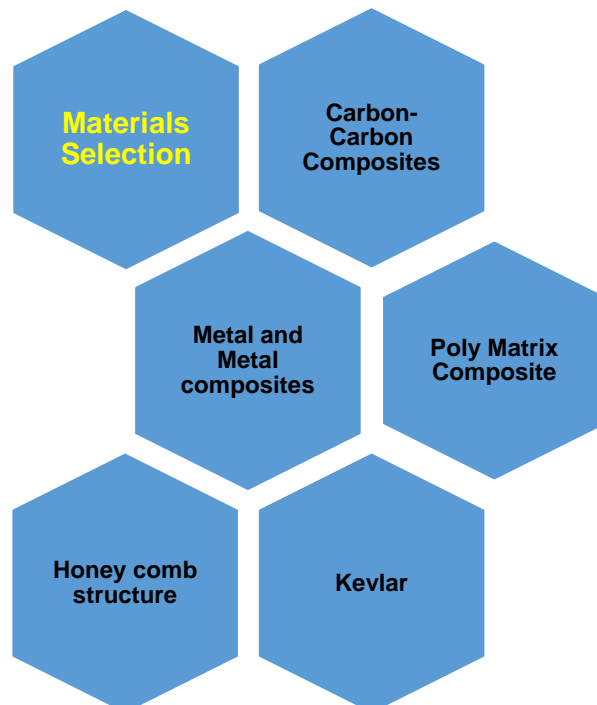


Figure 11. 1- The figure shows the different materials considered for the spacecraft

The materials that were considered are shown in the Figure 11.1 and their respective properties and advantages are:

a) Kevlar

Kevlar is lightweight and sturdy material suitable for space travel. It has high strength, and is resistant to temperature changes making it ideal for the orbiting structures that move in and out of an eclipse. Kevlar's toughness and durability also makes it ideal for protecting the space craft.

b) Metal and Metal composites

Aluminium, Titanium and their alloys are used for the spacecraft bus and the framework as they can bear heavy loads without buckling.

c) Poly matrix composites

Organic-matrix composites can save up to 25 % weight of overall spacecraft mass.

d) Carbon-Carbon composites

They are used in structural parts requiring high temperatures.

This section gives an overview on the possible materials for the spacecraft. Stress analysis of the spacecraft and material selection is part of future work.

11.4 Critique and Final Satellite Configuration

The final spacecraft configuration complies with the fairing dimensions of the launcher (max of 5m for SLS Block 1) as shown in figures 11.2, 11.3, 11.4 which includes:

- a) EPS : 32 batteries of size 0.09m each and mass 0.6 kg each ; ~9 m² of solar array pointing towards the sun vector
- b) Propulsion: 1 spherical Oxidiser tank of diameter 1.42m; 1 spherical Fuel tank of diameter 1.64m; 1 spherical pressurant tank of diameter 0.76m ; 22 impulse manoeuvre thrusters
- c) Communication : 1 High gain Antenna of 2m pointing towards nadir
- d) OBDH: 1 OBC
- e) AOCS : 10 thrusters ; 4 reaction wheels; 1 IMU
- f) Mining: Regolith ore storage container cube of sides ~2m
- g) Optical payload : 1 NAC, 1 WAC
- h) 1 LIDAR system of size 14×20.6×16.5 cm [9]
- i) 1 Thermal Imager
- j) 1 X-ray Spectrometer of size 32×14×20 cm [9]
- k) 1 Microthermogravimeter
- l) 1 Infrared Spectrometer

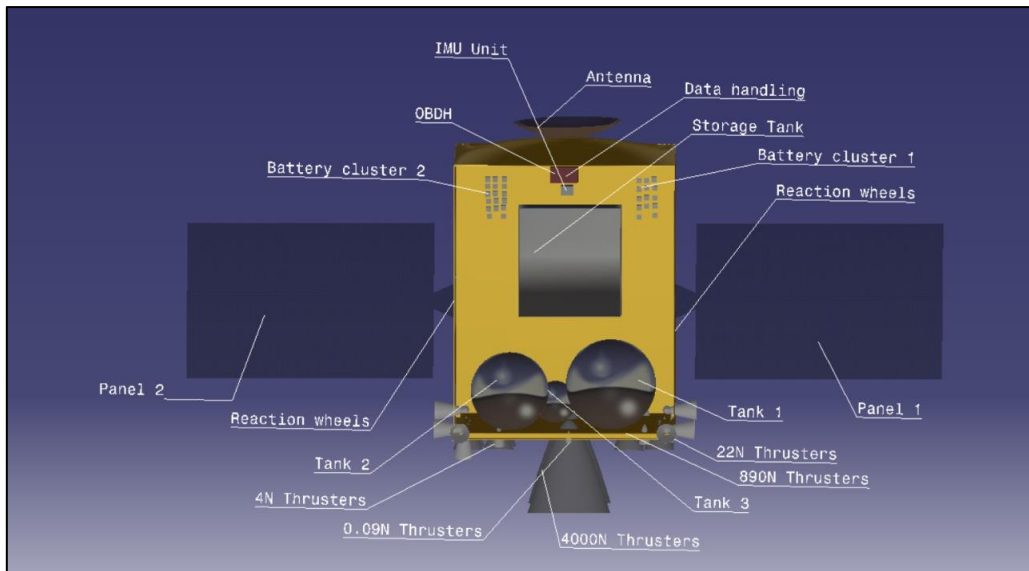


Figure 11. 2- Placement of payloads and tanks within the spacecraft configuration

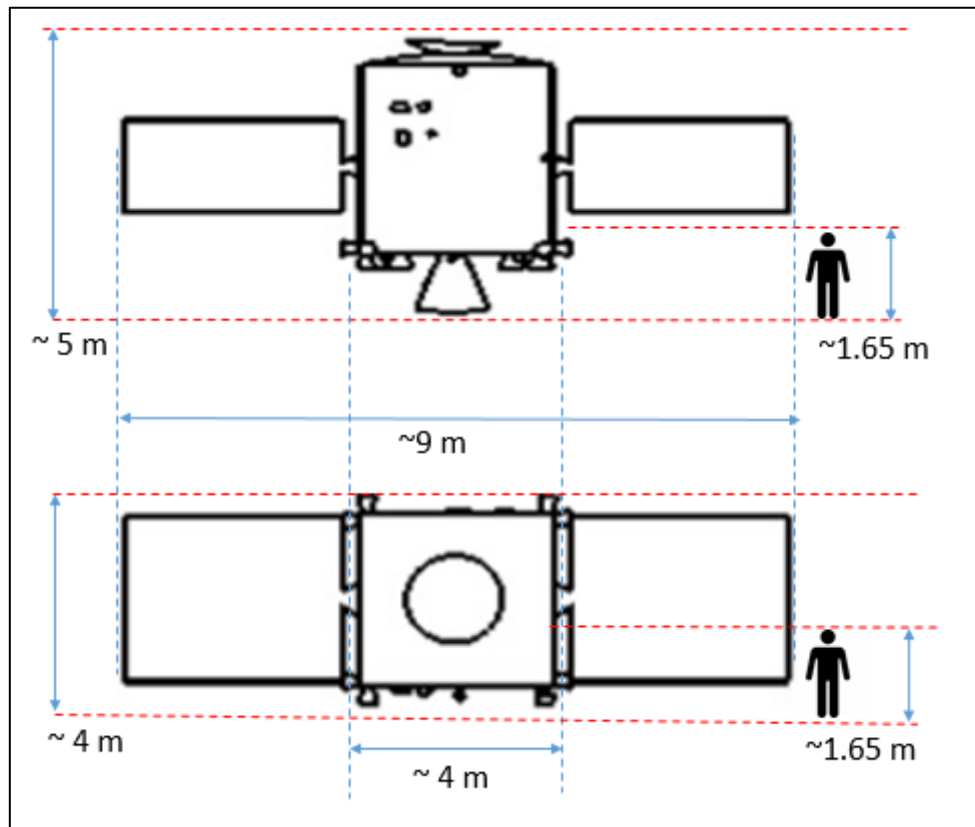


Figure 11. 3- Image to compare the size of spacecraft with a reference standard Indian human of average height of 1.65m

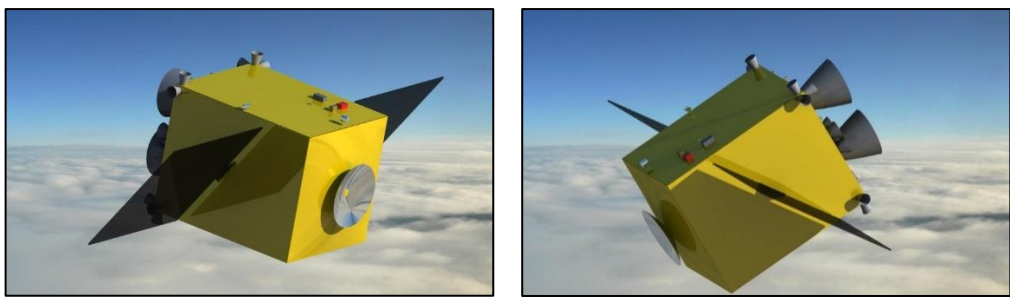


Figure 11. 4- The figure shows the rendered spacecraft module for the mission (Nadir/Earth pointing)

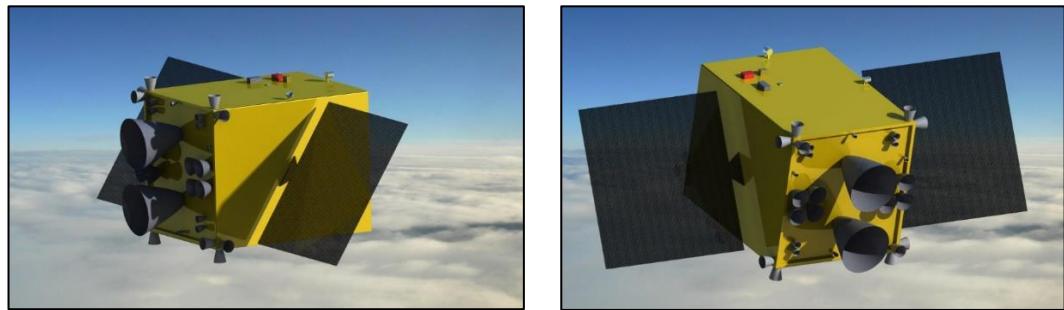


Figure 11. 5- The figure shows the rendered spacecraft module for the mission (Sun pointing; De-orbiting operations)

12 Mining Operations Sub-System

12.1 Introduction to different Mining Operational techniques used in Space

The best way to characterise mining operations for our mission is by looking to previously flown missions that have collected asteroid samples. OSIRIS Rex and Hayabusa missions were looked into as a part of literature survey.

- a) Osiris Rex used TAGSAM – Touch and Go sample acquisition for sample collection [9] [8]
- b) Hayabusa used ballistic methods to break asteroid regolith and collect the projectile regolith ejected towards the spacecraft for sample collection [14] [15]
- c) Phobos-Grunt although not an asteroid mission collected rock samples using a robotic arm [30]

All these methods had a very small resource collection of < 1kg. This cannot be scaled up to mine and collect 500 kg of ore and hence traditional earth mining methods were looked into.

Since traditional Earth mining methods have never been implemented in low gravity conditions like the Asteroid environment they have very low TRL. Hence, because of these uncertainties the report focuses on potential mining architecture concepts. These concepts are detailed in Section 12.2

12.2 Alternative Mining Architecture Concepts and Critique

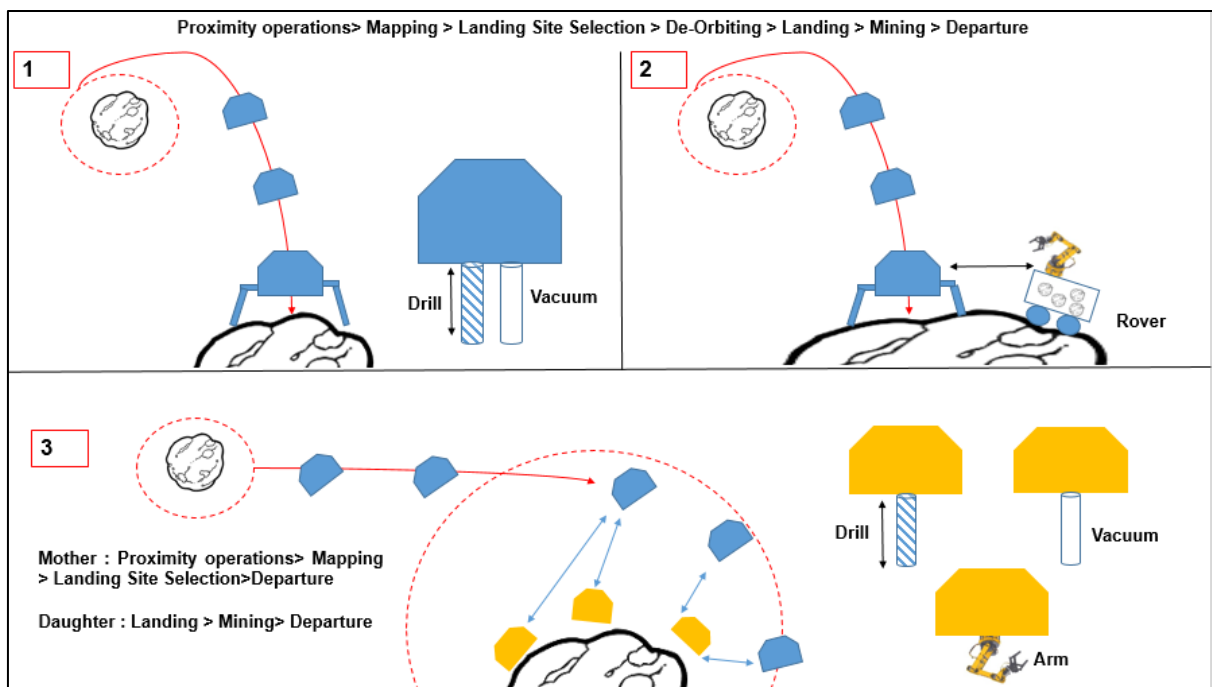


Figure 12. 1- The figure shows the different mining operational architectures

Figure 12.1 shows the different mining concept of operations which are:

a) Single Spacecraft Mining operations

The mining operations will be conducted by the spacecraft itself. The spacecraft after proximity operations, mapping, deorbits and lands on a suitable mining site. The Drill extension/Auger extension breaks the Asteroid regolith down into small handle able pieces and the vacuum extension/Arm extension collects the regolith and stores it in the spacecraft. Once a certain amount of regolith is collected, the spacecraft launches itself to find another suitable mining target. This process is repeated till 500kg of ore is collected. This kind of operational system is not redundant and has high failure rates.

b) Rover Mining Operations

The mining operations will be conducted by a rover that is deployed by the spacecraft once it lands on the Asteroid. The method has a very uncertainty than the other 2 mission architectures as the rover is likely going to escape the Asteroid due to very low gravity conditions of the order 0.00198 m/s^2 or $1.98E-06 \text{ km/s}^2$ which is 0.02 times the gravity of Earth. The velocity of escape is 0.77 m/s and if the rover needs to be operational then its velocity must be less than 2.7 km/hr. Curiosity travels at 0.14 km/hr, our rover probably also would have similar speeds.

c) Mother-Daughter Spacecraft Mining Operations

The mining operations will be conducted using multiple daughter space crafts that are launched from the mother orbiter spacecraft. These daughter space crafts are equipped with mining equipment. The daughter space crafts will return the mined ore to the orbiter that then departs to Earth. This comes at a very high ΔV cost and Mass constraint. These kind of operational systems are also quite complex and have high failure modes.

12.3 Critique of the Feasibility of Selected mining Technique

The Mining concept with a single spacecraft was chosen because of time constraints to explore and design other mining operational methods. It is to be noted that, any operational concept that is chosen needs to be further studied for feasibility, reliability, redundancy, complexity and for low-risk.

Furthermore a few possible parameters to consider for future that are currently uncertain are:

- a) The landing system of the spacecraft (Self, Daughter or rover systems) as the mining operation takes places in low gravity conditions.(Micro spines are considered as an
- b) The mining technique (operational and from a design standpoint)
- c) The power required for said mining technique
- d) The operational time of mining (This report assumes 1 year)
- e) The different structural load constraints caused because of mining
- f) Regolith Collection method (Arm extensions or vacuum or other Methods as such employed by OSIRIS Rex and Hayabusa)
- g) Ore extraction techniques (other non-mechanical techniques)
- h) ΔV and Mass constraints
- i) Regolith storage device for 500 kg of ore
- j) Spacecraft/ Rover anchoring method(Micro spines considered in this report based on a previous report study of SSERD intern batch –Team Vulcans; Design IP of Stanford University) [5]

13 Space Environmental Analysis

13.1 Introduction to Characteristics of Space Environment and its implications

Environmental Analysis of space is a well-researched subject and this report tries to capture the most common space threats that could potentially damage the spacecraft. This chapter does not detail the design outcomes to protect the spacecraft but rather establishes a risk framework for future design work such but not limited to radiation protection , solar cycle prediction for radiation , effective thermal protection etc.

Spacecraft design is heavily affected by space environmental characteristics such as:

- a) Thermal environment
- b) Ionising radiation(GCR and SEP)
- c) Plasma
- d) Vacuum of space
- e) Meteoroids/debris

Figure 13.1 shows some of the implications of the aforementioned factors on the spacecraft

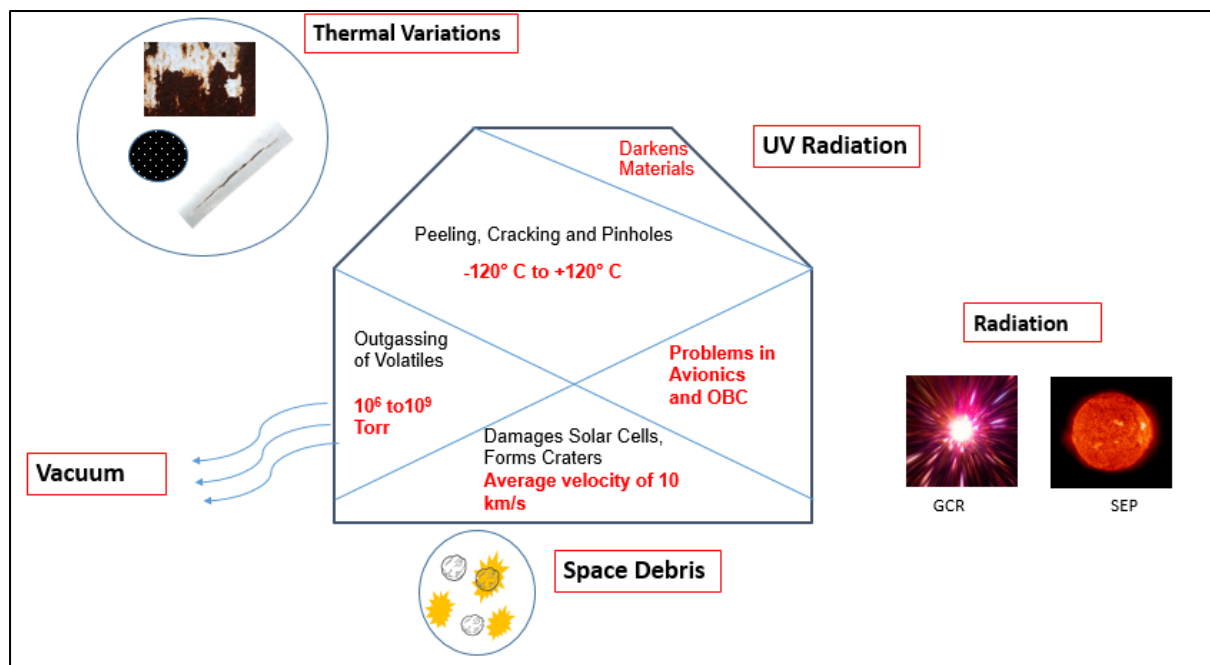


Figure 13. 1- The figure shows how space environment affects the spacecraft

Table 13.1 details the different threats and their magnitude of effects on the spacecraft

Table 13. 1- The table details how space environment affects the spacecraft

Threats	Effects of threats	Suitable conditions / materials	Range that it gets effected
Vacuum	1.Causes outgassing-releasing volatiles from materials 2. Molecular contamination can affect optical properties of the vehicle, payload surfaces, and space craft performance	Below 10^{-6} Torr	(10^{-6} to 10^{-9} Torr)
Atomic Oxygen	1. AO reacts with carbon, nitrogen, sulphur, hydrogen bonds. 2. Many polymers react and erode, AO increases longer exposure to UV radiation.	Thermal energy AO eliminates heating problem. Kapton*H and Kapton*HN polyimide are the most common materials used. Polyethylene, polypropylene, pyrolytic graphite.	N/A
Ultraviolet Radiation	1. Generally darkens materials, particularly in the presence of contamination. 2. Damages polymers by cross linking or chain scission.		N/A
Particulate or Ionizing Radiation	Main sources 1.Galactic cosmic rays 2.Solar proton events 3.Trapped radiation belts Greater effect is seen in "avionics" namely single-event upsets, bit errors		1.Radiation testing of a thermal control coating 3-5 mm thick could include protons and electrons Range 40 – 700 Kev (effect optical properties and coating chemistry) 2.Higher energy particles (1 to 70

			Mev) have been used to study single- event upsets
Plasma	Ion sputtering, arcing and parasitic currents in solar arrays as well as retraction of contamination.		
Temperature Extremes and thermal cycling	Leads to cracking, peeling, spalling, and formation of pinholes in the coating.		-120°C to +120°C
Micro meteoroid / Orbital Debris Impact	1.All areas of the spacecraft may be impacted by micrometeoroids travelling as fast as 60km/s 2.May crater the material 3.spall off a coating 4.Shot out solar cell		Surfaces facing the ram direction are more likely than those in the wake direction to be hit with space debris, travelling at an average velocity of 10km/s

Table 13.2 details the effect and magnitude of effect of ionising radiation caused due to Van Allen Belts on different spacecraft components.

Table 13. 2- The table shows how GCR and SEPs affect the spacecraft

Device type	Total Dose	Neutron	Prompt Dose Rate
Optical Fibres	≥100 k rad, polymer clad silica, 20°C , 0.85μm: 0.02-0.5 dB/m loss(1-2 orders less loss at 1.5μm)	>10 ¹⁴ n/cm ² for 0.02-0.5 dB/m loss	Losses increases 1-2 orders, depending on dose, dose rate, wavelength and temperature. Nearly complete annealing in≤24 hrs
Transmitters	1-10 M rad (up to 3.0 dB light loss) for LEDs and laser diodes, peak wavelength shifts, threshold current increases, beam pattern distorts, power loss	10 ¹² -10 ¹⁴ n/cm ² for LEDs (threshold) 10 ¹³ -10 ¹⁵ n/cm ² for laser diodes (threshold). Light output loss and peak wavelength shifts.	Ionization induced burnout at 10 ⁹ -10 ¹⁰ rad/s Pulsed lasers turn-on delays are up to 100ns *Power loss, wavelength shifts

Detectors	Decrease in responsivity of 10-30% at 10Mrad. Dark current increase of 1-2 orders at 10-100 M rads (for SI PIN photodiodes, worse for APDs, better for AlGAsAs/GaAs photodiodes)	Displacement damage thresholds of -10^{14} n/cm ² for SI PIN photodiodes and -10^{12} for APDs. Dark current increases, responsibility decreases.	Dark current increases linearly up to -10^{10} rads/s False signal generation by radiation pulse. Upset at $\geq 10^7$ rads/s. Burnout at $\geq 10^9$ rads/s. APDs much more sensitive than PIN photodiodes
Opto modulators	Depends on device and device technology	Depends on device and device technology	Depends on device and device technology. Circuit upset and burnout possible.

14 Budgets

14.1 Mass Budget

Table 14. 1- The table shows the Mass budget for the mission

Mass budget		
Propellant	4620.86	kg
Helium	15.9	kg
Thrusters	72.25	kg
Fuel tank	63.9	kg
Ox Tank	63.9	kg
Helium Tank	20.4	kg
Battery	24	kg
Solar panels	406.56	kg
Reaction wheels	35.6	kg
Hammer	83.1	kg
Auger	81	kg
Robotic arm	100	kg
MGA	0.3	kg
HGA	2.5	kg
OBC	1	kg
Thermal	76.8	kg
Total Mass	5668.074	kg
Total Mass + 30% margin	7368.497	kg

15 Conclusion and Future Work

This report presents a feasibility study and preliminary spacecraft design for an asteroid mining mission whose objective is to return 500kg of resources and be launched between the year 2027 and 2030.

A detailed study on near-earth asteroids was conducted to select the most suitable candidates for this mission. Trade parameters included asteroid composition, size, minimum ΔV requirements and the number of possible launch opportunities within the timeframe. The asteroid selected for this mission was 1989ML due to its high metallic composition.

The mission analyses conducted to plot the optimum trajectory to the asteroid (and back), considered seven possible scenarios. The option which showed the most feasibility and fuel savings was to use a Mars fly-by to reach the asteroid. The Delta – V requirements for this option was found to be ~1.6km/s, and the mission duration is 4 years.

Preliminary spacecraft design was conducted to solve subsystem designs to meet the payload and delta-V targets. The final spacecraft mass after subsystem design is ~7 tonnes (which includes a 25% margin). Based on preliminary design results, this mission concept is considered to be feasible using the SLS launcher and is compliant with the requirements mentioned in Section 3.

It is clear that for a mission such as this there are a number of technical, socio-political and financial challenges that have to be overcome to make this a reality.

For areas covered in this report some of these are addressed however there are also a number of areas beyond the scope of the report.

The actual environment of the asteroid needs to be better understood. Yarkovsky effect, Shape model of the asteroid, tumbling properties, spin state, asteroid mass need to be refined and better understood. Radiation environment for a long term mission also need to be studied.

Landing site analysis needs to be performed and selected potentially before launch for the purposes of the mission based on the key criteria outlined. With further analysis, better defined scientific and mining aims, as well as future data from missions to Target Asteroid is necessary.

The work presented in this report explores the feasibility of an Asteroid mining mission and the top-level sub system design. The mission is driven by the need to launch within the timeframe of 2027 to 2030, ΔV (km/s) and the return of 500 kg of regolith ore to LEO or cis-lunar orbits. The need and objectives for the mission are captured in Chapter 1.

Chapter 2 reviews previously flown asteroid sample return missions which sets a baseline framework for our mission architecture and its relevant sub-system work.

Literature is fed into evaluation of requirements in Section 3, Selection of Target asteroid in Chapter 4 and all the other sub-system designs. The literature review gives us the limitations and opportunities in mission and spacecraft design

Following literature review, critical requirements are derived based on the selection of key-subsystem drivers for the spacecraft sub-system and mission.

Selection of target asteroid sets a baseline for design of all the other sub-systems. The trade parameters considered are ΔV requirements, composition, size and number of launch opportunities available. This data is found using the NASA Small Body Database by analysis of pork chop plots.

1989ML is selected as the target asteroid as it is an X-type asteroid with high metallic content and has 5 launch opportunities within the launch window. The preliminary ΔV for a direct transfer is found to be 4.4 km/s. Using NASA SSD the maximum launch mass is also found for minimum ΔV . The maximum launch mass for asteroid rendezvous is 10 to 15 tonnes for SLS Block 1 launcher. SLS block 1 has a maximum 5m fairing envelope and our spacecraft of dimensions $< 4 \times 4 \times 5$ m (solar arrays folded) is compliant with fairing dimensions as discussed in Chapter 11. The spacecraft is also compliant with the total lift-off mass of ~7 tonnes.

Furthermore, the ΔV requirements of the mission is refined to 1.6 km/s by including a Mars gravity assist. The ΔV requirements for proximity operations is found to be ~13 cm/s. These values are calculated using the standard patched conics method and Hohmann transfers and further STK analysis needs to be conducted to get the appropriate ΔV requirements for all phase of the mission.

Sub-system budgets are found subsequently through Chapters 6 to 12 and Mass budget is found in Chapter 14

Chapter 6 captures the propulsion system for the mission. The spacecraft uses a bi-propellant system of hydrazine and nitrogen tetroxide with overall propellant mass of 4.62 tonnes for the entire mission and is pressurised using Helium of mass 15.9 kg. The total thrust requirements for the mission is found using the Thrust to weight ratio of Soyuz MS spacecraft that has similar weight to our spacecraft. The thrust to weight ratio for our spacecraft is found to be 2.20 with a net effective ISP of 296 seconds. The spacecraft has a total of 32 thrusters (AOCS included) with varying thrust outputs which are selected based on the preliminary total thrust required for the mission. Feedline system components and architecture and thruster design need to be done as a part of future work.

Chapter 7 captures the AOCS system for the mission. The AOCS architecture consists of 4 reaction wheels, thrusters and sun and star sensors for a complete 3-axis stabilisation during orbit keeping for low gravity mining conditions.

Chapter 8 captures the Electrical system for the mission. The total area the spacecraft spends in eclipse around the Asteroid with a parking orbit of 10km is 75 minutes. The system is designed for this constraint and has a Li-ion battery mass of ~23 kg and a GaS solar array panel of area ~9 m² for a maximum power usage of ~1000 W

Chapter 9 captures the Communication and OBDH system for the mission. The communication takes place over 4 X-band antennae: 1 HGA of 2m ø, 1 MGA of 0.4m ø and 2 LGA. The total Link Budget for the X-band is 18.82 dB and for DSN is 5.02 dB. Electrical interface mapping and Data rates is considered part of future work. Further detailed study of OBDH systems also need to be done and justified for the needs of the mission.

Chapter 10 captures the Thermal system for our mission. Equilibrium temperatures of the spacecraft for different spacecraft scenarios (Around Earth and Around Asteroid) are found. Passive thermal control finishes are traded using the Heat balance equation and MLI –Kapton with aluminium back covering is picked as it provides good thermal control for the spacecraft payloads operating between a ranges of -70° to 166° Celsius. Active thermal control like the radiators need to be explored as a part of future work.

Chapter 11 captures the Structures system for the mission. Different spacecraft materials are explored and their respective advantages are listed. However the material is not selected as Structural and thermal analysis needs to be performed. The spacecraft orientation and placement of payloads within the spacecraft framework is rendered in CATIA V5 and a

preliminary spacecraft module is produced. Vibrational load analysis needs to be performed as the spacecraft undergoes high stresses due to mining operations which is part of future work.

Chapter 12 captures the Mining Operations system for the mission. Different mining concepts are looked into and critiqued and the Mining concept with a single spacecraft is chosen due to time constraints of the internship. This sub-system has high uncertainties as there are no previous flown missions that have a resource return of >500 kg. The biggest sample size returned to earth is around the range of ~ 60 g. Hence, there is no reliable way to justify the sub-system elements. A great deal of future work needs to be done in designing the mining mechanism for low gravity environments and mining operations that has low failure rates for the mission duration.

Chapter 13 captures the Space Environment for the mission. Space environmental analysis is pretty standard as there is a lot of data regarding the impacts of space environment on spacecraft. Effectors are discussed and possible impact on the spacecraft is captured.

Chapter 14 captures the Mass Budget for the mission. The mass budget gives us the overall mass of the spacecraft including the propellants and dry mass (all sub-system mass) which is necessary to check if it compliant with the lift-off mass capability of the launcher. The overall lift-off mass of the spacecraft is ~7 tonnes.

Overall, the internship was a success; the scope and complexity of the mission meant that a significant amount of time was devoted to the definition of the project at the start, however this was essential for the clarity of the work that followed. A suitable and functional baseline was established for the mission and a viable engineering solution was developed. This report could be a good baseline for any further work and development on the project.

Due to the scope of the project some areas could only be examined at a top level, these are identified in the relevant Chapters as areas that require future work. Given more time and resources these areas could have been developed further to give a better overall design concept.

APPENDIX A
TEAM MEMBERS AND TEAM LOGO



Figure A. 1- The figure shows the logo created for the internship batch 4

The figure above shows the team logo created for the internship by team leader - Akanksha Maskeri and Team Member – Abhijeeth Someshwar using the online tool Canva.

The figure below shows the team members for the SSERD batch 4 internship.



Figure A. 2- The figure shows the different team members for the IPS batch 4 of the internship

APPENDIX B

MATLAB CODE FOR ORBIT PLOTS

The MATLAB code below gives the Orbital Transfers and orbital plots for our Mission

```
%% MATLAB Code for Orbit Transfers and Orbit diagrams
% V V K Lalithej SSERD IPD Batch 4 Pathfinders

%% Matlab Code

%% Initialization of values

au = 149598073; %km to au
eccen_earth = 0.0167086; % eccentricity of earth
semimajor = au + 500;
Rpe = 147.10*10^6; %Perigee distance km
Rpeau = Rpe/au; %Perigee distance au
mu = 1.3271*10^11; %Gravitational Constant
VE = orbit_vel(Rpe,semimajor,mu); %Orbital Velocity

%% Transfer Orbit Parameters

transfer_apogee = 1.15*au; %Transfer orbit apogee
VTE = orbit_vel(Rpe,au2,mu); %V at TO
delV = abs(VE-VTE); %delV for TO

%% Earth Orbit
theta = [0:0.001:2*pi];
a_earth = 1;
e_earth = 0.0137;
b_earth = eccen(a_earth,e_earth);
x_earth = a_earth*cos(theta);
y_earth = b_earth*sin(theta);
plot(x_earth,y_earth,'LineWidth',1.5)
hold on

%% Mars Orbit
a_mars = 1.52366;
e_mars = 0.0937;
b_mars = eccen(a_mars,e_mars);
x_mars = a_mars*cos(theta);
y_mars = b_mars*sin(theta);
plot(x_mars,y_mars,'LineWidth',1.5)
hold on

%% Asteroid 1989 ML Orbit
%Orbit Parameters
a_DL = 1.272206355146454;
e_DL = .1364029076489758;
b_DL = eccen(a,e);
q_DL = 1.098673709174972;
x_DL = a*cos(theta)-0.1735;
y_DL = b*sin(theta);
deg = pi/3 - pi/15;

x_1989ML = x_DL*cos(deg) - y_DL*sin(deg);
```

```

y_1989ML = y_ML*cos(deg) + x_ML*sin(deg);

hold on
grid on
plot(x_1989ML,y_1989ML,'-', 'LineWidth',1.5)

% Calculation of Transfer Ellipse using co-ordinates

theta_TO = [0:0.001:pi*6/7 + pi/11];
a_TO = 1.265;
e_TO = 0.01;
b_TO = eccen(a_TO,e_TO);
x_TO = a_TO*cos(theta2)-0.265;
y_TO = b_TO*sin(theta2);
plot(x_TO,y_TO,'--m','LineWidth',1.5)

%% Mars to Asteroid Orbit

theta_MTO = [(pi + pi/4.55) :0.001:pi*1.98];
a_MTO = 1.4107;
e_MTO = 0.281;
b_MTO = eccen(a,e);
x_MTO = -(a*cos(theta2)+ (1.524 - 1.4107));
y_MTO = b*sin(theta2);
deg = -pi/10;

x_MarsTO = x_MTO*cos(deg) - y_MTO*sin(deg);
y_MarsTO = y_MTO*cos(deg) + x_MTO*sin(deg);

plot(x_MarsTO,y_MarsTO,'--b','LineWidth',1.5)
xlabel('X (au)')
ylabel('Y (au)')
hold on

%% Return Transfer based on porkchop plots

theta_RTO = [pi :0.001:pi*3/2];
a_RTO = 1.374;
b_RTO = 1;
X_RTO = a_RTO*cos(theta_RTO);
Y_RTO = b_RTO*sin(theta_RTO);
plot(X_RTO,Y_RTO,'--k','LineWidth',1.5)

% Planet Instantaneous Positions

plot(0,0,'or') %Sun
plot(1, 0,'ob') %Earth
plot(0,-1,'ok') % Mars
plot(-1.493,0.3004,'dr') %1989ML

plot(0.6601,-1.121,'db')
plot(-1.374,0,'dk')
xlim([-2 3])
legend('Earth Orbit','Mars orbit','1989 ML orbit','Earth to Mars Transfer','Mars to A')

```

```

Asteroid','Return Trajectory','Sun','Earth(12/7/2028)','Earth(1/5/2034)','Mars
(15/2/2029)', '1989 ML(20/11/2029)', '1989 ML(2/12/2033)')
legend('Location','NorthEast');
title('Orbit Diagram')

function b = eccen(a,e)

b = a*sqrt(1 - e^2);

end

```

The output of the Code is as shown below:

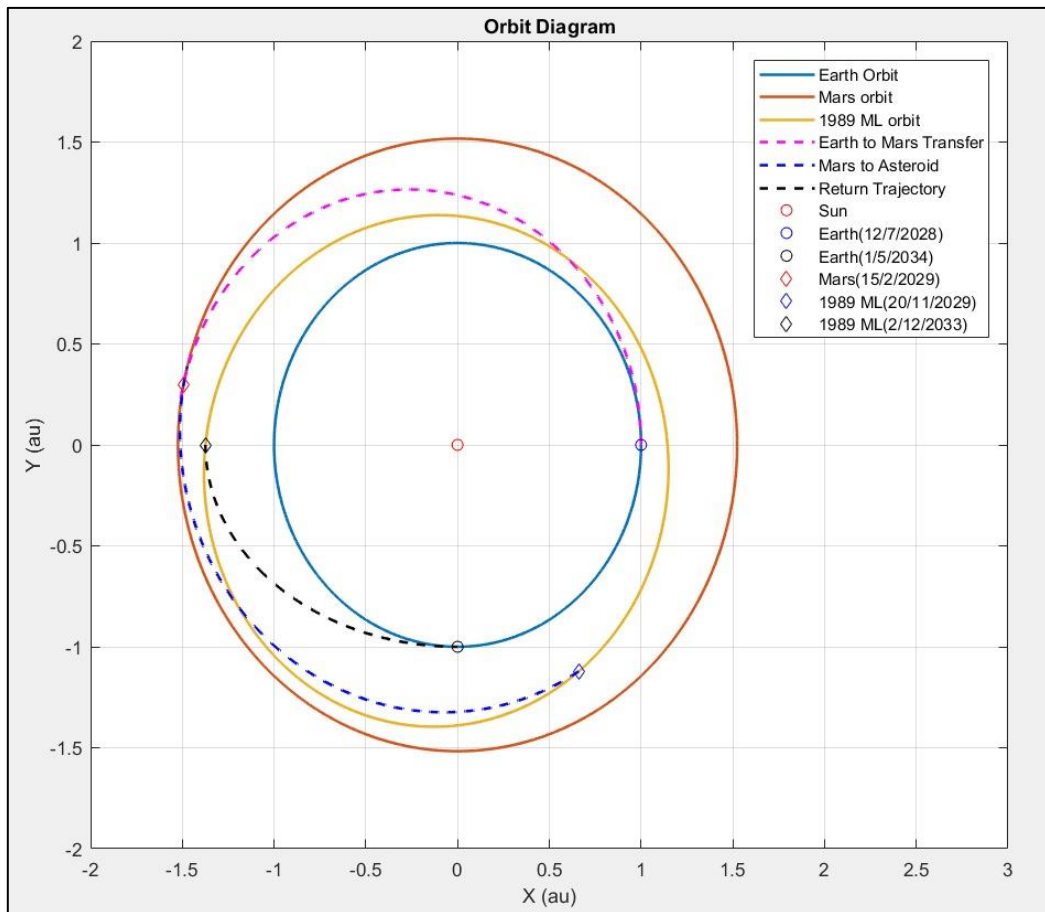


Figure B. 1- The figure shows the orbits for our mission

APPENDIX C

ΔV CALCULATIONS FOR VARIOUS MISSION ARCHITECTURES

MISSION SCENARIO 1: DIRECT TRANSFER FROM EARTH TO ASTEROID

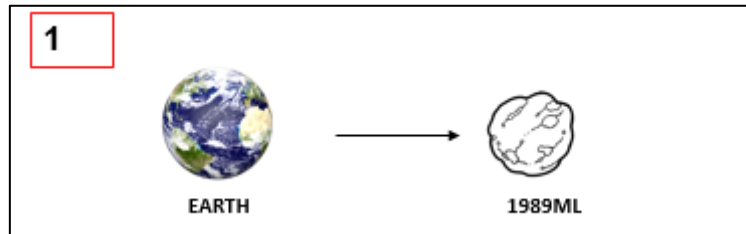


Figure C. 1- Mission scenario 1

Table C. 1- ΔV Calculation for Mission Scenario 1 using Hohmann Transfer

ΔV Calculation						
Heliocentric cruise Earth Departure, Asteroid Rendevous						
Standard Hohmann Transfer						
μ_{Sun}	1.33E+20		m3/s2			
Earth distance from Sun	1	AU	1.50E+11	m		
Asteroid distance from Sun	1.1	AU	1.65E+11	m		
ΔV_1 - Earth Departure						
$\Delta v_1 = v_2 - v_1 = \sqrt{\frac{\mu}{r_1}} \left[\sqrt{\frac{2r_2}{r_1 + r_2}} - 1 \right]$						
ΔV_1	700.87	m/s	0.70	km/s		
ΔV_2 - Asteroid Arrival						
$\Delta v_2 = v_4 - v_3 = \sqrt{\frac{\mu}{r_2}} \left[1 - \sqrt{\frac{2r_1}{r_1 + r_2}} \right]$						
ΔV_2	6.84E+02	m/s	0.68	km/s		
ΔV_{total}	$\Delta V_1 + \Delta V_2$		1.39	km/s		
Heliocentric cruise Asteroid Departure, Earth Rendevous						
Standard Hohmann Transfer						
μ_{Sun}	1.33E+20		m3/s2			
Earth distance from Sun	1	AU	1.50E+11	m		
Asteroid distance from Sun	1.1	AU	1.65E+11	m		
ΔV_1 - Asteroid Departure						
$\Delta v_2 = v_4 - v_3 = \sqrt{\frac{\mu}{r_2}} \left[1 - \sqrt{\frac{2r_1}{r_1 + r_2}} \right]$						

ΔV_1	6.84E+02	m/s	0.68	km/s
ΔV_2 - Earth Arrival				
$\Delta v_1 = v_2 - v_1 = \sqrt{\frac{\mu}{r_1}} \left[\sqrt{\left(\frac{2r_2}{r_1 + r_2} \right)} - 1 \right]$				
ΔV_2	700.87	m/s	0.70	km/s
ΔV_{total}	$\Delta V_1 + \Delta V_2$		1.39	km/s
$\Delta V_{\text{totalTrip}}$	2.77			km/s
Time of Flight to Asteroid Orbit insertion				
$T = 2\pi \sqrt{\frac{a^3}{\mu_{\text{Sun}}}}$				
a	1.5708E+11		m	
T	3.93E+02		days	
ToF	1.08E+00		years	

Table C. 2- ΔV Calculation for Mission Scenario 1 using Patched Conics

True ΔV Calculation without any Gravity Assists		
Patched Conic Method		
μ_{Sun}	1.33E+20	m3/s2
Earth radius	6378	km
Asteroid radius	0.15	km
μ_{Earth}	3.99E+05	km3/s2
$\mu_{1989\text{ML}}$	4.47E-08	km3/s2
Earth parking	16378	km
Heliocentric cruise		
VEarth	29.78	km/s
VParking	30.48	km/s
V^∞ Earth Departure	0.70	km/s
V1989ML	28.40	km/s
VApproach	27.71	km/s
V^∞ Asteroid arrival	0.68	km/s
ΔV_1 - Earth Hyperbolic Departure		
VParking	7.01	km/s
VCircular	4.93	km/s
ΔV_1	2.08	km/s
ΔV_2 - Asteroid Hyperbolic Arrival		
Asteroid Parking	10.15	km
VcircularAsteroid	0.00006637	km/s
VparkingAsteroid	0.68	km/s

$\Delta V2$	0.68	km/s
ΔV_{total}	2.76	km/s
$\Delta V_{\text{mission}}$	5.53	km/s

MISSION SCENARIO 2: EARTH GRAVITY ASSIST TO ASTEROID

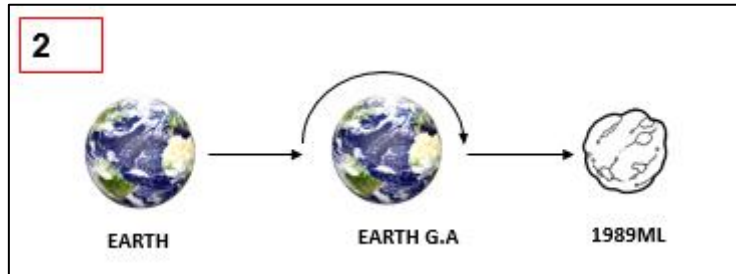


Figure C. 2- Mission Scenario 2

Table C. 3- ΔV Calculation for Mission Scenario 2

True ΔV Calculation using Earth Gravity Assist							
Patched Conic Method							
μ_{Sun}	1.33E+20	m3/s2					
Earth distance from Sun	1	AU	1.50E+11	m			
1989ML distance from Sun	1.1	AU	1.65E+11	m			
Earth radius	6371	km					
Asteroid radius	0.15	km					
μ_{Earth}	3.99E+05	km3/s2					
μ_{1989ML}	4.47E-08	km3/s2					
Earth parking	16371	km					
Earth fly-by altitude	50000	km					
Heliocentric Earth Departure							
VEarth	29.78	km/s					
Vparking	30.48	km/s					
V_{∞} Earth Departure=Approach	0.70	km/s					
Eccentricity of Arrival Trajectory at Earth							
$e = 1 + \frac{r_p v_e^2}{\mu}$							
eEarth	1.06						
Deflection Angle							
δ	2.456829238	rad	140.7659	deg			
$\Delta V_{\text{fly-by}}$	1.34	km/s					
Heliocentric Earth Departure							
V_{∞} Earth Departure	0.70	km/s					
V1989ML	28.40	km/s					

VApproach	27.71	km/s
V ∞ Asteroid Approach	0.68	km/s
ΔV Earth Hyperbolic Departure		
Vparking around Earth	4.05	km/s
Vcircular around Earth	2.82	km/s
$\Delta V1$	1.23	km/s
ΔV Asteroid Arrival Hyperbolic Capture		
Asteroid Parking distance	10.15	km
VcircularAsteroid	0.00006637	km/s
VparkingAsteroid	0.68	km/s
$\Delta V2$	0.68	km/s
ΔV total to asteroid	1.91	km/s
Heliocentric Earth Arrival		
V1989ML	28.40	km/s
VApproach	27.71	km/s
V ∞ Asteroid departure	0.68	km/s
VEarth	29.78	km/s
VParking	30.48	km/s
V ∞ Earth Arrival	0.70	km/s
ΔV Asteroid Hyperbolic Departure		
Asteroid Parking	10.15	km
VcircularAsteroid	0.00006637	km/s
VparkingAsteroid	0.68	km/s
$\Delta V1$	0.68	km/s
ΔV Earth Hyperbolic Arrival		
VParking	7.01	km/s
VCircular	4.93	km/s
$\Delta V2$	2.08	km/s
ΔV total to Earth	2.76	km/s
ΔV total mission	3.34	km/s

MISSION SCENARIO 3: MOON GRAVITY ASSIST TO ASTEROID

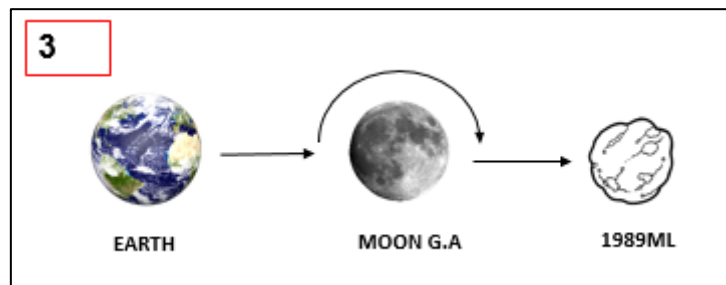


Figure C. 3- Mission scenario 3

Table C. 4- ΔV Calculation for Mission Scenario 3

True ΔV Calculation using Moon Gravity Assist						
Patched Conic Method						
μ_{Sun}	1.33E+20	m^3/s^2				
Earth distance from Sun	1	AU	1.50E+11	m		
Moon distance from Sun	1.002569	AU	1.50E+11	m		
1989ML distance from Sun	1.1	AU	1.65E+11	m		
Earth radius	6371	km				
Asteroid radius	0.15	km				
μ_{Earth}	3.99E+05	km^3/s^2				
$\mu_{1989\text{ML}}$	4.47E-08	km^3/s^2				
μ_{Moon}	4.90E+03	km^3/s^2				
Earth parking	16371	km				
Moon fly-by altitude	50000	km				
Heliocentric Earth Departure						
V _{Earth}	29.78	km/s				
V _{parking}	29.80	km/s				
V _{&infty} Earth Departure	0.02	km/s				
V _{Moon}	29.74	km/s				
V _{Approach}	29.73	km/s				
V _{&infty} Moon Approach	0.02	km/s				
Eccentricity of Arrival Trajectory at Moon						
$e = 1 + \frac{r_p v_\infty^2}{\mu}$						
e _{Moon}	1.00					
Deflection Angle						
δ	2.969422065	rad	170.1354	deg		
$\Delta V_{\text{fly-by}}$	0.01	km/s				
Heliocentric Moon Departure						
V _{&infty} Moon Departure	0.02	km/s				
V _{1989ML}	28.40	km/s				
V _{Aapproach}	27.73	km/s				
V _{&infty} Asteroid Approach	0.67	km/s				
ΔV Moon Hyperbolic Departure						
V _{parking around Moon}	0.44	km/s				
V _{circular around Moon}	0.31	km/s				
ΔV_1	0.13	km/s				
ΔV Asteroid Arrival Hyperbolic Capture						
Asteroid Parking distance	10.15	km				
V _{circularAsteroid}	0.00006637	km/s				
V _{parkingAsteroid}	0.67	km/s				
ΔV_2	0.67	km/s				
$\Delta V_{\text{total to asteroid}}$	0.80	km/s				

Heliocentric Earth Arrival		
V1989ML	28.40	km/s
VApproach	27.71	km/s
V∞ Asteroid departure	0.68	km/s
VEarth	29.78	km/s
VParking	30.48	km/s
V∞ Earth Arrival	0.70	km/s
ΔV Asteroid Hyperbolic Departure		
Asteroid Parking	10.15	km
VcircularAsteroid	0.00006637	km/s
VparkingAsteroid	0.68	km/s
ΔV_1	0.68	km/s
ΔV Earth Hyperbolic Arrival		
VParking	7.01	km/s
VCircular	4.93	km/s
ΔV_2	2.08	km/s
$\Delta V_{\text{total to Earth}}$	2.76	km/s
$\Delta V_{\text{total mission}}$	3.55	km/s

MISSION SCENARIO 4: MARS GRAVITY ASSIST TO ASTEROID

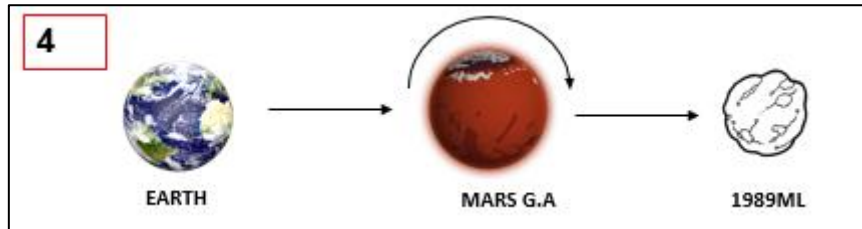


Figure C. 4 – Mission Architecture Scenario 4

Table C. 5- ΔV Calculation for Mission Scenario 4

True ΔV Calculation using Mars Gravity Assist				
Patched Conic Method				
μ_{Sun}	1.33E+20		m^3/s^2	
Earth distance from Sun	1	AU	1.50E+11	m
Mars distance from Sun	1.45	AU	2.17E+11	m
1989ML distance from Sun	1.1	AU	1.65E+11	m
Earth radius	6371		km	
Asteroid radius	0.15		km	
μ_{Earth}	3.99E+05		km^3/s^2	
μ_{1989ML}	4.47E-08		km^3/s^2	
μ_{Mars}	4.28E+04		km^3/s^2	
Earth parking	16371		km	
M fly-by altitude	50000		km	
Heliocentric Earth Departure				

VEarth	29.78	km/s
Vparking	32.40	km/s
V ∞ Earth Departure	2.62	km/s
VMars	24.73	km/s
Vapproach	22.35	km/s
V ∞ Mars Approach	2.39	km/s
Eccentricity of Arrival Trajectory at Mars		
eMars	7.65	
Deflection Angle		
δ	0.262158416	rad 15.02057 deg
$\Delta V_{\text{fly-by}}$	4.49	km/s
Heliocentric Mars Departure		
V ∞ Mars Departure	2.39	km/s
V1989ML	28.40	km/s
VApproach	30.28	km/s
V ∞ Asteroid Approach	1.89	km/s
ΔV Mars Hyperbolic Departure		
Vparking around Mars	2.72	km/s
Vcircular around Mars	0.93	km/s
ΔV_1	1.80	km/s
ΔV Asteroid Arrival Hyperbolic Capture		
Asteroid Parking distance	10.15	km
VcircularAsteroid	0.00006637	km/s
VparkingAsteroid	1.89	km/s
ΔV_2	1.89	km/s
$\Delta V_{\text{total to asteroid}}$	3.68	km/s
Heliocentric Earth Arrival		
V1989ML	28.40	km/s
Vparking	27.71	km/s
V ∞ Asteroid departure	0.68	km/s
VEarth	29.78	km/s
VParking	30.48	km/s
V ∞ Earth Arrival	0.70	km/s
ΔV Asteroid Hyperbolic Departure		
Asteroid Parking	10.15	km
VcircularAsteroid	0.00006637	km/s
VparkingAsteroid	0.68	km/s
ΔV_1	0.68	km/s
ΔV Earth Hyperbolic Arrival		
VParking	7.01	km/s
VCircular	4.93	km/s
ΔV_2	2.08	km/s
$\Delta V_{\text{total to Earth}}$	2.76	km/s
$\Delta V_{\text{total mission}}$	1.95	km/s

Table C. 6- Optimised ΔV Calculation for Mission Scenario 4

True ΔV Calculation using Mars Gravity Assist (OPTIMISED)							
Patched Conic Method							
μ_{Sun}	1.33E+20	m^3/s^2					
Earth distance from Sun	1	AU	1.50E+11	m			
Mars distance from Sun	1.45	AU	2.17E+11	m			
1989ML distance from Sun	1.1	AU	1.65E+11	m			
Earth radius	6371	km					
Asteroid radius	0.15	km					
μ_{Earth}	3.99E+05	km^3/s^2					
$\mu_{1989\text{ML}}$	4.47E-08	km^3/s^2					
μ_{Mars}	4.28E+04	km^3/s^2					
Earth parking	16371	km					
M fly-by altitude	31897.55217	km					
Heliocentric Earth Departure							
VEarth	29.78	km/s					
Vparking	32.40	km/s					
V^∞ Earth Departure	2.62	km/s					
VMars	24.73	km/s					
Vapproach	22.35	km/s					
V^∞ Mars Approach	2.39	km/s					
Eccentricity of Arrival Trajectory at Mars							
$e = 1 + \frac{r_p v_\infty^2}{\mu}$							
eMars	5.24						
Deflection Angle							
δ	0.383817949	rad	21.99115	deg			
$\Delta V_{\text{fly-by}}$	4.77	km/s					
Heliocentric Mars Departure							
V^∞ Mars Departure	2.39	km/s					
V1989ML	28.40	km/s					
VAapproach	30.28	km/s					
V^∞ Asteroid Approach	1.89	km/s					
ΔV Mars Hyperbolic Departure							
Vparking around Mars	2.89	km/s					
Vcircular around Mars	1.16	km/s					
ΔV_1	1.74	km/s					
ΔV Asteroid Arrival Hyperbolic Capture							
Asteroid Parking distance	10.15	km					
VcircularAsteroid	0.00006637	km/s					
VparkingAsteroid	1.89	km/s					
ΔV_2	1.89	km/s					

$\Delta V_{\text{total to asteroid}}$	3.62	km/s
Heliocentric Earth Arrival		
V1989ML	28.40	km/s
VApproach	27.71	km/s
V^∞ Asteroid departure	0.68	km/s
VEarth	29.78	km/s
VParking	30.48	km/s
V^∞ Earth Arrival	0.70	km/s
ΔV Asteroid Hyperbolic Departure		
Asteroid Parking	10.15	km
VcircularAsteroid	0.00006637	km/s
VparkingAsteroid	0.68	km/s
ΔV_1	0.68	km/s
ΔV Earth Hyperbolic Arrival		
VParking	7.01	km/s
VCircular	4.93	km/s
ΔV_2	2.08	km/s
$\Delta V_{\text{total to Earth}}$	2.76	km/s
$\Delta V_{\text{total mission}}$	1.61	km/s

MISSION SCENARIO 5: MOON AND MARS GRAVITY ASSIST TO ASTEROID

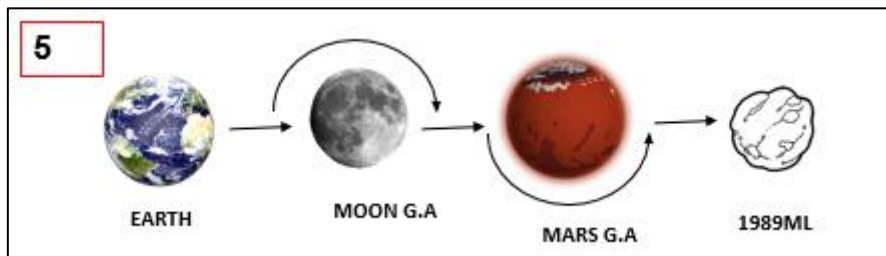


Figure C. 5 – Mission Architecture Scenario 5

Table C. 7- ΔV Calculations for Mission Scenario 5

True ΔV Calculation using Moon and Mars Gravity Assists				
Patched Conic Method				
μ_{Sun}	1.33E+20	m3/s2		
Earth distance from Sun	1	AU	1.50E+11	m
Moon distance from Sun	1.002569	AU	1.50E+11	m
1989ML distance from Sun	1.1	AU	1.65E+11	m
Mars distance from Sun	1.45	AU	2.17E+11	m
Earth radius	6371	km		
Asteroid radius	0.15	km		
μ_{Earth}	3.99E+05	km3/s2		

μ_{1989ML}	4.47E-08	km ³ /s ²
μ_{Moon}	4.90E+03	km ³ /s ²
μ_{Mars}	4.28E+04	km ³ /s ²
Earth parking	16371	km
Moon fly-by altitude	50000	km
Mars fly-by altitude	50000	km
Heliocentric Earth Departure		
V_{Earth}	29.78	km/s
V_{parking}	29.80	km/s
$V^{\infty}_{\text{Earth}} \text{ Departure}$	0.02	km/s
V_{moon}	29.74	km/s
V_{approach}	29.73	km/s
$V^{\infty}_{\text{Moon Approach}}$	0.02	km/s
Eccentricity of Arrival Trajectory at Moon		
$e = 1 + \frac{r_p v_p^2}{\mu}$		
e_{Moon}	1.00	
Deflection Angle		
δ	2.969422065	rad 170.1354 deg
$\Delta V_{\text{fly-by}}$	0.01	km/s
Heliocentric Moon Departure		
$V^{\infty}_{\text{Moon Departure}}$	0.02	km/s
V_{Mars}	24.73	km/s
V_{approach}	22.36	km/s
$V^{\infty}_{\text{Mars Approach}}$	2.37	km/s
Eccentricity of Arrival Trajectory at Mars		
e_{Mars}	7.56	
Deflection Angle		
δ	0.265446154	rad 15.20894 deg
$\Delta V_{\text{fly-by}}$	4.59	km/s
Heliocentric Mars Departure		
ΔV Mars Hyperbolic Departure		
$V^{\infty}_{\text{Mars Approach}}$	2.37	km/s
$V_{\text{parking around Mars}}$	2.71	km/s
$V_{\text{circular around Mars}}$	0.93	km/s
ΔV_1	1.78	km/s
V_{1989ML}	28.40	km/s
$V_{\text{Aapproach}}$	30.28	km/s
$V^{\infty}_{\text{Asteroid Approach}}$	1.89	km/s
ΔV Asteroid Arrival Hyperbolic Capture		
Asteroid Parking distance	10.15	km
$V_{\text{circularAsteroid}}$	0.00006637	km/s
$V_{\text{parkingAsteroid}}$	1.89	km/s
ΔV_2	1.89	km/s

$\Delta V_{\text{total to asteroid}}$	3.67	km/s
Heliocentric Earth Arrival		
V1989ML	28.40	km/s
VApproach	27.71	km/s
V_{∞} Asteroid departure	0.68	km/s
VEarth	29.78	km/s
VParking	30.48	km/s
V_{∞} Earth Arrival	0.70	km/s
ΔV Asteroid Hyperbolic Departure		
Asteroid Parking	10.15	km
VcircularAsteroid	0.00006637	km/s
VparkingAsteroid	0.68	km/s
ΔV_1	0.68	km/s
ΔV Earth Hyperbolic Arrival		
VParking	7.01	km/s
VCircular	4.93	km/s
ΔV_2	2.08	km/s
$\Delta V_{\text{total to Earth}}$	2.76	km/s
$\Delta V_{\text{total mission}}$	1.83	km/s

MISSION SCENARIO 6: EARTH AND MARS GRAVITY ASSIST TO ASTEROID

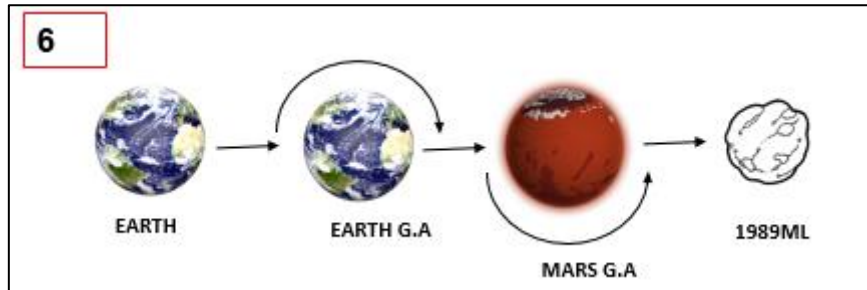


Figure C. 6 - Mission Architecture Scenario 6

Table C. 8 - ΔV Calculations for Mission Scenario 6

True ΔV Calculation using Earth and Mars Gravity Assists				
Patched Conic Method				
μ_{Sun}	1.33E+20		m^3/s^2	
Earth distance from Sun	1	AU	1.50E+11	m
1989ML distance from Sun	1.1	AU	1.65E+11	m
Mars distance from Sun	1.45	AU	2.17E+11	m
Earth radius	6371		km	
Asteroid radius	0.15		km	
μ_{Earth}	3.99E+05		km^3/s^2	
μ_{1989ML}	4.47E-08		km^3/s^2	
μ_{Mars}	4.28E+04		km^3/s^2	

Earth parking	16371	km
Earth fly-by altitude	10000	km
Mars fly-by altitude	10000	km
Heliocentric Earth Departure		
VEarth	29.78	km/s
Vparking	30.48	km/s
V∞ Earth Departure =Approach	0.70	km/s
Eccentricity of Arrival Trajectory at Moon		
$e = 1 + \frac{r_p v_\infty^2}{\mu}$		
eEarth	1.01	
Deflection Angle		
δ	2.829201765	rad
ΔVfly-by	0.83	km/s
Heliocentric Earth Departure		
V∞ Earth Departure	0.70	km/s
VMars	24.73	km/s
Vapproach	22.35	km/s
V∞ Mars Approach	2.39	km/s
Eccentricity of Arrival Trajectory at Mars		
eMars	2.33	
Deflection Angle		
δ	0.887108918	rad
ΔVfly-by	1.32	km/s
Heliocentric Mars Departure		
ΔV Mars Hyperbolic Departure		
V∞ Mars Approach	2.39	km/s
Vparking around Mars	3.78	km/s
Vcircular around Mars	2.07	km/s
ΔV1	1.71	km/s
V1989ML	28.40	km/s
VApproach	30.28	km/s
V∞ Asteroid Approach	1.89	km/s
ΔV Asteroid Arrival Hyperbolic Capture		
Asteroid Parking distance	10.15	km
VcircularAsteroid	0.00006637	km/s
VparkingAsteroid	1.89	km/s
ΔV2	1.89	km/s
ΔVtotal to asteroid	3.59	km/s
Heliocentric Earth Arrival		
V1989ML	28.40	km/s
VApproach	27.71	km/s
V∞ Asteroid departure	0.68	km/s
VEarth	29.78	km/s

VParking	30.48	km/s		
V∞ Earth Arrival	0.70	km/s		
ΔV Asteroid Hyperbolic Departure				
Asteroid Parking	10.15	km		
V_{circular}Asteroid	0.00006637	km/s		
VparkingAsteroid	0.68	km/s		
$\Delta V1$	0.68	km/s		
ΔV Earth Hyperbolic Arrival				
VParking	7.01	km/s		
VCircular	4.93	km/s		
$\Delta V2$	2.08	km/s		
$\Delta V_{\text{total to Earth}}$	2.76	km/s		
$\Delta V_{\text{total mission}}$	4.21	km/s		

APPENDIX D TIME OF FLIGHT CALCULATIONS

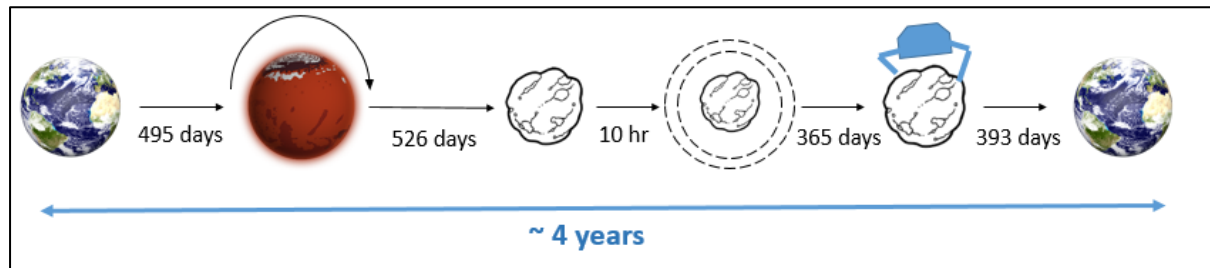


Figure D. 1- Mission lifetime

Table D. 1- Time of flight calculations for the mission

ToF Calculations for mission			
μ_{Sun}	1.33E+20	m3/s2	
Earth distance from Sun	1	AU	1.50E+11 m
Asteroid distance from Sun	1.1	AU	1.65E+11 m
Mars distance from Sun	1.45	AU	2.17E+11 m
Time of Flight Earth to Mars			
$T = 2\pi \sqrt{\frac{a^3}{\mu_{Sun}}}$			
a	1.8326E+11	m	
T	4.95E+02	days	
ToFe2m	6.78E-01	years	
Time of Flight Mars to Asteroid			
$T = 2\pi \sqrt{\frac{a^3}{\mu_{Sun}}}$			
a	1.9074E+11	m	
T	5.26E+02	days	
ToFm2a	7.20E-01	years	
Time of Proximity Operations			
$T = 2\pi \sqrt{\frac{a^3}{\mu_{Asteroid}}}$			
τ_{10km}	9.61E+05	s	
τ_{5km}	3.47E+05	s	
τ_{3km}	1.66E+05	s	
τ_{2km}	9.37E+04	s	
τ_{1km}	3.66E+04	s	
τ_{Total}	1.60E+06	s	
	4.46E+02	hr	

	5.09E-02	years
τProximity+50%margin	7.63E-02	years
Time of Mining Operations		
Time of Mining Operations	1	year
Time of Flight Asteroid to Earth		
$T = 2\pi \sqrt{\frac{a^3}{\mu_{Sun}}}$		
a	1.5708E+11	m
T	3.93E+02	days
ToFa2e	5.38E-01	years
Total Time of Mission	3.01E+00	years
Total Time of Mission+30%	3.92E+00	Years
	~4	Years

References

- [1] C. Shaffer, ThermoFisher Scientific, 2014. [Online]. Available: <https://www.thermofisher.com/blog/mining/key-issues-facing-the-mining-industry-in-2014/>. [Accessed 2020].
- [2] “Wikipedia,” [Online]. Available: https://en.wikipedia.org/wiki/Environmental_impact_of_mining. [Accessed 2020].
- [3] A. Sandstrom, “Epiroc,” 2018. [Online]. Available: <http://www.sandstromanders.com/portfolio/project-1/#:~:text=Mining%20in%20Zero%20Gravity%20is,development%20of%20our%20space%20industry..> [Accessed 2020].
- [4] P. H. Diamandis, Harvesting Asteroids to fuel human exploration and prosperity, Planetary Resources, 2013.
- [5] T. Vulcans, “SSERD,” [Online]. Available: <https://teamvulcans.sserd.org/>. [Accessed 2020].
- [6] R. m. B. a. D. F. Andreas M Heina, “A Techno-Economic Analysis of Asteroid Mining,” International astronautical Congress, 2018.
- [7] M. J. Sonter, “The Technical and Economic Feasibility of Mining the Near-Earth Asteroids,” University of Wollongong, 2012.
- [8] NASA, “OSIRIS-REX,” 2020. [Online]. Available: <https://www.nasa.gov/osiris-rex>. [Accessed 2020].
- [9] NASA, “Spaceflight101, OSIRIS-REX,” 2020. [Online]. Available: <https://spaceflight101.com/osiris-rex/>. [Accessed 2020].
- [10] D. Lauretta, “Osiris-rex: Sample return from asteroid (101955) bennu,” Space Sci Review, 2017.
- [11] P. A. a. E. C. B William, “Osiris-rex flight dynamics and navigation design,” Space Sci Review, 2018.
- [12] J. a. K. Hitoshi Kuninaka, “Lessons learned from round trip of hayabusa asteroid explorer in deep space,” IEEE, 2010.
- [13] A. M. C. M. W. W. J. H. Gary A Allen, “Hayabusa re-entry: Trajectory analysis and observation mission design,” IEEE, 2011.
- [14] JAXA, “Hayabusa 2,” 2013. [Online]. Available: <https://www.hayabusa2.jaxa.jp/en/>. [Accessed 2020].
- [15] JAXA, “Hayabusa,” 2016. [Online]. Available: <https://www.isas.jaxa.jp/en/missions/spacecraft/past/hayabusa.html>. [Accessed 2020].
- [16] NASA, “Asteroids,” [Online]. Available: [https://solarsystem.nasa.gov/asteroids-comets-and-meteors/asteroids/in-depth/#:~:text=The%20three%20broad%20composition%20classes,are%20dark%20in%20appearance.&text=The%20S%2Dtypes%20\(%22stony,metallic%20\(nickel%2Diron\)..](https://solarsystem.nasa.gov/asteroids-comets-and-meteors/asteroids/in-depth/#:~:text=The%20three%20broad%20composition%20classes,are%20dark%20in%20appearance.&text=The%20S%2Dtypes%20(%22stony,metallic%20(nickel%2Diron)..) [Accessed 2020].

- [17] “Asteroid,” [Online]. Available: <https://en.wikipedia.org/wiki/Asteroid>. [Accessed 2020].
- [18] NASA, “JPL Small-Body Mission-Design Tool,” [Online]. Available: https://ssd.jpl.nasa.gov/?mdesign_server&sstr=1989ML. [Accessed 2020].
- [19] A. W. H. A. F. Michael Mueller, “Science Direct,” 2007. [Online]. Available: <https://www.sciencedirect.com/science/article/abs/pii/S0019103507000425>. [Accessed 2020].
- [20] “1989ML,” [Online]. Available: [https://en.wikipedia.org/wiki/\(10302\)_1989_ML](https://en.wikipedia.org/wiki/(10302)_1989_ML). [Accessed 2020].
- [21] j. R. Wertz, Space Mission Engineering: The New SMAD, Microcosm press, 2011.
- [22] A. Rocketdyne, “In-Space propulsion Data Sheets,” 4 08 2020. [Online]. [Accessed 2020].
- [23] N. Grumman, “PMD Tank Datasheet,” 2020. [Online]. Available: <https://www.northropgrumman.com/space/pmd-tanks-data-sheets-sorted-by-volume/>. [Accessed 2020].
- [24] N. Grumman, “Pressurant Tank Data Sheet,” 2020. [Online]. Available: <https://www.northropgrumman.com/space/pressurant-tanks-data-sheets-sorted-by-volume/>. [Accessed 2020].
- [25] M. M. B. Viorel, The International Handbook of Space Technology.
- [26] S. 101, “Progress MS Spacecraft,” [Online]. Available: <https://spaceflight101.com/spacecraft/progress-ms/#:~:text=The%20engine%20operates%20at%20a,202.1m%20in%20diameter..> [Accessed 2020].
- [27] “Soyuz MS,” [Online]. Available: https://en.wikipedia.org/wiki/Soyuz_MS. [Accessed 2020].
- [28] C. D. Brown, Elements of Spacecraft Design, American Institute of Aeronautics and Astronautics, 2002.
- [29] K. E. Boushon, “Thermal analysis and control of small satellites in low Earth orbit,” Missouri University Of Science and technology, 2018.
- [30] NASA, “Phobos-Grunt,” [Online]. Available: <https://solarsystem.nasa.gov/missions/phobos-grunt/in-depth/>. [Accessed 2020].